Demonstration of the Updated Bays Eutrophication Model

Massachusetts Water Resources Authority
Environmental Quality Department
Report 2021-02

Deltares, 2021. Demonstration of the updated Bays Eutrophication Model. Boston: Massachusetts Water Resources Authority. Report 2021-02. 138 p. plus appendices.
www.mwra.com/media/file/demonstration-updated-bays-eutrophication-model-2021-02

Cover image: Boston Harbor Islands (MWRA photo)

Executive Summary

Background. The Massachusetts Water Resources Authority (MWRA) manages a sewage system that collects wastewater from 43 communities in Greater Boston and sends it to the Deer Island Treatment Plant. Before September 2000, discharges went into Boston Harbor and contributed to its poor water quality. As part of efforts to clean up the harbor, MWRA diverted effluent through a new outfall farther offshore in Massachusetts Bay. There was general concern about how the treated effluent would affect Massachusetts Bay, and whether it might affect neighboring Cape Cod Bay. Nutrients in the effluent could potentially contribute to eutrophication, an overgrowth of phytoplankton which as it decays can deplete dissolved oxygen and harm marine life. Federal and state regulators require MWRA to monitor water quality in the bays, through a National Pollutant Discharge Elimination System permit. MWRA has collected extensive measurements of nutrients, chlorophyll (an indicator for phytoplankton), and zooplankton, as well as temperature, salinity, and circulation patterns. These field observations have shown that eutrophication is not a concern.

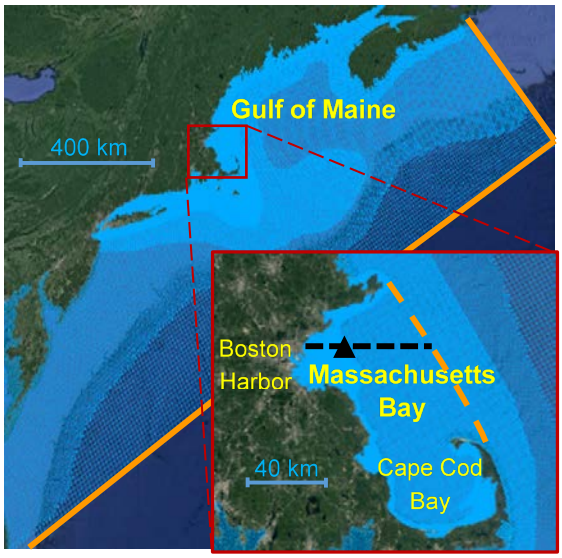

Updated model domain spans beyond Gulf of Maine (background map, offshore boundary solid orange line) to best simulate the important influence of water outside the bays; dashed orange line in inset is offshore boundary of water quality component of former model. Black triangle is outfall site. Model results in figure on next page are from east-west transect along black dashed line. Also shown: model grid resolution, which varies from finest in the bays (brighter blues) to most coarse farthest offshore (darker blues), for computational efficiency.

The Bays Eutrophication Model. The permit requires MWRA to maintain and annually run a Bays Eutrophication Model (BEM). It is a combined water quality and hydrodynamics model; the water quality component simulates processes influencing phytoplankton, including nutrients, light, and potential effects on oxygen, and the hydrodynamic component simulates physical processes controlling water temperature, salinity, and circulation. Simulations of the years 2000 to 2016 are complete. During that period the modeling methods were updated several times, as better techniques became available. Recently MWRA contracted Deltares to update BEM again. This report demonstrates that the updated model is ready for use in simulations of 2017 onward.

Development of updated model. The updated model is built on a widely used software platform that is continually improved to include modeling methods based on the latest research. The updated and former models are similar in many ways. Both models include realistic river, atmospheric, and offshore conditions; track several nutrients; represent multiple groups of phytoplankton; simulate decaying organic materials at the seafloor; use a grid that captures the complex coastline, with spatially varying resolution

for computational speed; and treat effluent dilution directly above the outfall using the same grid as for other parameters for efficiency. A difference of the updated model is its larger domain (see figure on previous page), which spans beyond the Gulf of Maine so it more directly simulates exchange between the bays and waters farther offshore, for example inflow to Massachusetts Bay from the Merrimack River. In addition, the water quality component does not require measurements within the bays because conditions at the far offshore boundary are set by an independent North Atlantic simulation. The hydrodynamic component also captures physical processes more independently because it treats temperature and salinity without using data assimilation, a method for guiding models with observations.

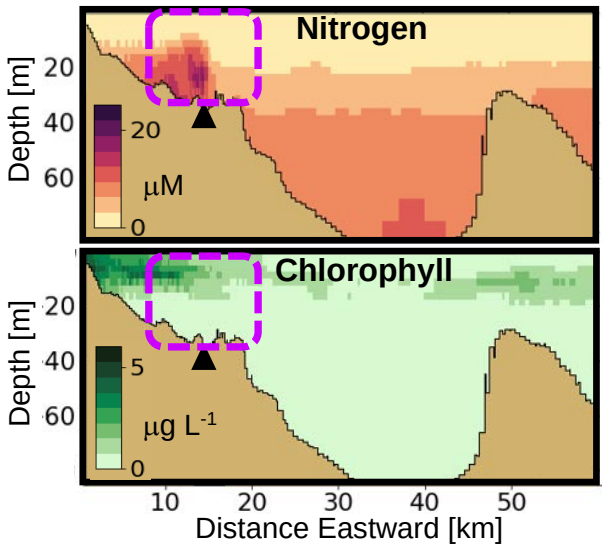

Subset of results from updated model, on vertical slice through outfall (black triangle) along dashed east-west black line in bays map above. This example shows monthly-mean June 2016 stratified conditions, for dissolved inorganic nitrogen and chlorophyll. Over the outfall (dashed violet boxes) an effluent plume is evident in nitrogen. For chlorophyll, in contrast, effluent impacts are difficult to detect. This general pattern is representative of overall model results for other times and other parameters. It is characteristic of both field observations and results from the former model, and indicates that eutrophication is not a concern.

Model calibration and performance. Calibration of the updated model relied on established methods and used five years of observations (2012 to 2016) to include a representative range of year-to-year variability. The calibration improved agreement of model results with observations based on both visual comparisons and quantitative indicators. This report presents a series of graphics demonstrating the performance of the updated model compared with observations, for the year 2016, with side-by-side comparisons to performance of the former model for the same year. In general, both models performed equally well. Results of the updated model support the conclusions from field monitoring, that water quality in the bays is controlled mainly by exchange with Gulf of Maine waters, the outfall is a minor influence, and discharged nutrients do not lead to strongly enhanced phytoplankton growth. For example, both models show increased dissolved inorganic nitrogen concentrations near and above the outfall, while chlorophyll concentrations remain at normal levels throughout the bays including over the outfall (see figure at left). For some water quality parameters, including chlorophyll, the updated model shows variability in depth that is more realistic than the former model, with values near the ocean surface differing more from those at the seafloor. In addition, the updated model accurately captures seasonal density stratification, caused by temperature and salinity changes, without relying on data assimilation.

Conclusion. This report demonstrates using 2016 simulations that the updated BEM agrees with field observations at least as well as the former model, which met the permit requirement through that year. Therefore, the updated model is suitable for MWRA to use in meeting its permit requirement on simulations of 2017 onward.

Contents

	Executive Summary	**1**
	List of Figures	**5**
1	**Introduction**	**11**
2	**Hydrodynamics**	**12**
2.1	Distinctions between former BEM and updated BEM	12
2.1.1	Data Assimilation	12
2.1.2	Proximity of offshore boundary	13
2.2	Model-observation comparisons	13
2.2.1	MWRA observations: Temporal variability	14
2.2.1.1	Temperature	14
2.2.1.2	Salinity	17
2.2.2	MWRA observations: Spatial structure	20
2.2.2.1	Surface temperature	20
2.2.2.2	Bottom temperature	23
2.2.2.3	Surface salinity	26
2.2.2.4	Bottom salinity	29
2.2.3	Mooring observations time series	32
2.2.3.1	Temperature and salinity	32
2.2.3.2	Non-tidal currents	34
2.3	Model monthly-mean temperature, salinity and circulation	40
2.3.1	Temperature	40
2.3.2	Salinity	46
2.3.3	Residual currents	52
2.4	Conclusions on updated/former model comparisons for hydrodynamics	58
3	**Water Quality**	**59**
3.1	Distinctions between former BEM and updated BEM	60
3.1.1	Location of the open boundary	60
3.1.2	Non-oceanic loads	61
3.1.3	Representation of biogeochemical processes	61
3.1.3.1	Phytoplankton model	61
3.1.3.2	Attenuation of light	62
3.1.3.3	Representation of organic matter	62
3.1.3.4	Sediment processes	62
3.2	Model-observation comparisons	63
3.2.1	Model-observation correlation analysis	64
3.2.2	Light climate	67
3.2.3	Dissolved Inorganic Nitrogen	74
3.2.4	Chlorophyll-a and primary productivity	83

3.2.5 Dissolved and Particulate Organic Nitrogen 95
3.2.6 Particulate Organic Carbon 108
3.2.7 Dissolved Oxygen 115
3.2.8 Sediment fluxes 123
3.3 Discussion 128
3.3.1 Role of model boundary 128
3.3.2 Outfall plume 128
3.3.3 Temporal variability of simulated concentrations 129
3.3.4 Vertical gradients of simulated concentrations 130
3.3.5 Residence times and flushing of study area; relative importance of outfall 130
3.3.6 Processes controlling dissolved oxygen 131
3.3.7 Relevance of sediments in mass balances 133
3.4 Conclusions on update/former model comparisons for water quality 133
4 Conclusion 134
5 References 135
Appendix A: Model attributes and methods 137
Appendix B: Multi-year calibration 138

List of Figures

Figure 2-1 MWRA observation locations. ARRS is Alexandrium Rapid Response Surveys. NERACOOS is Northeastern Regional Association of Coastal Ocean Observing Systems. 13
Figure 2-2 Temperature time-series, model-observation comparison for 2016 for the former BEM. Model results: black/red lines. MWRA observations: black/red symbols (Zhao et al. 2017, Figure 4-1)..... 15
Figure 2-3 Temperature time-series, model-observation comparison for 2016 for the updated BEM. Model results: black/blue lines. MWRA observations: black/blue symbols 16
Figure 2-4 Salinity time-series, model-observation comparison for 2016 for the former BEM. Model results: black/red lines. MWRA observations: black/red symbols (Zhao et al. 2017, Figure 4-2). 18
Figure 2-5 Salinity time-series, model-observation comparison for 2016 for the updated BEM. Model results: black/blue lines. MWRA observations: black/blue symbols. 19
Figure 2-6 Temperature spatial structure, at/near sea surface, model-observation comparison for 2016 for former BEM (Zhao et al. 2017, Figure 4-3a). Contours in the “Observations” plots are based on the observations at discrete sample locations shown by black dots..... 21
Figure 2-7 Temperature spatial structure, at/near sea surface, model-observation comparison for 2016 for updated BEM. 22
Figure 2-8 Temperature spatial structure, at/near seafloor, model-observation comparison for 2016 for former BEM (Zhao et al. 2017, Figure 4-3b). 24
Figure 2-9 Temperature spatial structure, at/near seafloor, model-observation comparison for 2016 for updated BEM. 25
Figure 2-10 Salinity spatial structure, at/near sea surface, model-observation comparison for 2016 for former BEM (Zhao et al. 2017, Figure 4-4a). 27
Figure 2-11 Salinity spatial structure, at/near sea surface, model-observation comparison for 2016 for updated BEM. 28
Figure 2-12 Salinity spatial structure, at/near seafloor, model-observation comparison for 2016 for former BEM (Zhao et al. 2017, Figure 4-4b). 30
Figure 2-13 Salinity spatial structure, at/near seafloor, model-observation comparison for 2016 for updated BEM. 31
Figure 2-14 Former BEM model results compared to observed time series at Mooring A01 for 2016 for three depths:1m, 20m and 50m. Top: Temperature. Bottom: Salinity (psu) (Zhao et al.2017, Figure 4-5). 32
Figure 2-15 Updated BEM results compared to observed time series at Mooring A01 for 2016 for three depths:1m, 20m and 50m. Top: Temperature. Bottom: Salinity (psu). 33
Figure 2-16 Updated BEM model results compared against observed time series at Mooring A01 for 2016 for 1 to 20 meter and 1 to 50-meter stratification. Top: Temperature. Bottom: Salinity (psu) 34
Figure 2-18 Former BEM modeled against observed current time-series, for 2016 Jul-Dec. Sticks point in the direction of flow, away from zero line: north/eastward flow up/rightward (Zhao et al. 2017, Figure 4-6b). 37

Figure 2-19 Updated BEM modeled against observed current time-series, for 2016 Jan-Jun. Sticks point in the direction of flow, away from zero line: north/eastward flow up/rightward. 38
Figure 2-20 Updated BEM modeled against observed current time-series, for 2016 Jul-Dec. Sticks point in the direction of flow, away from zero line: north/eastward flow up/rightward. 39
Figure 2-21 Former BEM model monthly mean temperature at sea surface for 2016 (Zhao et al. 2017, Figure 4-7a). 41
Figure 2-22 Updated BEM model monthly mean temperature at sea surface for 2016. 42
Figure 2-23 Former BEM model monthly mean temperature at seafloor for 2016 (Zhao et al. 2017, Figure 4-7b). 44
Figure 2-24 Updated BEM model monthly mean temperature at seafloor for 2016. 45
Figure 2-25 Former BEM model monthly mean salinity at sea surface for 2016 (Zhao et al. 2017, Figure 4-8a). 47
Figure 2-26 Updated BEM model monthly mean salinity at sea surface for 2016. 48
Figure 2-27 Former BEM model monthly mean salinity at seafloor for 2016 (Zhao et al. 2017, Figure 4-8b). 50
Figure 2-28 Updated BEM model monthly-mean salinity at near the seafloor for 2016. 51
Figure 2-29 Schematic long-term mean circulation (Zhao et al. 2017, Figure 1-1). WMCC: Western Maine Coastal Current. 52
Figure 2-30 Former BEM model monthly-mean currents at sea surface for 2016 (Zhao et al.2017, Figure 4-9a). 54
Figure 2-31 Updated BEM model monthly-mean currents at sea surface for 2016. 55
Figure 2-32 Former BEM model monthly-mean currents at 15 m depth for 2016 (Zhao et al.2017, Figure 4-9b). 56
Figure 2-33 Updated BEM model monthly-mean currents at 15 m depth for 2016. 57
Figure 3-1 Zones over which mass balances are calculated in the updated BEM. 59
Figure 3-2 Extent of the updated BEM horizontal grid (colors indicate grid resolution: yellow=8km; orange=4km; green=2km; light blue=1km; royal blue=500m; dark blue=250m). 60
Figure 3-3 Water quality model domain of the former BEM. Red arc = Offshore boundary; Black line = East-west transect through outfall. Station groups: northern (circles), southern (squares), and harbor (triangles). (from Zhao et al. 2017, Figure 3-6). 63
Figure 3-4 Model-observation correlation/regressions of key water quality parameters for 2016 for the former BEM. All stations outside Boston Harbor; regressions are solid lines, dashed lines indicate equality between observed and model results (Zhao et al. 2017, Figure 5-1). 65
Figure 3-5 Model-observation regression plots for key water quality variables for 2016 for the updated BEM. The black line corresponds to the linear regression; the dotted line indicates equality between observations and model results. 66
Figure 3-6 Light extinction at Northern stations for 2016. Line: Model results from former BEM. Symbols: Observations. In this and all similar plots to follow, upper left of frame shows "station name (bathymetric depth)" (Zhao et al. 2017, Figure 5-2a). 68
Figure 3-7 Light extinction at Northern stations for 2016. Line: Model results from updated BEM. Symbols: Observations. 69

Figure 3-8 Light extinction at Southern stations for 2016. Line: Model results from former BEM. Symbols: Observations. (Zhao et al. 2017, Figure 5-2b). 70
Figure 3-9 Light extinction at Southern stations for 2016. Line: Model results from updated BEM. Symbols: Observations. 71
Figure 3-10 Light extinction at Harbor stations for 2016. Line: Model results from former BEM. Symbols: Observations. Note different y-axis scale than for bay stations in Figure 3-6 and Figure 3-8 (Zhao et al. 2017, Figure 5-2c). 72
Figure 3-11 Light extinction at Harbor stations for 2016. Line: Model results from updated BEM. Symbols: Observations. 73
Figure 3-12 Dissolved inorganic nitrogen at Northern stations. Model-observation comparisons for 2016 for former BEM (Zhao et al. 2017, Figure 5-3a). 75
Figure 3-13 Dissolved inorganic nitrogen at Northern stations. Model-observation comparisons for 2016 for updated BEM. Black: observations near surface, model at water surface. Blue: observations near seafloor, model at bottom. 76
Figure 3-14 Dissolved inorganic nitrogen at Southern stations. Model-observation comparisons for 2016 for former BEM (Zhao et al. 2017, Figure 5-3b). 77
Figure 3-15 Dissolved inorganic nitrogen at Southern stations. Model-observation comparisons for 2016 for updated BEM. Black: observations near surface, model at water surface. Blue: observations near seafloor, model at bottom. 78
Figure 3-16 Dissolved inorganic nitrogen. Harbor stations. Model-observation comparisons for 2016. Note different y-axis scale than for bay stations in Figure 3-12 and Figure 3-14 (Zhao et al. 2017, Figure 5-3c). 79
Figure 3-17 Dissolved inorganic nitrogen at Harbor stations. Model-observation comparisons for 2016 for updated BEM. Black: observations near surface, model at water surface. Blue: observations near seafloor, model at bottom. 80
Figure 3-18 Dissolved inorganic nitrogen (µM). Former BEM results for 2016 along east-west transect (Figure 3-3). Horizontal axis is distance eastward from coast; outfall is on seafloor at approximately 13 km (Zhao et al. 2017, Figure 5-3d). 81
Figure 3-19 Dissolved inorganic nitrogen (µM). Updated BEM results for 2016 along east-west transect (Figure 3.1). Horizontal axis is distance eastward from coast; black triangle indicates the location of the outfall on seafloor. 82
Figure 3-20 Chlorophyll at Northern stations. Model-observation comparisons for 2016 for former BEM (Zhao et al. 2017, Figure 5-4a). 84
Figure 3-21 Chlorophyll at Northern stations. Model-observation comparisons for 2016 for updated BEM. Black: observations near surface, model at water surface. Blue: observations near seafloor, model at bottom. 85
Figure 3-22 Chlorophyll at Southern stations. Model-observation comparisons for 2016 for former BEM (Zhao et al. 2017, Figure 5-4b). 86
Figure 3-23 Chlorophyll at Southern stations. Model-observation comparisons for 2016 for updated BEM. Black: observations near surface, model at water surface. Blue: observations near seafloor, model at bottom. 87
Figure 3-24 Chlorophyll at Harbor stations. Model-observation comparisons for 2016 for former BEM (Zhao et al. 2017, Figure 5-4c). 88
Figure 3-25 Chlorophyll at Harbor stations. Model-observation comparisons for 2016 for updated BEM. Black: observations near surface, model at water surface. Blue: observations near seafloor, model at bottom. 89

Figure 3-26 Chlorophyll (µg L^{-1}). Former BEM results along east-west transect for 2016 (Figure 3.1). Horizontal axis is distance eastward from coast; outfall is on seafloor at approximately 13 km (Zhao et al. 2017, Figure 5-3d). 90
Figure 3-27 Chlorophyll (µg L^{-1}). Updated BEM results along east-west transect for 2016 (Figure 3.1). Horizontal axis is distance eastward from coast; black triangle indicates the location of the outfall on seafloor. 91
Figure 3-28 Primary production, vertically integrated, model-observation comparison for the former BEM. Line is 2016 model result. Box-whiskers are 1995-2010 observations; box shows 25th, 50th, 75th percentiles and whiskers are 9th and 91st percentiles (Zhao et al., 2017)..... 93
Figure 3-29 Primary production, vertically integrated, model-observation comparison for the updated BEM. Line is 2016 model result. Box-whiskers are 1995-2010 observations; box shows 25th, 50th, 75th percentiles and whiskers are 9th and 91st percentiles. 94
Figure 3-30 Dissolved organic nitrogen at Northern stations. Model-observation comparisons for 2016 for former BEM (Zhao et al. 2017, Figure 5-6a). 96
Figure 3-31 Dissolved organic nitrogen at Northern stations. Model-observation comparisons for 2016 for updated BEM. Black: observations near surface, model at water surface. Blue: observations near seafloor, model at bottom. 97
Figure 3-32 Dissolved organic nitrogen at Northern stations. Model-observation comparisons for 2016 for former BEM (Zhao et al. 2017, Figure 5-6b). 98
Figure 3-33 Dissolved organic nitrogen at Southern stations. Model-observation comparisons for 2016 for updated BEM. Black: observations near surface, model at water surface. Blue: observations near seafloor, model at bottom. 99
Figure 3-34 Dissolved organic nitrogen (µM). Former BEM results for 2016 along east-west transect (Figure 3.1). Horizontal axis is distance eastward from coast; outfall is on seafloor at approximately 13 km (Zhao et al. 2017, Figure 5-6c). 100
Figure 3-35 Dissolved organic nitrogen (µM). Updated BEM results for 2016 along east-west transect (Figure 3.1). Horizontal axis is distance eastward from coast; black triangle indicates the location of the outfall on seafloor. 101
Figure 3-36 Particulate organic nitrogen at Northern stations. Model-observation comparisons for 2016 for former BEM (Zhao et al. 2017, Figure 5-7a). 102
Figure 3-37 Particulate organic nitrogen at Northern stations. Model-observation comparisons for 2016 for updated BEM. Black: observations near surface, model at water surface. Blue: observations near seafloor, model at bottom. 103
Figure 3-38 Particulate organic nitrogen at Southern stations. Model-observation comparisons for 2016 for former BEM (Zhao et al. 2017, Figure 5-7b). 104
Figure 3-39 Particulate organic nitrogen at Southern stations. Model-observation comparisons for 2016 for updated BEM. Black: observations near surface, model at water surface. Blue: observations near seafloor, model at bottom. 105
Figure 3-40 Particulate organic nitrogen (µM). Former BEM results for 2016 along east-west transect (Figure 3.1). Horizontal axis is distance eastward from coast; outfall is on seafloor at approximately 13 km (Zhao et al. 2017, Figure 5-7c). 106
Figure 3-41 Particulate organic nitrogen (µM). Updated BEM results for 2016 along east-west transect (Figure 3.1). Horizontal axis is distance eastward from coast; black triangle indicates the location of the outfall on seafloor. 107
Figure 3-42 Particulate organic carbon at Northern stations. Model-observation comparisons for 2016 for former BEM (Zhao et al. 2017, Figure 5-8a). 109

Figure 3-43 Particulate organic carbon at Northern stations. Model-observation comparisons for 2016 for updated BEM. Black: observations near surface, model at water surface. Blue: observations near seafloor, model at bottom. 110
Figure 3-44 Particulate organic carbon at Southern stations. Model-observation comparisons for 2016 for former BEM (Zhao et al. 2017, Figure 5-8b). 111
Figure 3-45 Particulate organic carbon at Southern stations. Model-observation comparisons for 2016 for updated BEM. Black: observations near surface, model at water surface. Blue: observations near seafloor, model at bottom. 112
Figure 3-46 Particulate organic carbon (µM). Former BEM results for 2016 along east-west transect (Figure 3.1). Horizontal axis is distance eastward from coast; outfall is on seafloor at approximately 13 km (Zhao et al. 2017, Figure 5-8c). 113
Figure 3-47 Particulate organic carbon (µM). Updated BEM results for 2016 along east-west transect (Figure 3.1). Horizontal axis is distance eastward from coast; black triangle indicates the location of the outfall on seafloor. 114
Figure 3-48 Oxygen concentrations at Northern stations. Model-observation comparisons for 2016 for former BEM (Zhao et al. 2017, Figure 5-9a). 116
Figure 3-49 Oxygen concentrations at Northern stations. Model-observation comparisons for 2016 for updated BEM. Black: observations near surface, model at water surface. Blue: observations near seafloor, model at bottom. 117
Figure 3-50 Oxygen concentrations at Southern stations. Model-observation comparisons for 2016 for former BEM (Zhao et al. 2017, Figure 5-9b). 118
Figure 3-51 Oxygen concentrations at Southern stations. Model-observation comparisons for 2016 for updated BEM. Black: observations near surface, model at water surface. Blue: observations near seafloor, model at bottom. 119
Figure 3-52 Oxygen concentration (mg L^{-1}). Former BEM results for 2016 along east-west transect (Figure 3.1). Horizontal axis is distance eastward from coast; outfall is on seafloor at approximately 13 km (Zhao et al. 2017, Figure 5-9c). 120
Figure 3-53 Oxygen concentration (mg L^{-1}). Updated BEM results for 2016 along east-west transect (Figure 3.1). Horizontal axis is distance eastward from coast; black triangle indicates the location of the outfall on seafloor. 121
Figure 3-54 Oxygen time series at A01 mooring site, model-observation comparison for 2016 for former BEM. The 2-m depth observations after late September did not meet quality standards (Zhao et al. 2017, Figure 5-11). 122
Figure 3-55 Oxygen time series at A01 mooring site, model-observation comparison for 2016 for updated BEM. 122
Figure 3-56 Sediment NH4+ flux. Former BEM 2016 results (line), and 2001-2010 observations (box-whiskers). Selected Boston Harbor stations (left column) and Massachusetts Bay stations (right column). (Zhao et al. 2017, Figure 5-12). 124
Figure 3-57 Sediment NH4+ flux. Updated BEM 2016 results (line), and 2001-2010 observations (box-whiskers). 125
Figure 3-58 Sediment oxygen demand. Former BEM 2016 results (line), and 2001-2010 observations (box-whiskers). Selected Boston Harbor stations (left column) and Massachusetts Bay stations (right column). (Zhao et al. 2017, Figure 5-13). 126
Figure 3-59 Sediment oxygen demand. Updated BEM 2016 results (line), and 2001-2010 observations (box-whiskers). 127
Figure 3-60 DIN measurements at MWRA station N21 (above outfall) at different water depths. 129

Figure 3-61 Model-computed vertically averaged monthly-mean values of DO fluxes in Cape Cod Bay for 2008 with the former BEM (Xue et al. 2014, figure 16). Fluxes are calculated for model grid cell at station F02. 132
Figure 3-62 Model-computed averaged DO fluxes in the MBS-CCB mass balance area (Figure 3-1) for 2016 with the updated BEM. Results are calculated at a 5-day timestep, which limits the ability to filter out the tidal signal and explains the “shakiness” of the curves. 132

1 Introduction

In May 2019, the Massachusetts Water Resources Authority (MWRA) awarded Deltares USA, working together with sub-contractor Stichting Deltares of the Netherlands (hereafter, “Deltares”), a contract to develop the updated Bays Eutrophication Model (BEM). This model will enable MWRA to comply with the nutrient- and eutrophication-related water quality modeling requirement of its National Pollution Discharge Elimination System (NPDES) permit for the Massachusetts Bay (Mass Bay) outfall.

The NPDES permit requires annual simulations which are used to support interpretation of field monitoring to assess the influence of the Mass Bay outfall on the water quality of Mass Bay. The BEM is a coupled water quality and hydrodynamics model implemented for Mass Bay, Boston Harbor and Cape Cod Bay.

The purpose of this report is to demonstrate that an updated BEM has been developed, that it performs comparably well (based on its agreement with observations) to the former BEM, and that it is suitable for use from here forward in simulations for compliance with the NPDES permit MWRA holds for its Massachusetts Bay outfall.

The updated BEM has been developed using Deltares Delft3D-Flexible Mesh Suite software (Delft3D-FM). For the MWRA, the integrated hydrodynamic and water quality modules (D-FLOW FM and D-Water Quality) have been configured for the application to Mass Bay and the assessment of the Mass Bay outfall.

The main body of the report presents the results of the *updated* BEM for the year 2016 compared to those of the *former* BEM for the same year, using model-observation figures equivalent to those for the former BEM presented in Zhao et al. (2017). Figures include time series and spatial plots as well as transects of the main model parameters relevant to characterize the hydrodynamics and water quality of Massachusetts Bay and Cape Cod Bay. Quantitative statistical and graphical approaches to documenting the strength of model-observation agreement were used in developing the updated BEM (see Appendix B). Because those methods were not as extensively used in modeling of 2016 with the former BEM (Zhao et al 2017), evaluations in this report rely heavily on visual comparisons between simulations of 2016 (updated BEM and former BEM) and corresponding field observations.

Section 2 presents the results for the *hydrodynamics* part of the model, while Section 3 presents the results of the *water quality* part of the model. Section 4 presents overall conclusions regarding the performance of the updated BEM model and its suitability for use for future annual simulations. References are in Section 5. Additionally, two technical appendices describe the main attributes and methods of the updated BEM (Appendix A) and the results of the multi-year calibration using available monitoring observations for the period 2012-2016 (Appendix B).

The content of this report is derived from internal Deltares reports: Deltares, March 2021, ref. 11203379-004-ZKS-0006 (main body), ref. 11203379-004-ZKS-0007 (Appendix A), and ref. 11203379-004-ZKS-0008 (Appendix B).

2 Hydrodynamics

In this section, the performance of the *updated* BEM hydrodynamics is evaluated in comparison to the *former* BEM. Specifically, the results from both models are compared for a series of plots, as published in Zhao et al. (2017). These plots show both time series as well as spatial fields for temperature, salinity and current velocity. In some of the plots, observations are shown also, allowing an assessment of the relative performance of the two models with respect to the observations.

2.1 Distinctions between former BEM and updated BEM

In order to facilitate the comparison of the models and assessment thereof, a few general differences in modeling approach between the former and the updated BEM hydrodynamics are presented.

2.1.1 Data Assimilation

The major difference between both models is the application of Data Assimilation (DA) in the *former* BEM, which has a significant impact on its model skill. As noted in Zhao et al. (2017), the former BEM assimilates the following information:

- Sea Surface Temperature fields: assimilated daily from a satellite product from the National Centers for Environmental Prediction, with a 0.1×0.1-degree resolution (http://polar.ncep.noaa.gov/sst/ophi/); and
- Point data: Assimilation of salinity and temperature, at all depths, for MWRA monitoring stations during approximately monthly-frequency surveys, and for instrumented moorings within the model domain at 3-day frequency.

Numerous measurements from moorings and research vessel surveys, spanning broad geographic coverage and with intensive temporal resolution at certain locations, were assimilated by the former BEM. These include measurements that were later compared to the former BEM simulations to assess its performance. This means that in the former BEM validation plots taken from the 2016 simulation report (Zhao et al., 2017) and shown in subsequent sections in this report, the former BEM is being evaluated against the same observations that have been used for assimilation. A good agreement with observations is therefore to be expected at these locations and times.

In the updated BEM, data assimilation is not applied, and the model skill is attributed purely to the physical processes resolved in the numerical model and its forcing conditions.

The use of assimilation decreases the difference between model results and observations. This holds for, but is not restricted to, the assimilated parameters at the measurement locations and time. However, this approach can potentially hide inconsistencies in the model's representation of physical processes affecting salinity and temperature, such as residual horizontal and vertical transport due to advection and diffusion. As the processes driving salinity and temperature are also key for a correct representation of water quality, it was decided not to apply assimilation in the updated

BEM. This means that achieving the same quality for salinity and temperature without DA in the updated BEM implies a better representation of physical processes affecting salinity, temperature and transport of water quality substances. A better representation of the underlying physical process subsequently gives more confidence in the applicability of the model for conducting scenario studies, for example, for assessing the impact of load changes.

2.1.2 Proximity of offshore boundary

Another potentially important difference between the former BEM and the updated BEM is the fact that the former model used a nesting approach for hydrodynamics, in which the area for the wider Gulf of Maine was modeled in a separate regional model. The area covering Massachusetts Bay and Cape Cod Bay was included in a standalone model, nested into the regional model, and therefore had an offshore boundary close to the area of interest (as seen, for example, in Figure 2-6 below). In the updated BEM, a single model covering all areas is used, and the offshore boundary lies much farther offshore. When analyzing some of the plots in this report, reference is made, where appropriate, to the consequences of this close offshore boundary in the former BEM.

2.2 Model-observation comparisons

For reference, Figure 2-1 gives an overview of the spatial distribution of the observations provided by MWRA (hereafter referred to as MWRA observations). The A01 mooring belonging to the NERACOOS (Northeastern Regional Association of Coastal Ocean Observing Systems) dataset, which is presented in the Appendix B of this report, is shown as a yellow diamond.

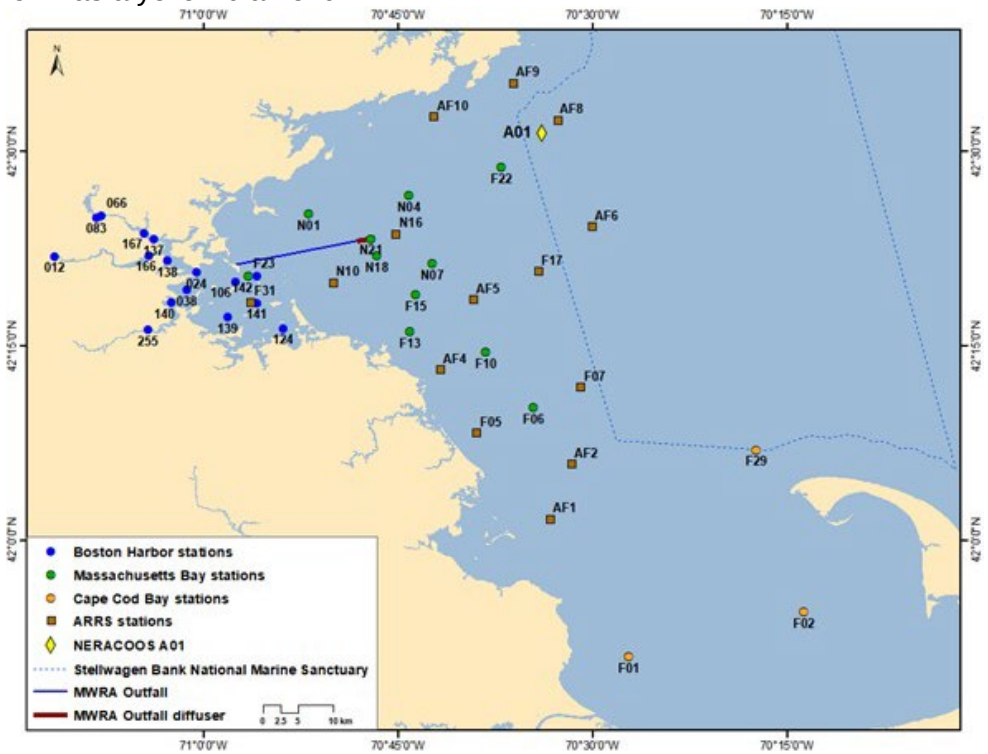

Figure 2-1 MWRA observation locations. ARRS is Alexandrium Rapid Response Surveys. NERACOOS is Northeastern Regional Association of Coastal Ocean Observing Systems.

2.2.1 MWRA observations: Temporal variability

In this section, the updated and former BEM model results for temperature and salinity are compared for a set of time series plots also showing the MWRA observations. The following locations are shown:

- Stations in Massachusetts Bay: N01, F22, N07, F06
- Stations in Cape Cod Bay: F01, F02, F29
- Stations at the mouth of Boston Harbor: F23

Mooring A01 is about 5 km to the northeast of F22 and provides a continuous hourly record of salinity and temperature at several depths. These mooring observations are assimilated by the former BEM.

2.2.1.1 Temperature

Figure 2-2 and Figure 2-3 show the temperature model-observations comparison for the former and updated BEM, respectively. The former and updated BEM show comparable and excellent skills in reproducing surface temperature values throughout the year and for all stations. For bottom waters, however, the former BEM shows temperatures that are too warm at most stations, whereas the updated BEM shows an excellent agreement with observations. This implies that temperature stratification is better represented in the updated BEM. A correct representation of stratification is especially important for modeling water quality since it affects the amount of vertical transport of substances like dissolved or particulate nutrients.

The effect of DA to correct the overestimation of bottom temperatures in the former BEM is evident in the plots, as sudden decreases in bottom temperature occur when observations are available. Between available observations, the bottom temperature rapidly increased, which is not expected and was not observed in the deep buoy A01 results plotted for station F22. Therefore, it appears that the former BEM underestimates seasonal temperature stratification. The updated BEM shows a smoother evolution of bottom temperature and consequently a better representation of seasonal temperature stratification.

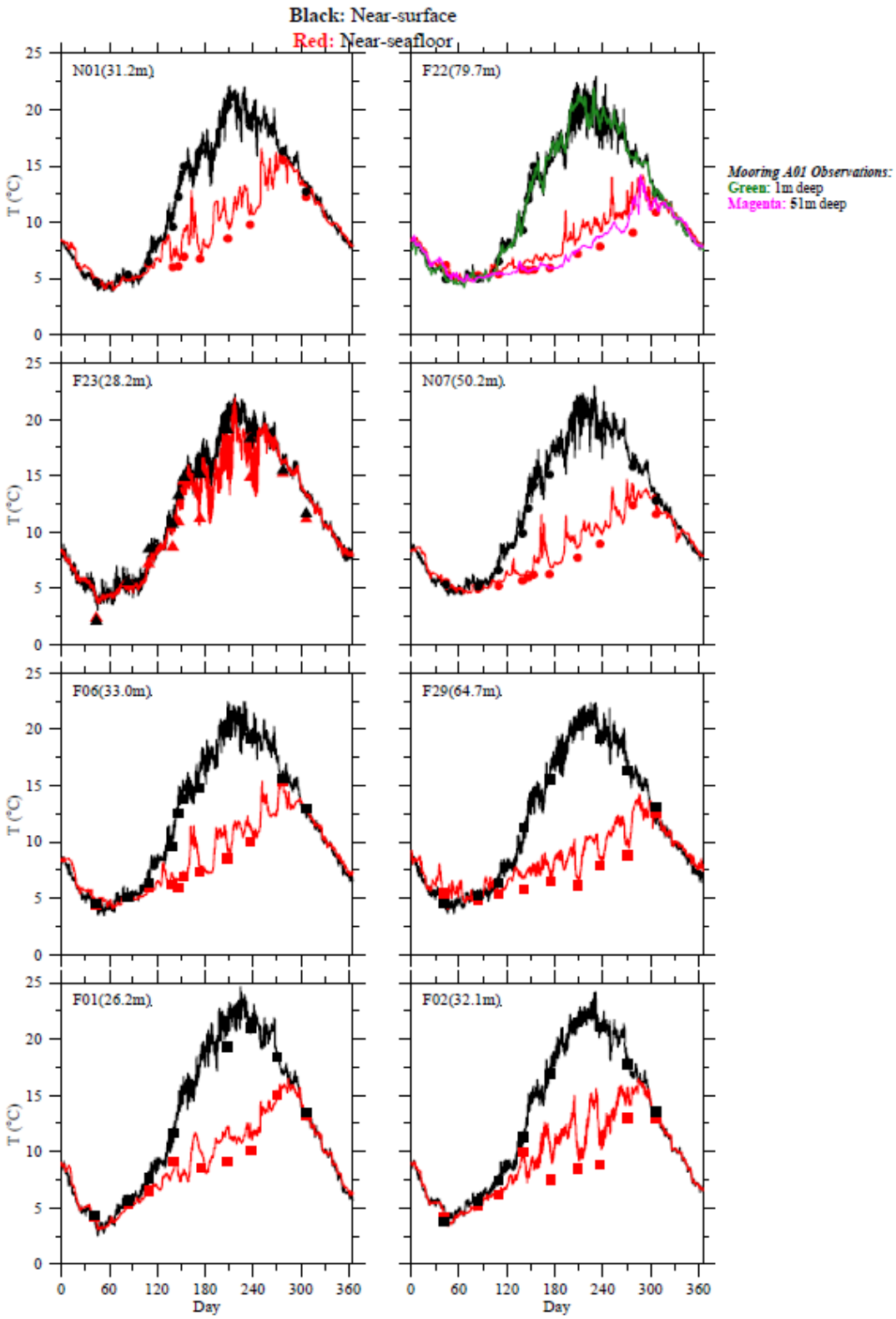

Figure 2-2 Temperature time-series, model-observation comparison for 2016 for the former BEM. Model results: black/red lines. MWRA observations: black/red symbols (Zhao et al. 2017, Figure 4-1).

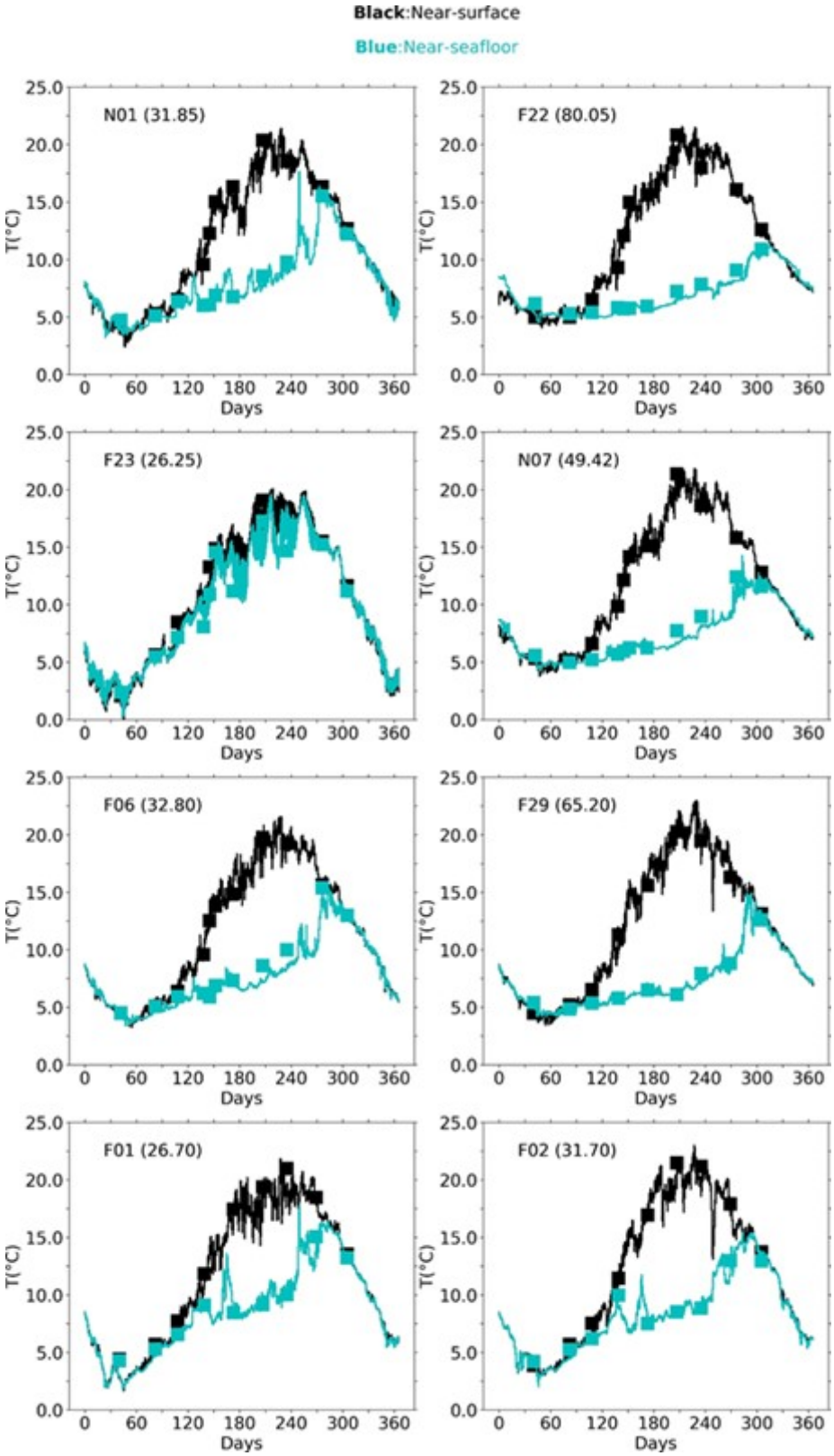

Figure 2-3 Temperature time-series, model-observation comparison for 2016 for the updated BEM. Model results: black/blue lines. MWRA observations: black/blue symbols

2.2.1.2 Salinity

Figure 2-4 and Figure 2-5 show the salinity model-observations comparison for the former and updated BEM respectively. The former BEM shows a tendency for salinities deeper in the water column to be higher than observed in some stations (e.g. F22 and F29), which is reduced by data assimilation when observations become available. This bias was reported by Zhao et al. (2017) to be in the order of 0.5 psu without DA. The results shown in Figure 2-4 show a smaller bias due to the use of DA.

The updated BEM shows a salinity bias in the order of 0.1 – 0.3 psu, in this case consistent on average throughout the MWRA measurement stations and throughout the water-column. This is larger than the bias in the former BEM plots, but it is similar to, or even smaller than, the reported bias of 0.5 psu in the former BEM without DA.

Despite this salinity bias, the stratification (vertical salinity difference) in the updated BEM is in excellent agreement with measurements. Stratification is one of the primary physical phenomena influencing water quality processes. Additionally, the former BEM showed large and abrupt salinity drops at the Boston Harbor station F23, which are not present in the MWRA observations. These salinity drops potentially reflect an overpredicted river discharge in the area (from Mystic, Charles and/or Neponset rivers). These salinity drops are not present in the updated BEM, which is consistent with observations.

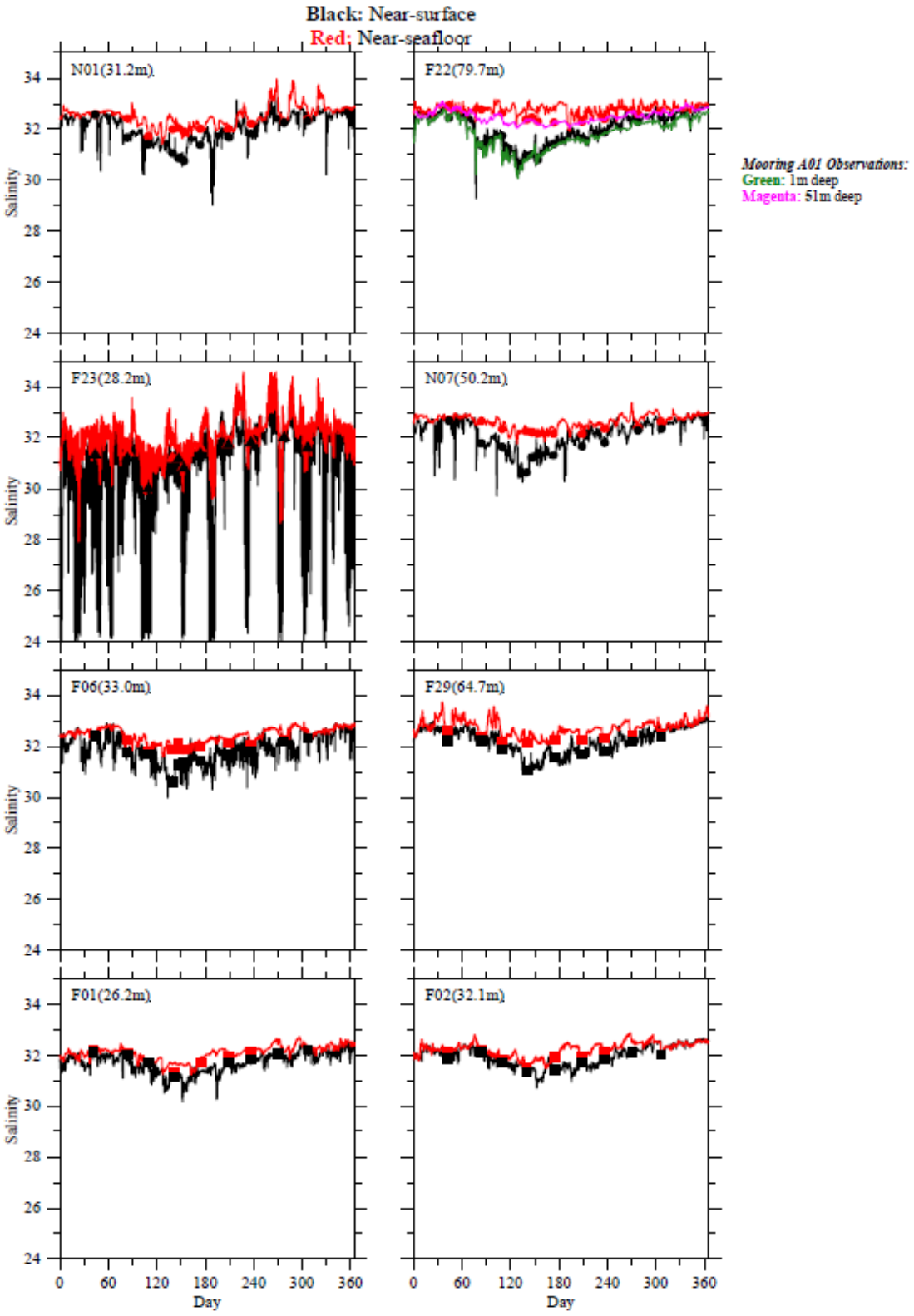

Figure 2-4 Salinity time-series, model-observation comparison for 2016 for the former BEM. Model results: black/red lines. MWRA observations: black/red symbols (Zhao et al. 2017, Figure 4-2).

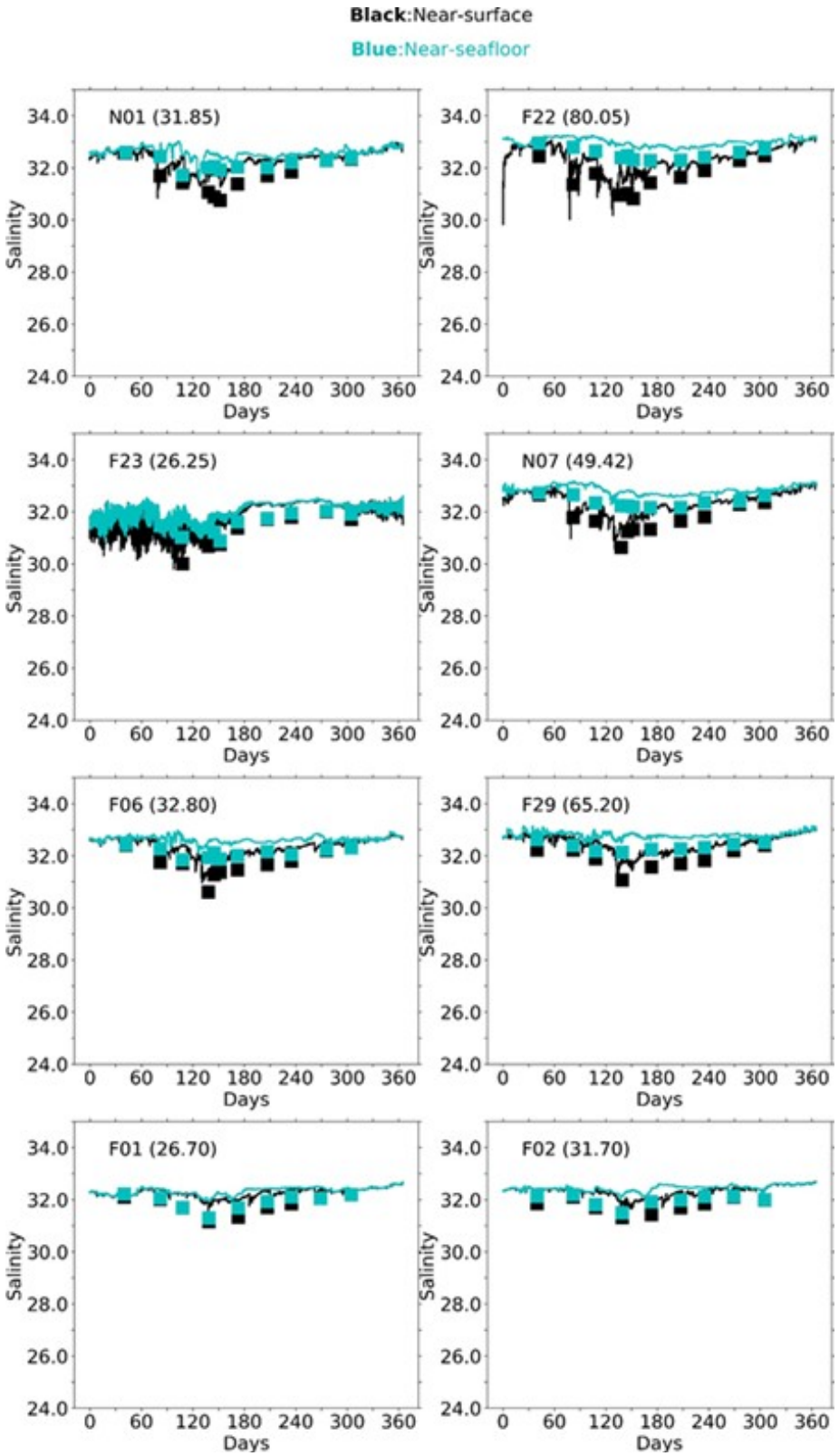

Figure 2-5 Salinity time-series, model-observation comparison for 2016 for the updated BEM. Model results: black/blue lines. MWRA observations: black/blue symbols.

2.2.2 MWRA observations: Spatial structure

The former and updated BEM skill in reproducing geographic patterns is presented in this section. Before describing these, it is important to clarify the methods used to create these plots and the differences therein between the former and updated BEM plots:

- Former BEM: Based on the explanations in Zhao et al (2017), figures for the former BEM were prepared as follows: Mean modeled fields were created by computing the mean of the modeled quantities at the MWRA observation locations at those times at which observations where available for each month, which vary between stations and depths. Some locations have one value per month, some two, some none. With those modeled and observed monthly mean point-values, fields were generated through interpolation between the dots and extrapolation to cover the remaining areas, producing separate fields for observations and model. Note this extrapolation potentially generates unrealistic values outside the area covered by the observation locations.
- Updated BEM: Mean modeled fields are the result of the monthly mean modeled quantities, using model results at every computational time-step, at each grid cell. These fields are therefore the same as the monthly fields shown in Section 2.3 below, with a slightly different color scale. The observations are plotted in this case on top of these monthly mean modeled fields, as colored dots. These observed values are the arithmetic mean of the available observations for each location and month. One can therefore expect a certain mismatch between model and observations. It is noted that temperature and salinity can vary significantly within one month, and the model results in these plots are the average across all model time-steps, whereas most observed mean values are computed using a single or at most two points per month.

2.2.2.1 Surface temperature

Figure 2-6 shows the monthly surface temperature spatial fields against observations for the former BEM. While the general seasonal pattern is captured, the former BEM shows a mismatch with the observed surface fields for February, June and October. For February and April, the model shows lack of spatial variability present in the observations; for October, the fields show completely different values throughout the model area. In general, the former BEM shows overpredicted surface temperatures and a lack of spatial variability, which was pointed out also by Zhao et al. (2017).

Figure 2-7 shows the same comparison for the updated BEM, with the observed values plotted as dots on top of the modeled fields. The updated BEM accurately represents the observed seasonal surface temperature variation and shows a good agreement with observations for every month and at all locations. (It is worth noting that the observed values for October that have been used in this report, which for an unknown reason are not the same as those presented in Zhao et al. (2017), better match both the updated and former BEM modeled fields.)

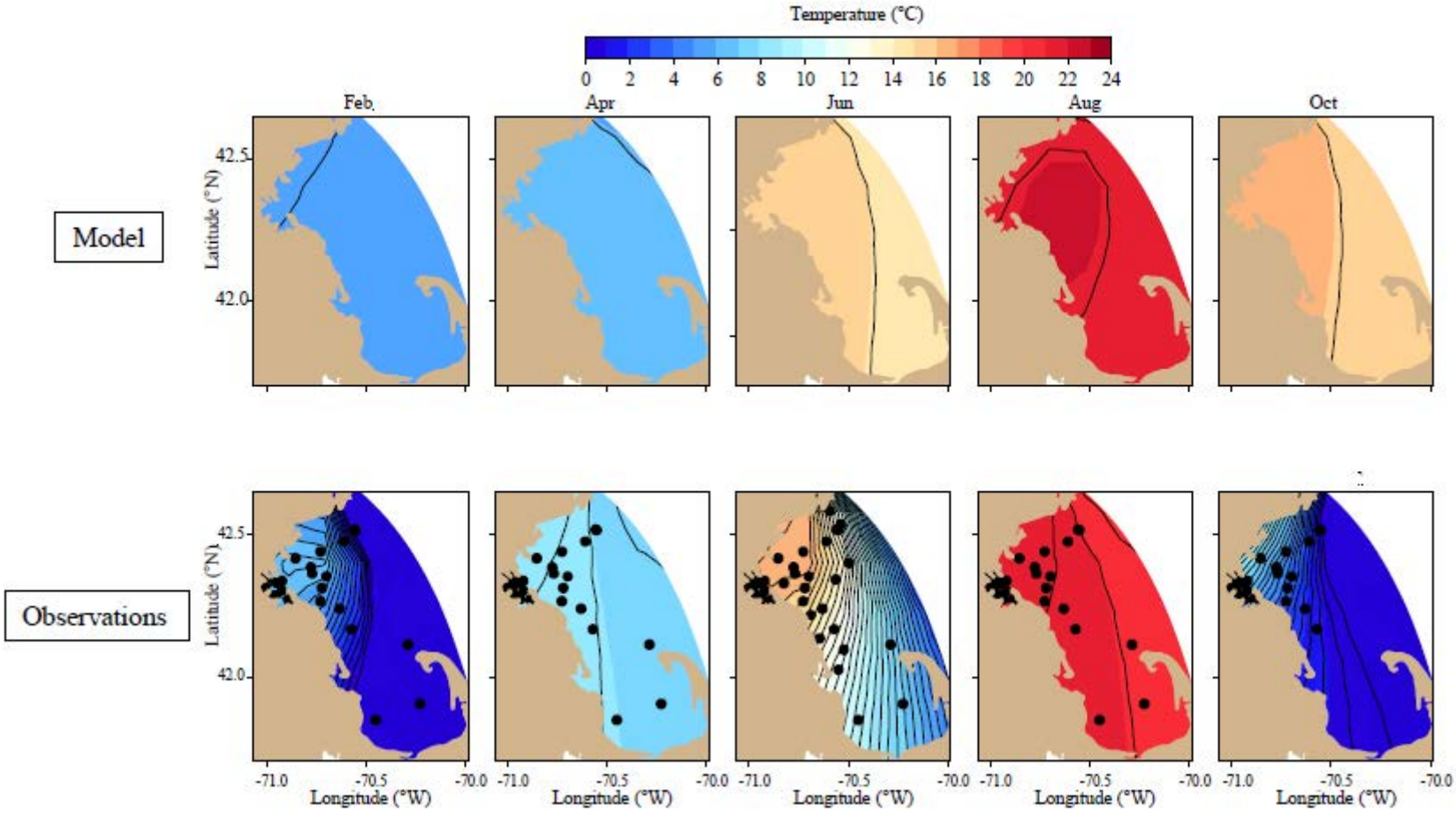

Figure 2-6 Temperature spatial structure, at/near sea surface, model-observation comparison for 2016 for former BEM (Zhao et al. 2017, Figure 4-3a). Contours in the "Observations" plots are based on the observations at discrete sample locations shown by black dots.

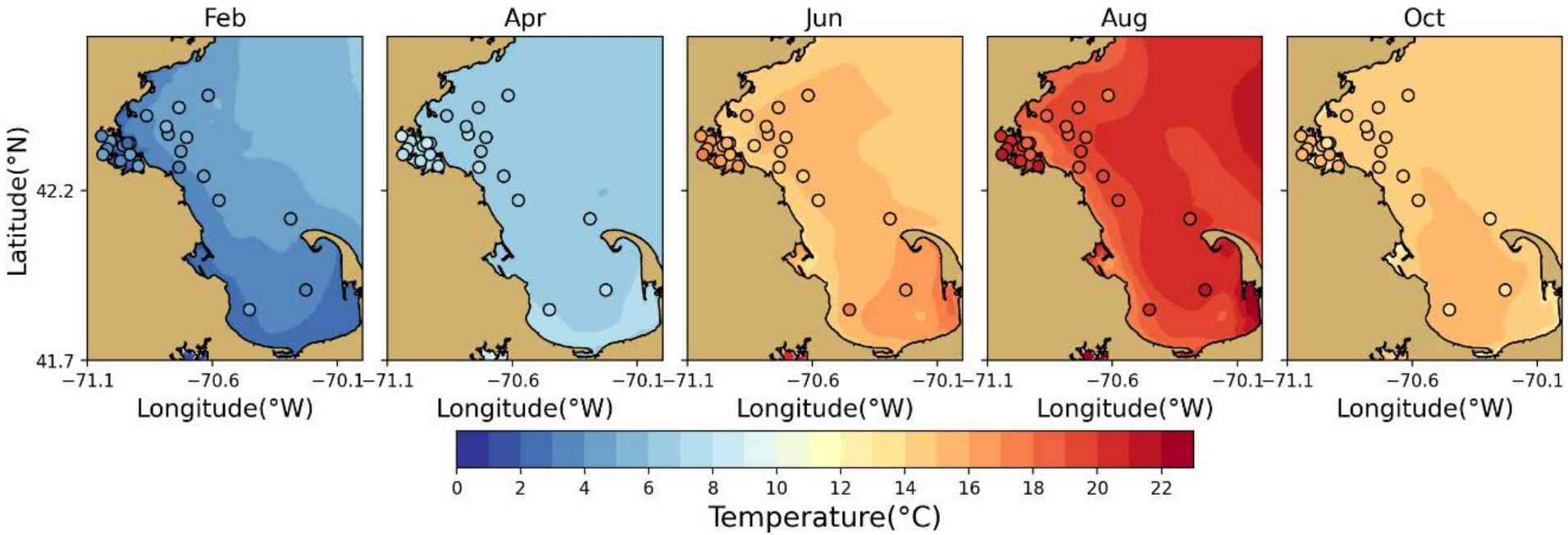

Figure 2-7 Temperature spatial structure, at/near sea surface, model-observation comparison for 2016 for updated BEM.

2.2.2.2 Bottom temperature

Figure 2-8 and Figure 2-9 presents the temperature comparison for the former BEM at the seafloor. While a good match is shown for August and October, the former BEM overpredicts seafloor temperatures in February and June. In April, in particular, there is a lack of spatial variability and an underprediction in the north-western part of the model domain. The updated BEM shows excellent agreement with observations in all months and locations, clearly capturing the spatial variability observed in June, August and October.

It is noted that the spatial fields for the updated BEM show stronger spatial variability than the former BEM. The contour plots of observations from Zhao et al. 2017 necessarily include interpolation and extrapolation outside the measurement locations. As an example, the spatial field of the updated BEM in October shows agreement with the observed cooler temperatures (pale blue) at the entrance of Massachusetts Bay (station F22) while neither observation-fields nor modeled fields of the former BEM showed this pattern at this location. It is also noteworthy that warm, summer seafloor temperatures in Boston Harbor, which are present in both observations and modeled fields for the updated BEM, were not present in the plots for the former BEM. The cause of this was not reported by Zhao et al. 2017.

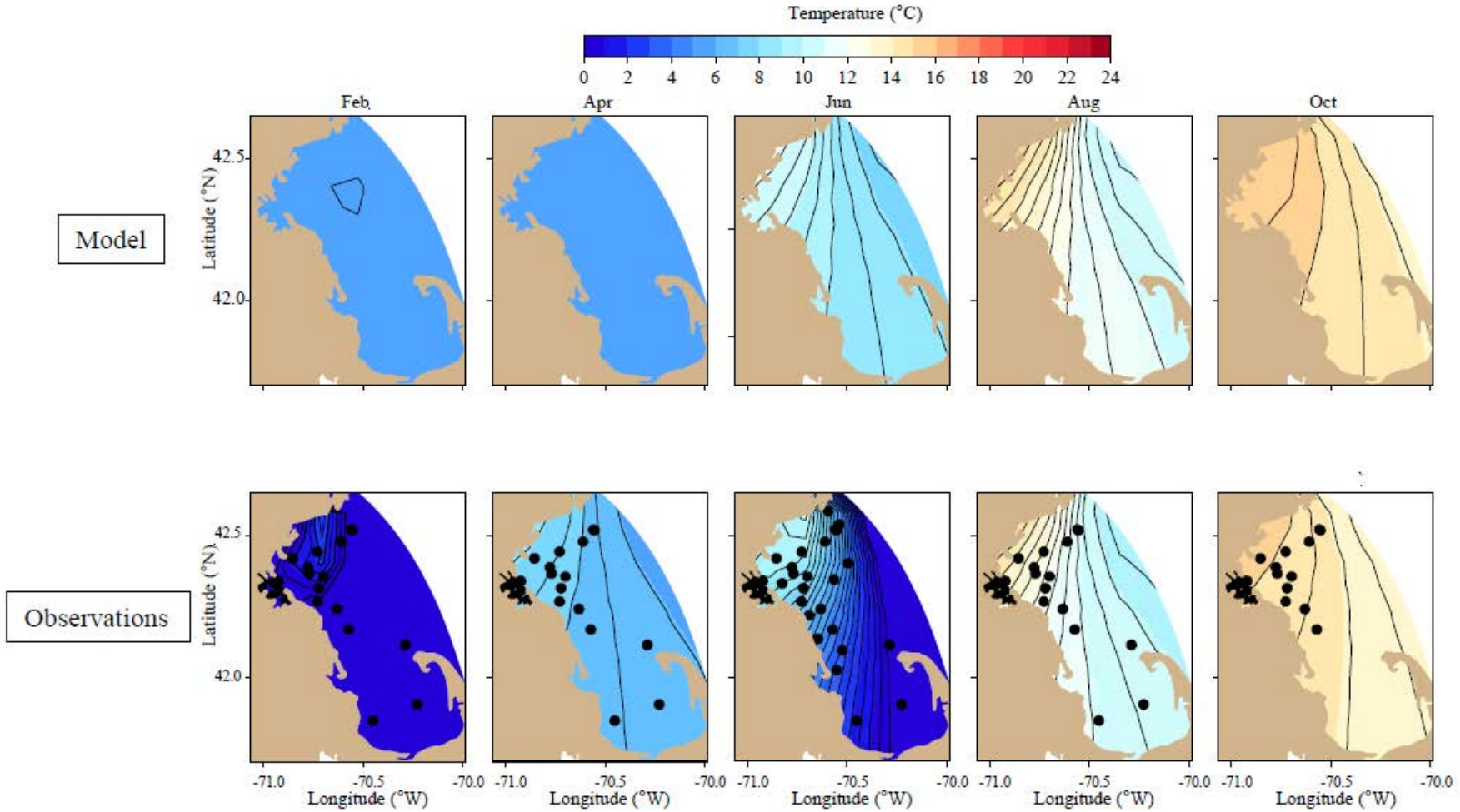

Figure 2-8 Temperature spatial structure, at/near seafloor, model-observation comparison for 2016 for former BEM (Zhao et al. 2017, Figure 4-3b).

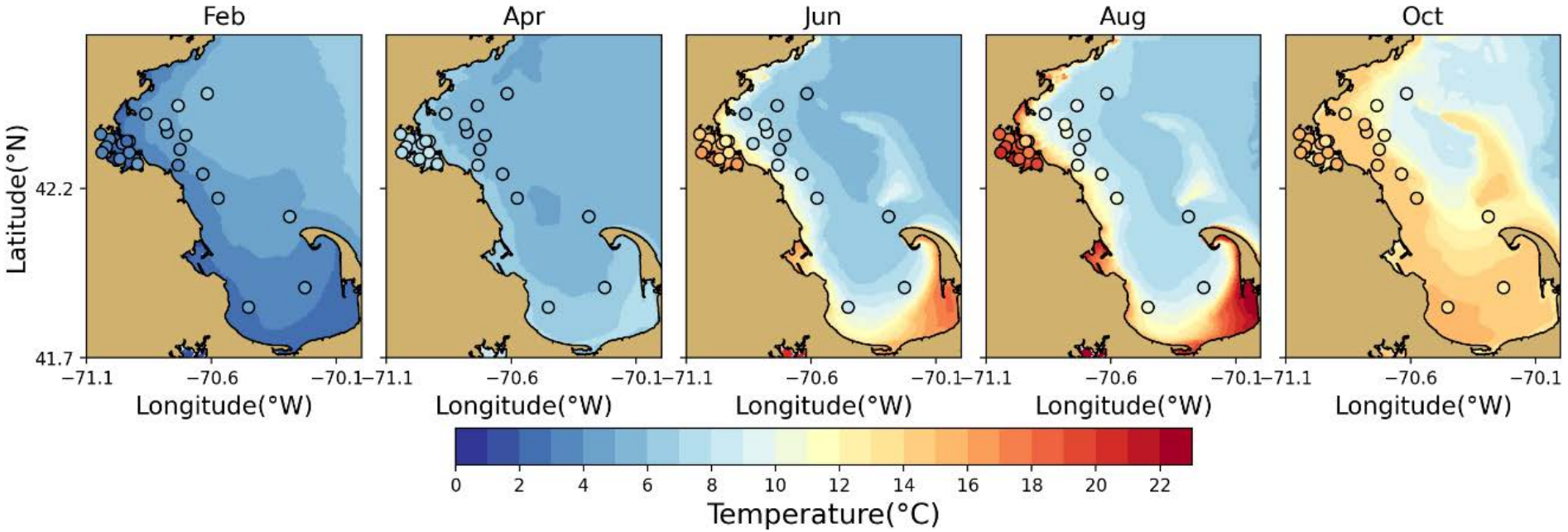

Figure 2-9 Temperature spatial structure, at/near seafloor, model-observation comparison for 2016 for updated BEM.

2.2.2.3 Surface salinity

Figure 2-10 and Figure 2-11 show the model-observation comparison of surface salinity fields for the former and updated BEM, respectively. For the former BEM, the agreement with observations was good. When using the same color scale, the updated BEM plots also show good agreement between model and observations, but the fields are more uniform and the values are generally higher, especially around Boston Harbor/ Massachusetts Bay, for which the former BEM shows values of 29-30 psu or lower.

It is noted that the former BEM plot for October is rather uniform, with values lower than 30 psu for both model and observations. When looking at the time-series plot for the former BEM (Figure 2-4), there is no evidence of such fresh water in any of the stations during October, and in general, salinity values only reduce to values around 30 psu very occasionally and for short durations, generally during the spring freshets. It is therefore not clear how these low salinity values were obtained for these plots. It is noteworthy that the surface salinity bias existing in the updated BEM of 0.1-0.3 psu on average is not evident in the Figure 2-11 for most months, which is likely due to the fact that the color scale employed uses steps of 1 psu and the error visually disappears for certain ranges. Although this color scale is useful for comparison between the former and the updated BEM, it is suggested that this is not suitable for distinguishing spatial and temporal patterns for surface salinities, as the spatial variability for this quantity is in general low throughout the year. In reports on simulations of 2017 and later, using the updated BEM, a different, more suitable color-scale will be used. Still, the fresher surface waters after the spring freshet season are evident in the plot for June.

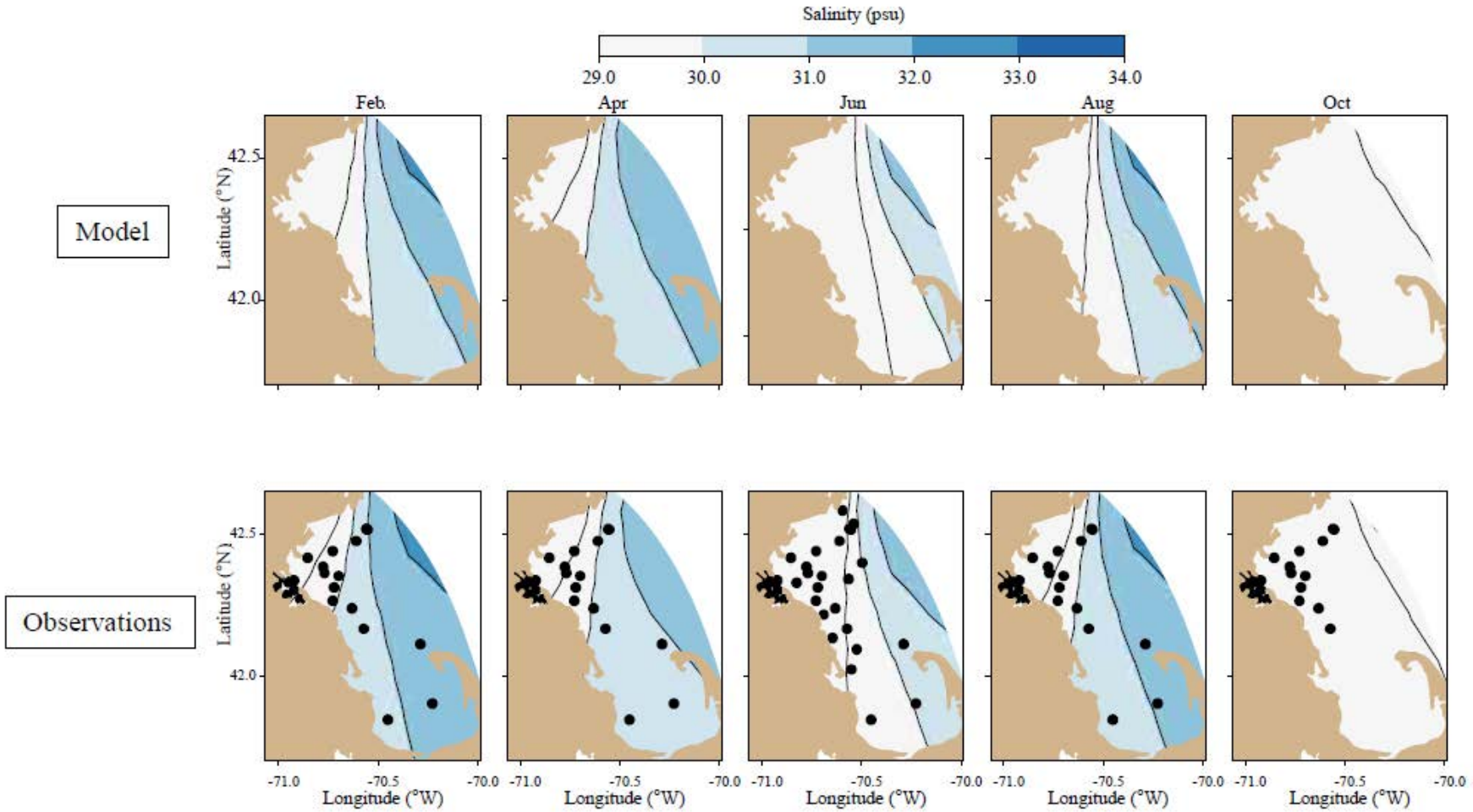

Figure 2-10 Salinity spatial structure, at/near sea surface, model-observation comparison for 2016 for former BEM (Zhao et al. 2017, Figure 4-4a).

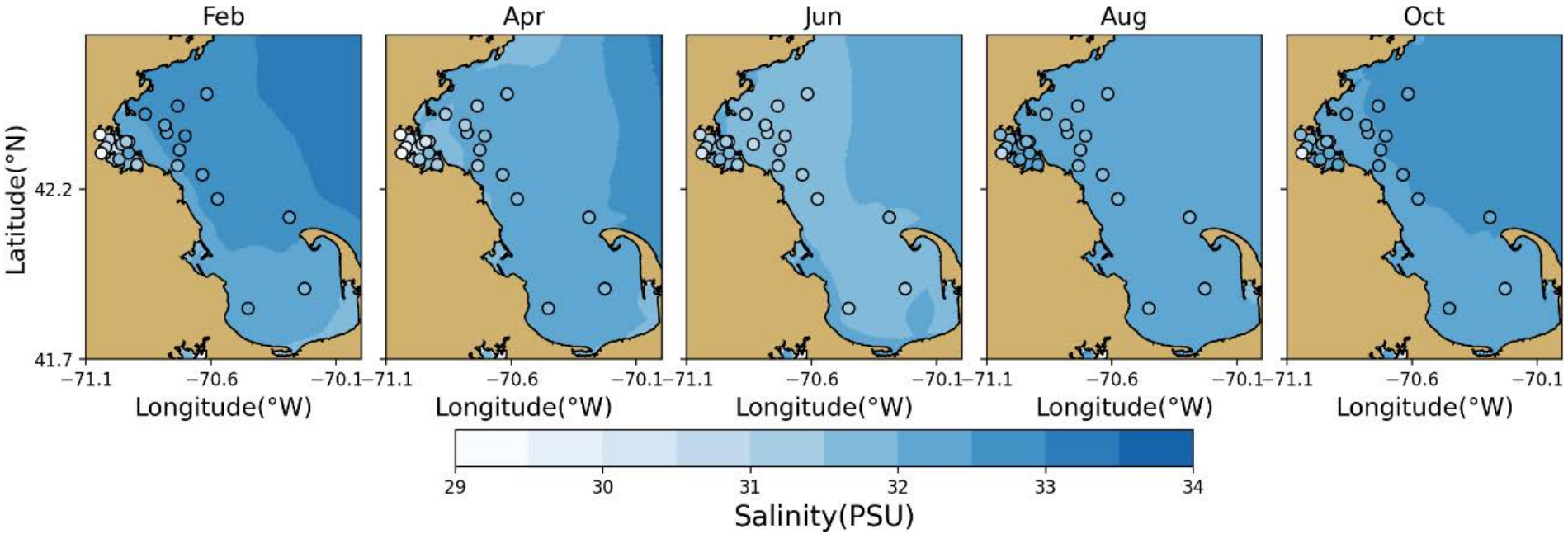

Figure 2-11 Salinity spatial structure, at/near sea surface, model-observation comparison for 2016 for updated BEM.

2.2.2.4 Bottom salinity

Figure 2-12 and Figure 2-13 show the spatial model-observation comparison for seafloor salinities, for the former and updated BEM, respectively. In this case, the former BEM shows overpredicted salinity values in April and underpredicted values around Boston Harbor and Massachusetts Bay in June and October. The updated BEM shows a good match with observations, although the salinity at stations toward the coast in Massachusetts Bay is somewhat underestimated in April and June, which is consistent with the time series results presented earlier. In general, observed and modeled bottom salinities are higher than for the surface in both models, which is as expected.

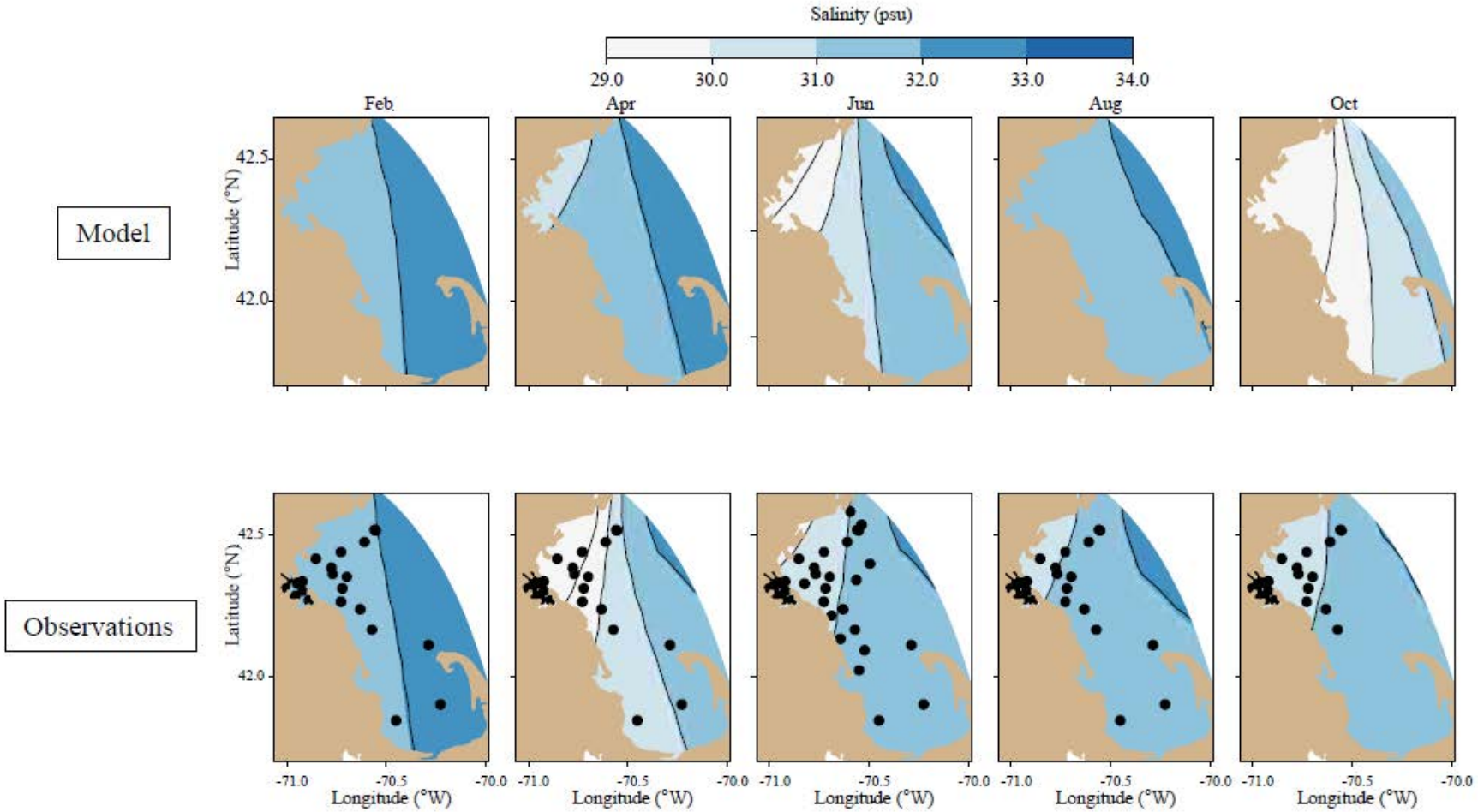

Figure 2-12 Salinity spatial structure, at/near seafloor, model-observation comparison for 2016 for former BEM (Zhao et al. 2017, Figure 4-4b).

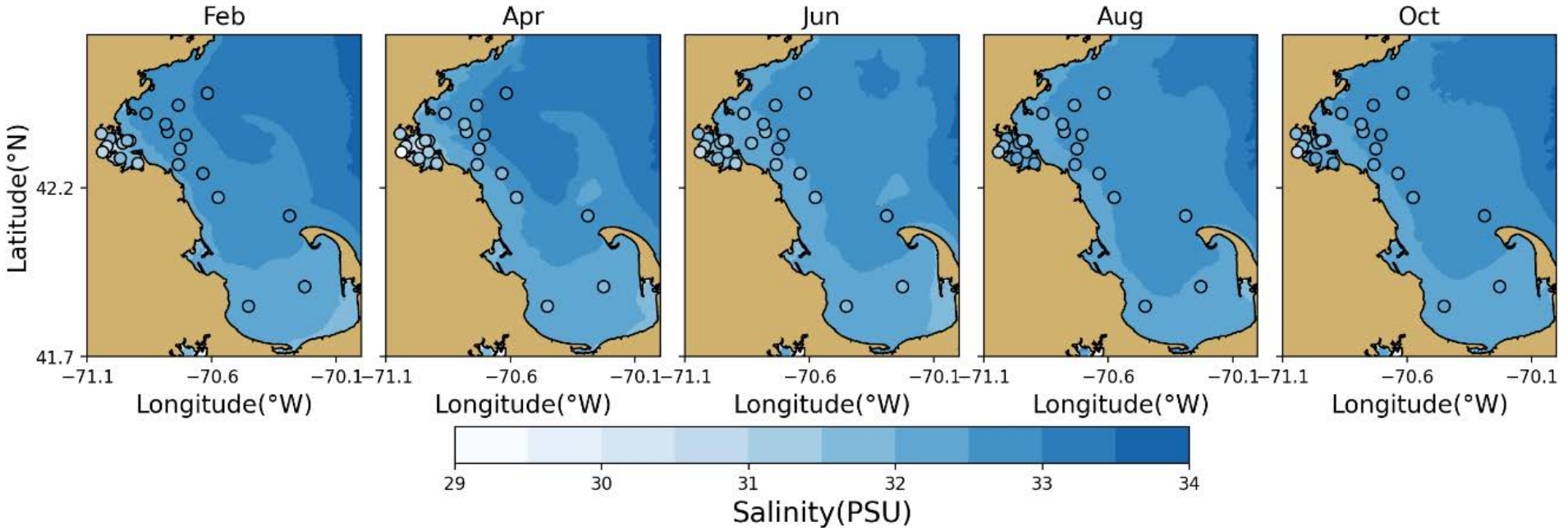

Figure 2-13 Salinity spatial structure, at/near seafloor, model-observation comparison for 2016 for updated BEM.

2.2.3 Mooring observations time series

2.2.3.1 Temperature and salinity

In this section, a set of plots is presented with model-observation comparisons for temperature and salinity time series at the mooring A01. This is the only location within the area of interest that provides a continuous, hourly record for both these quantities. Observations are available at 1m, 20m and 50m depths.

Figure 2-14 shows the *former* BEM results for temperature and salinity compared to mooring observations. Note that all the observation values presented in this plot (for both temperature and salinity, at all depths) are assimilated every 3 days in the former BEM, and therefore an excellent performance is expected. This is indeed the case for both temperature and salinity at all depths. The largest difference is observed at 50 m depth, where the former BEM model predicts slightly too warm temperatures and slightly too high salinities. The sign of the bias is consistent with results at the MWRA observation locations (see Figure 2-2 and Figure 2-4), but is of lower magnitude due to the benefits of assimilating these measurements.

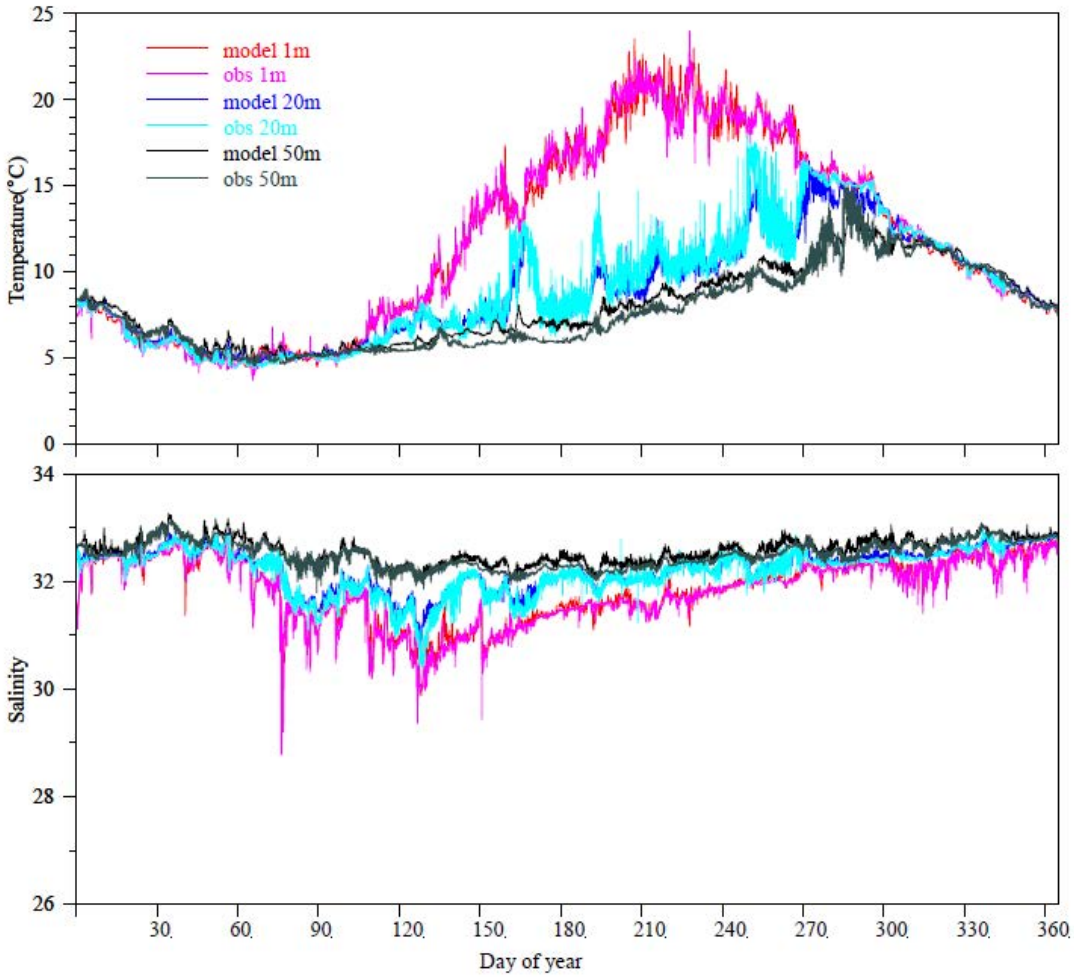

Figure 2-14 Former BEM model results compared to observed time series at Mooring A01 for 2016 for three depths:1m, 20m and 50m. Top: Temperature. Bottom: Salinity (psu) (Zhao et al.2017, Figure 4-5).

Figure 2-15 provides the same model-observation comparison for the updated BEM. For temperature, the model agreement with observations is very satisfactory and comparable to the former BEM. The updated BEM also shows the most noticeable error at the 50 m depth, in this case predicting slightly too cold temperatures. Overall, the model shows good skill in reproducing the vertical temperature structure, seasonal patterns as well as shorter episodes on weather-related time-scales. For salinity, the 0.1-0.3 psu bias present in the updated BEM throughout the water column is clearly evident in the plot.

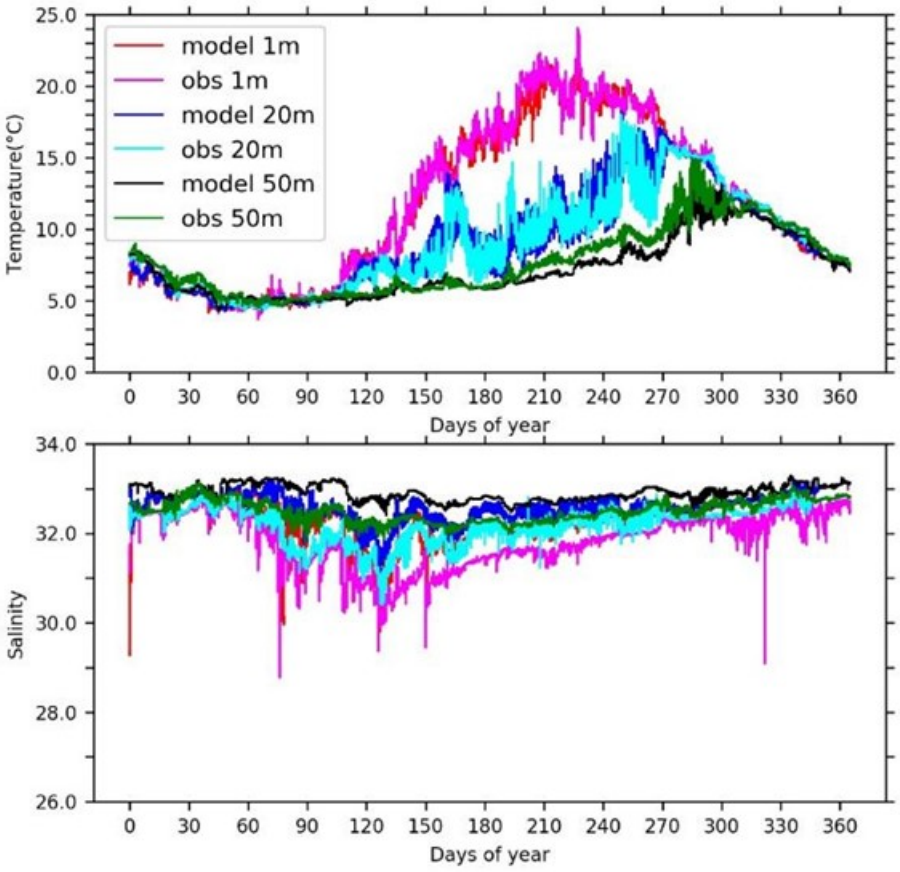

Figure 2-15 Updated BEM results compared to observed time series at Mooring A01 for 2016 for three depths:1m, 20m and 50m. Top: Temperature. Bottom: Salinity (psu).

However, when looking at stratification (Figure 2-16), the agreement with observations is quite satisfactory. Due to the local effects of data assimilation, it appears that the former BEM performs better for salinity at this location. However, the spatial plots presented previously illustrate that data assimilation, while effective locally, does not propagate all its benefits to those areas (and time-periods) that purely rely on the model physics to compute salinity and temperature. This is evident as the former BEM shows a non-uniform model skill in time and throughout the Massachusetts and Cape Cod Bays.

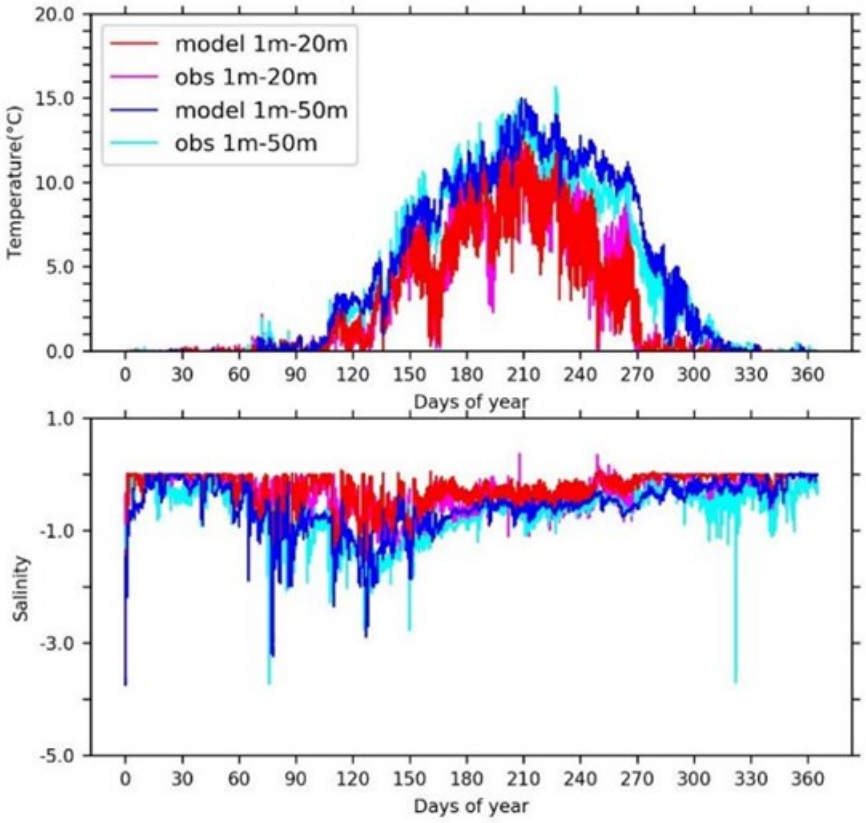

Figure 2-16 Updated BEM model results compared against observed time series at Mooring A01 for 2016 for 1 to 20 meter and 1 to 50-meter stratification. Top: Temperature. Bottom: Salinity (psu)

2.2.3.2 Non-tidal currents

In this section, the comparison of non-tidal currents at mooring A01 is presented. Specifically, the non-tidal currents at 2 m,10 m, 22 m and 50 m depth are evaluated. In the updated BEM, the non-tidal currents have been derived using a PL33 low-pass filter, as described in Alessi et al., (1985). As explained in Appendix B of this report (Multi-year calibration), this filter seems somewhat different to the PL66TN filter mentioned in Zhao et al. (2017), but leads to visually identical observed residual currents, and is therefore deemed suitable.

The plots are produced for the first and second half of 2016 in order to provide higher detail of the current patterns. *Figure 2-17* and Figure 2-18 show the model-observations comparison for the former BEM. For context, the local wind at mooring A01 has also been included in the figure and filtered using the same method as the model results (i.e. the PL66TN filter). As described in Zhao et al. (2017), the winds at this location show highly variable directions, spanning the full compass range, with weather-band variations every 3-10 days. The weaker, long-term (monthly mean) average winds are directed eastward year-round. There are alternating southward/northward components in winter/summer. Summer winds are generally weaker.

From observations, the currents at A01 are generally directed toward the southwest, into Massachusetts Bay. Some high-current episodes seem to be correlated with the local wind (e.g. the episode in first half of February), however there does not seem to be a general correlation between wind and current direction. It is noteworthy that the strong current episode around the beginning of June is thought to be related to strong river discharges, which enhance the Western Maine Coastal Current (WMCC). As described in Appendix B of this report (Multi-year calibration), the former BEM showed a general overprediction of higher magnitudes (see the June episode, for example) and a tendency for 50-meter deep currents to have a notable northward component not visible in observations. In general, the former BEM was able to capture the general flow patterns, including individual storm events.

Figure 2-19 and Figure 2-20 show the same comparison for the updated BEM. In these plots, instead of the observed wind from A01, the modeled wind at the A01 location is plotted in the top panel. This is the wind derived from a meteorological model. This same model (ECWMF ERA5) is also the source of the wind fields used for the updated BEM forcing, see Appendix A. By showing the modeled winds, it is possible to compare the modeled wind in the updated BEM to observations (shown in Figure 2-17 and Figure 2-18). Visually, the modeled wind compares well to the observed wind in both magnitudes and direction. Therefore, the wind can be discarded as a possible source for model-observation differences that might be visible in the comparison of the currents.

The updated BEM shows comparable skill to the former BEM in reproducing mean flow directions as well as low and high (storms) frequency current variations. While the former BEM showed a general overprediction of current magnitudes, the updated BEM shows a general underprediction of magnitudes only at the surface. Moreover, the updated BEM does not show the notable northward current component at deep levels that was shown by the former BEM, and which was not detected in observations. At deeper locations (22m and 50m), the agreement with observations is seen to be in general better for the updated BEM, both in magnitude and direction. The updated BEM shows very good skill in reproducing in magnitude and direction certain episodes of strong and variable currents, such as the one mentioned in June (days 150 to 165 in the plots), for all depths. As Zhao et al. (2017) mentions, the detailed velocity evaluation performed through these plots forms a challenging test for the hydrodynamic model. In this regard, the new and the former BEM show comparable skill and overall satisfactory skill in the reproduction of observed currents.

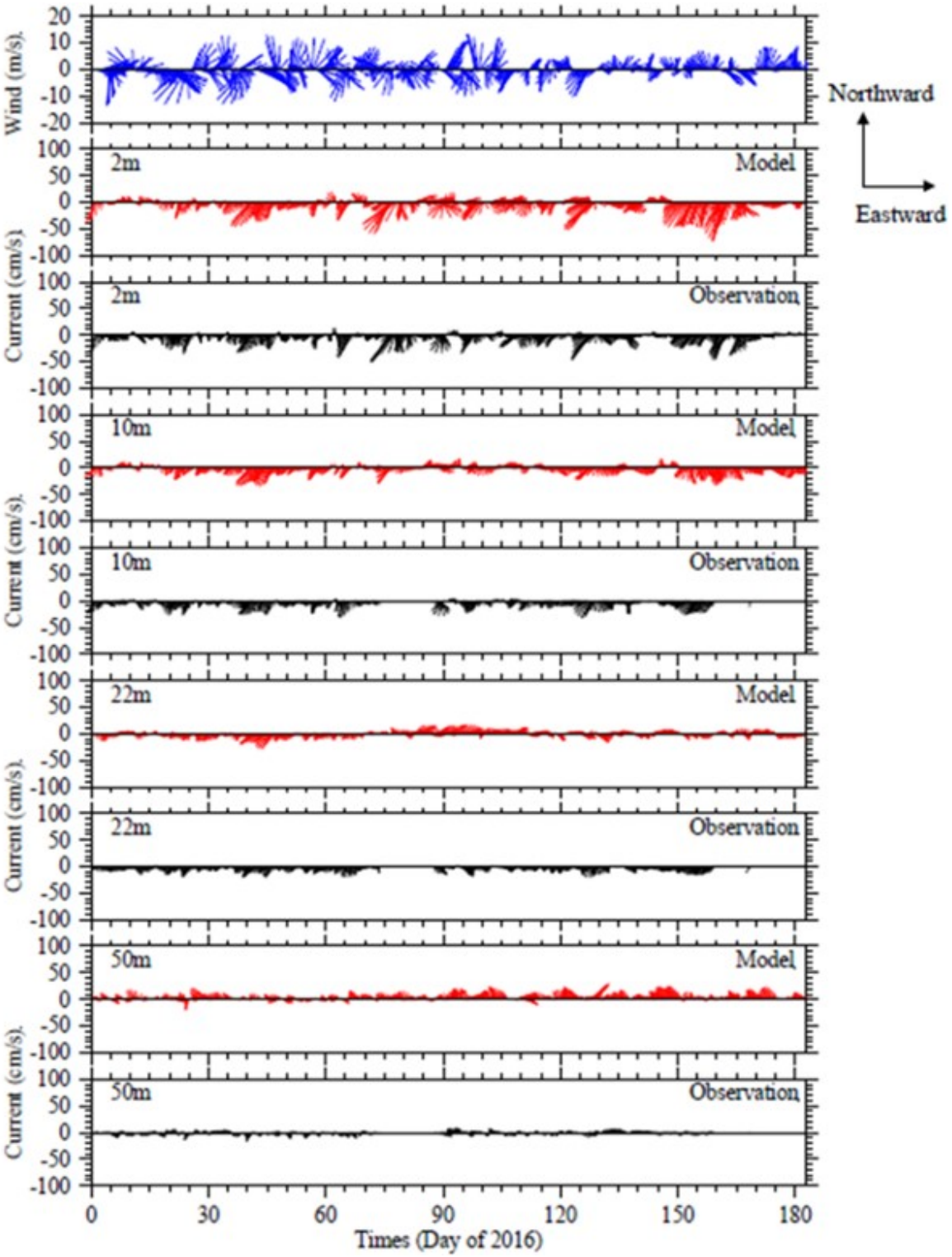

Figure 2-17 Former BEM modeled against observed current time-series, for 2016 Jan-Jun. Sticks point in the direction of flow, away from zero line: north/eastward flow up/rightward (Zhao et al. 2017, Figure 4-6a).

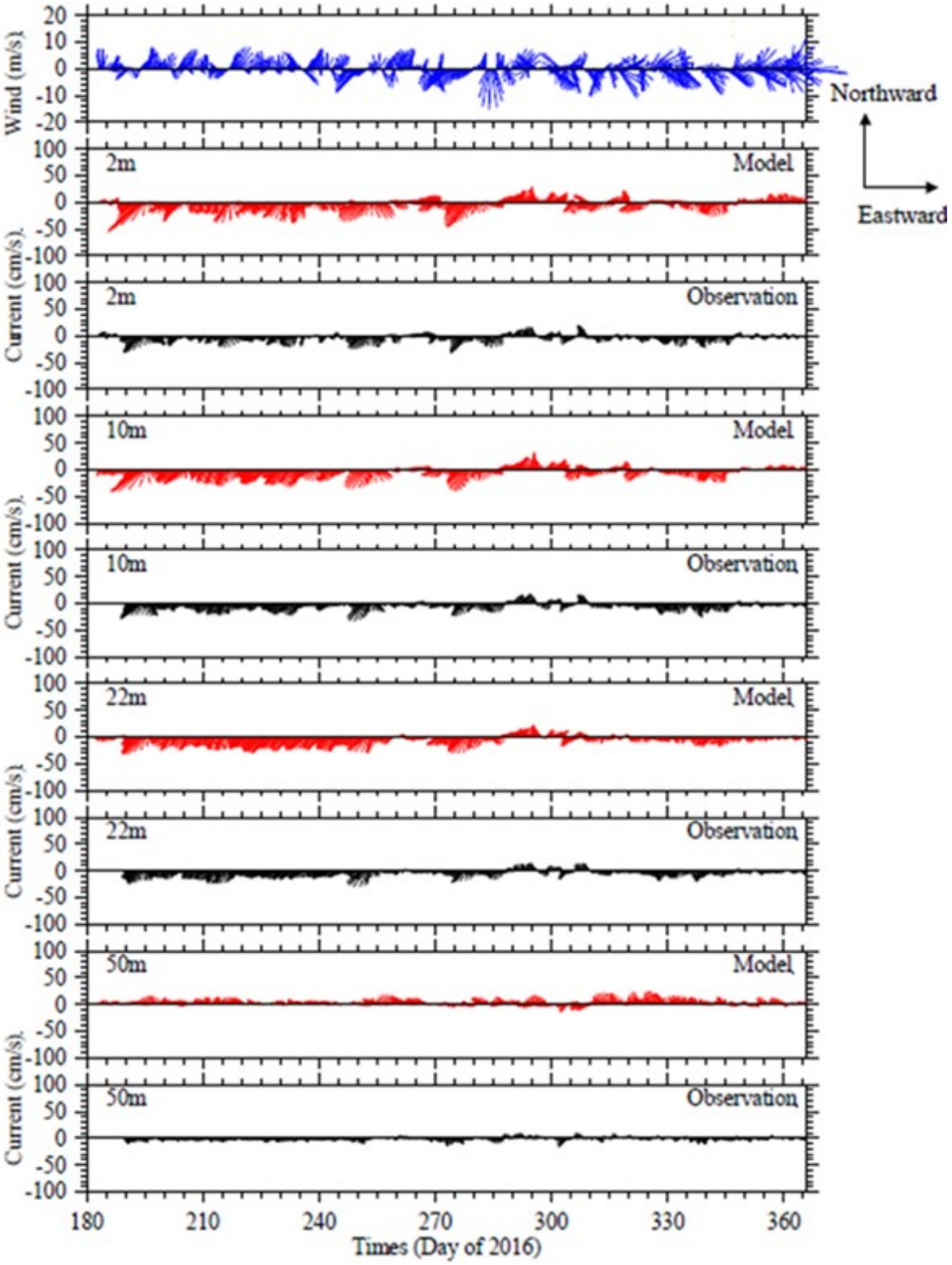

Figure 2-18 Former BEM modeled against observed current time-series, for 2016 Jul-Dec. Sticks point in the direction of flow, away from zero line: north/eastward flow up/rightward (Zhao et al. 2017, Figure 4-6b).

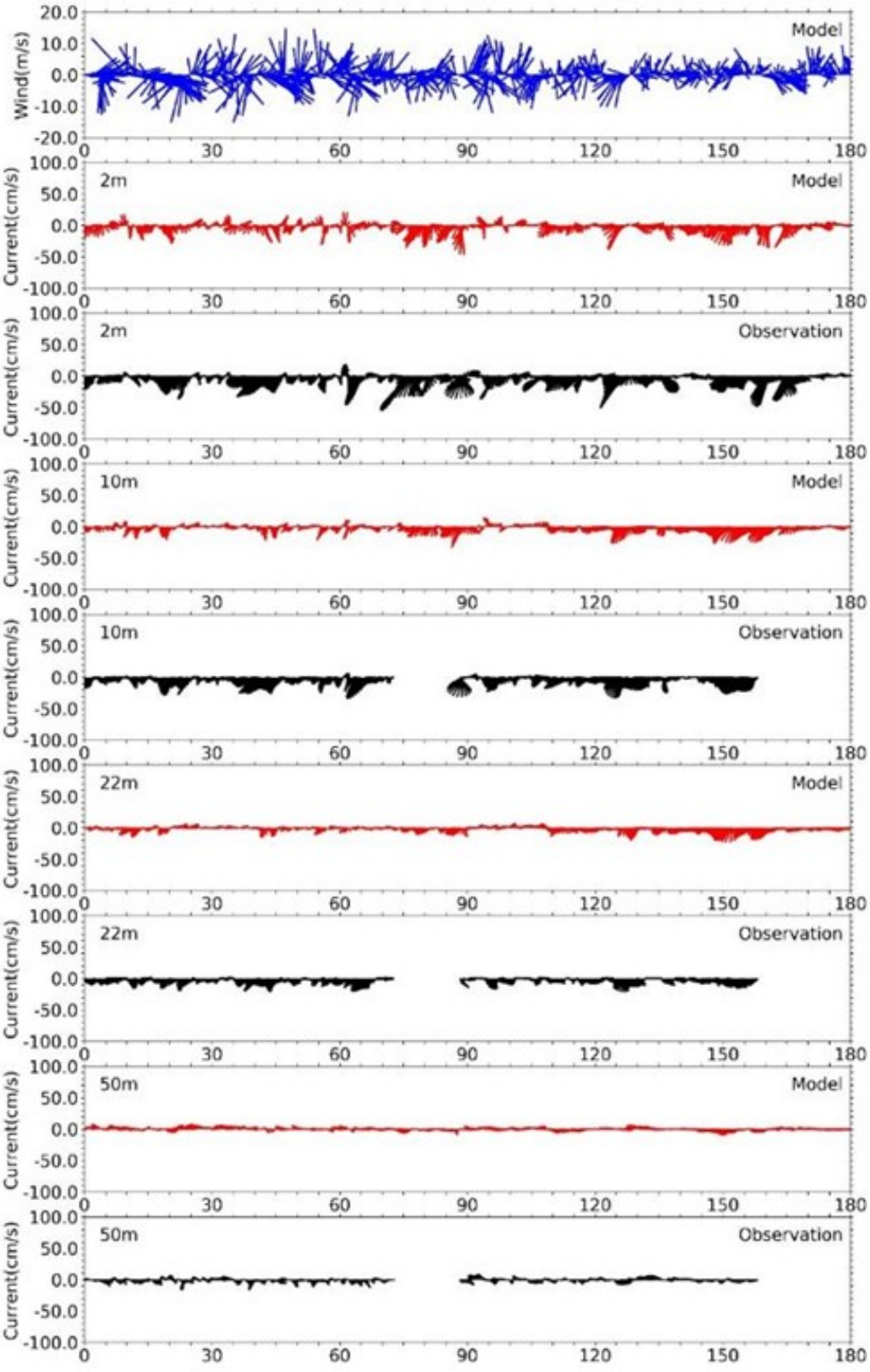

Figure 2-19 Updated BEM modeled against observed current time-series, for 2016 Jan-Jun. Sticks point in the direction of flow, away from zero line: north/eastward flow up/rightward.

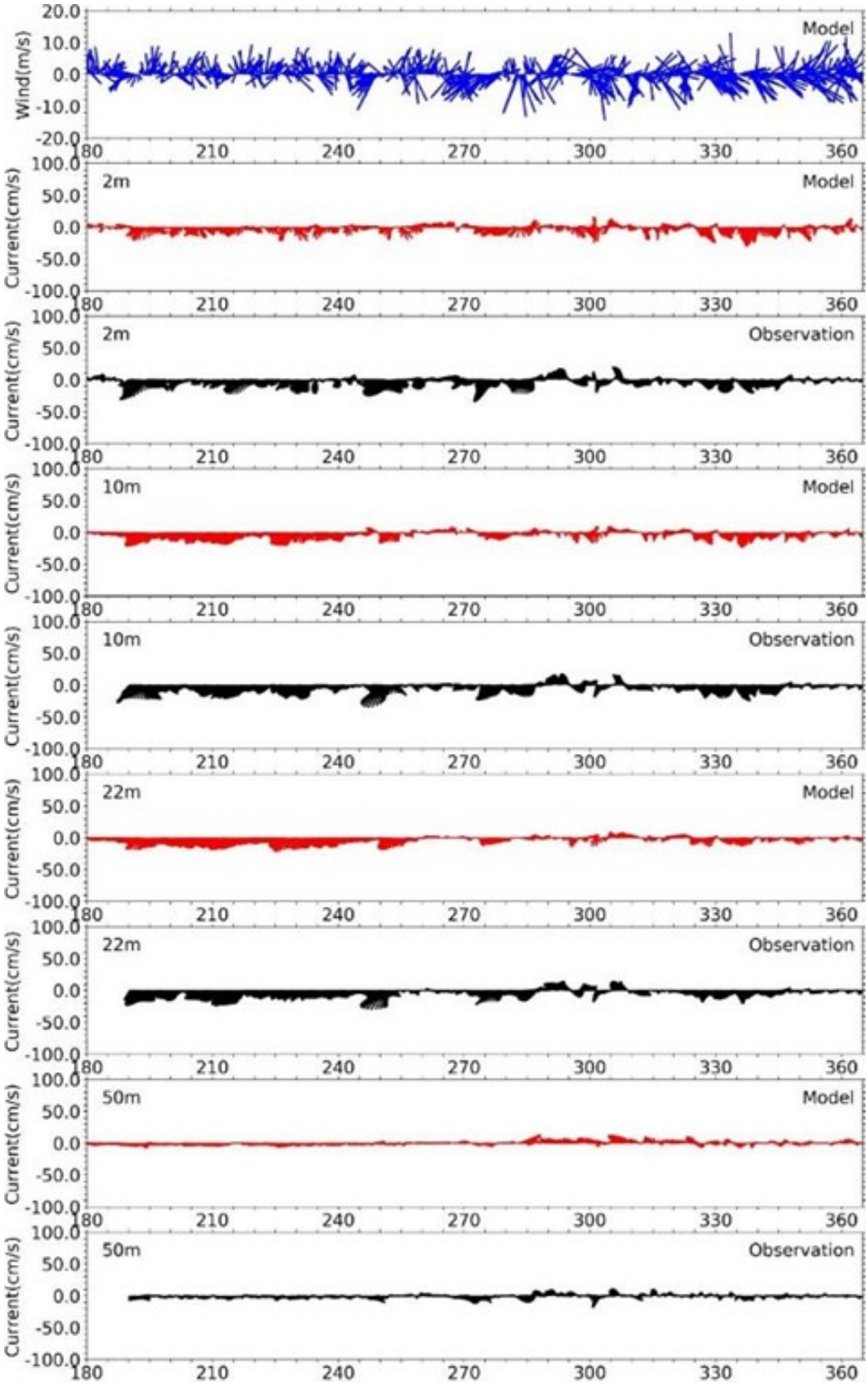

Figure 2-20 Updated BEM modeled against observed current time-series, for 2016 Jul-Dec. Sticks point in the direction of flow, away from zero line: north/eastward flow up/rightward.

2.3 Model monthly-mean temperature, salinity and circulation

In this section, the former BEM and the updated BEM are compared by looking at monthly mean spatial fields for the whole year, for both surface and near-seafloor depths. The modeled results for temperature, salinity and residual currents (circulation) are presented. There are no observation data in these plots and the focus is purely on how the models compare to each other with respect to spatial patterns and seasonal variation.

2.3.1 Temperature

Figure 2-21 and Figure 2-22 show the monthly-mean surface temperature fields for the former and updated BEM, respectively. For the former BEM, it is noted that some of these fields show significantly different values and spatial patterns than the ones presented when validating against point data (Figure 2-6), which is expected due to the different methods used for the two plots, as explained by Zhao et al (2017). From the temperature monthly-mean plots below, the former and updated BEM show very comparable seasonal behavior at the surface, with maximum temperatures in August and lowest values in February, and comparable warming and cooling periods. Spatially, the updated BEM generally shows more variability. The large temperature gradients in the former BEM near the open boundaries, most prominent in July to September, are an exception to this. These large gradients might be related to surface and lateral boundary forcing in the former BEM. In winter, the updated BEM predicts cooler temperatures along the coast, especially at the shallowest areas such as Boston Harbor. In the summer, the updated BEM predicts a stable coastal band that is slightly cooler than the surrounding waters within the bay, and which persists throughout the summer period (July, August, September). This is not visible in the former BEM.

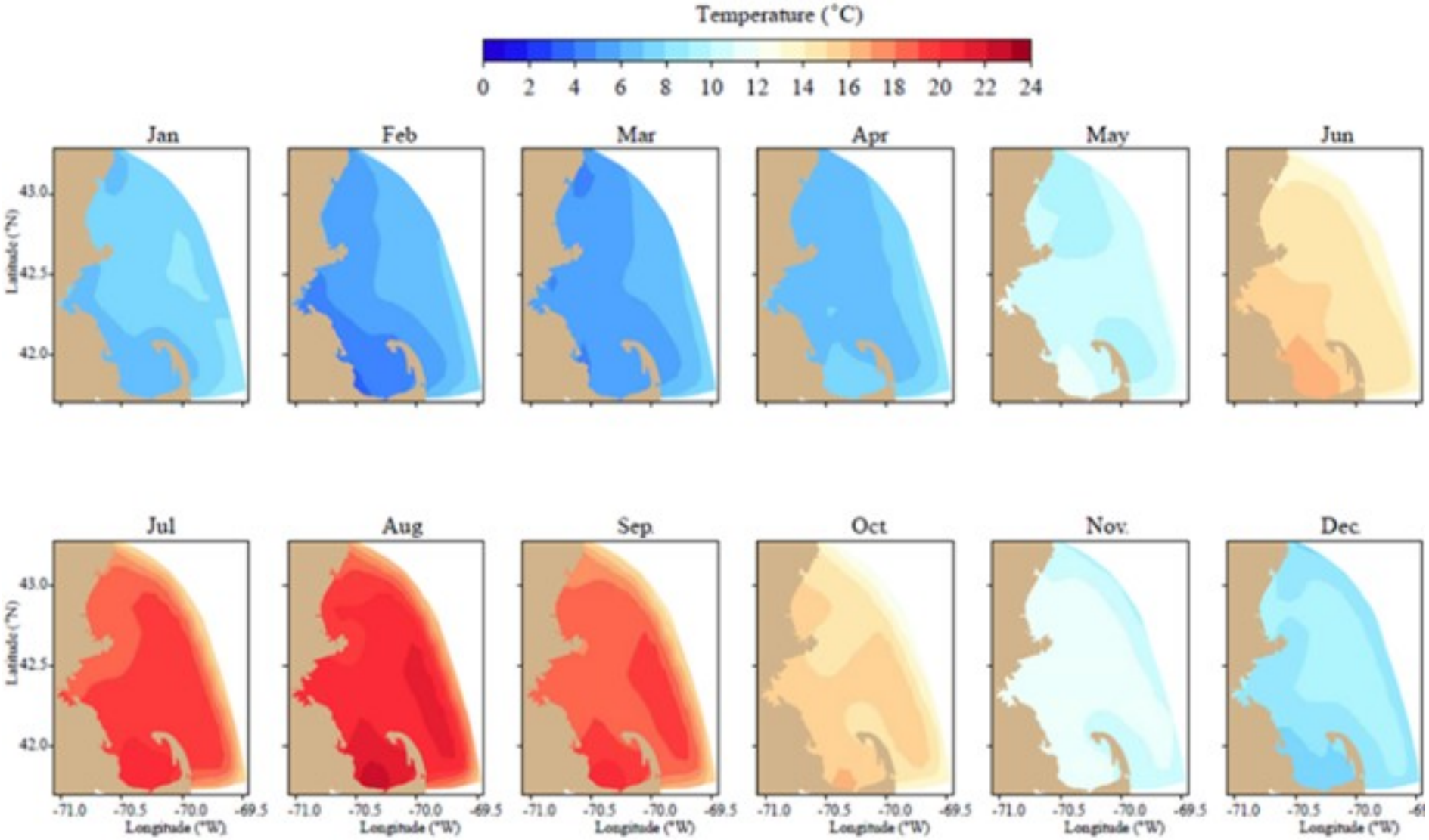

Figure 2-21 Former BEM model monthly mean temperature at sea surface for 2016 (Zhao et al. 2017, Figure 4-7a).

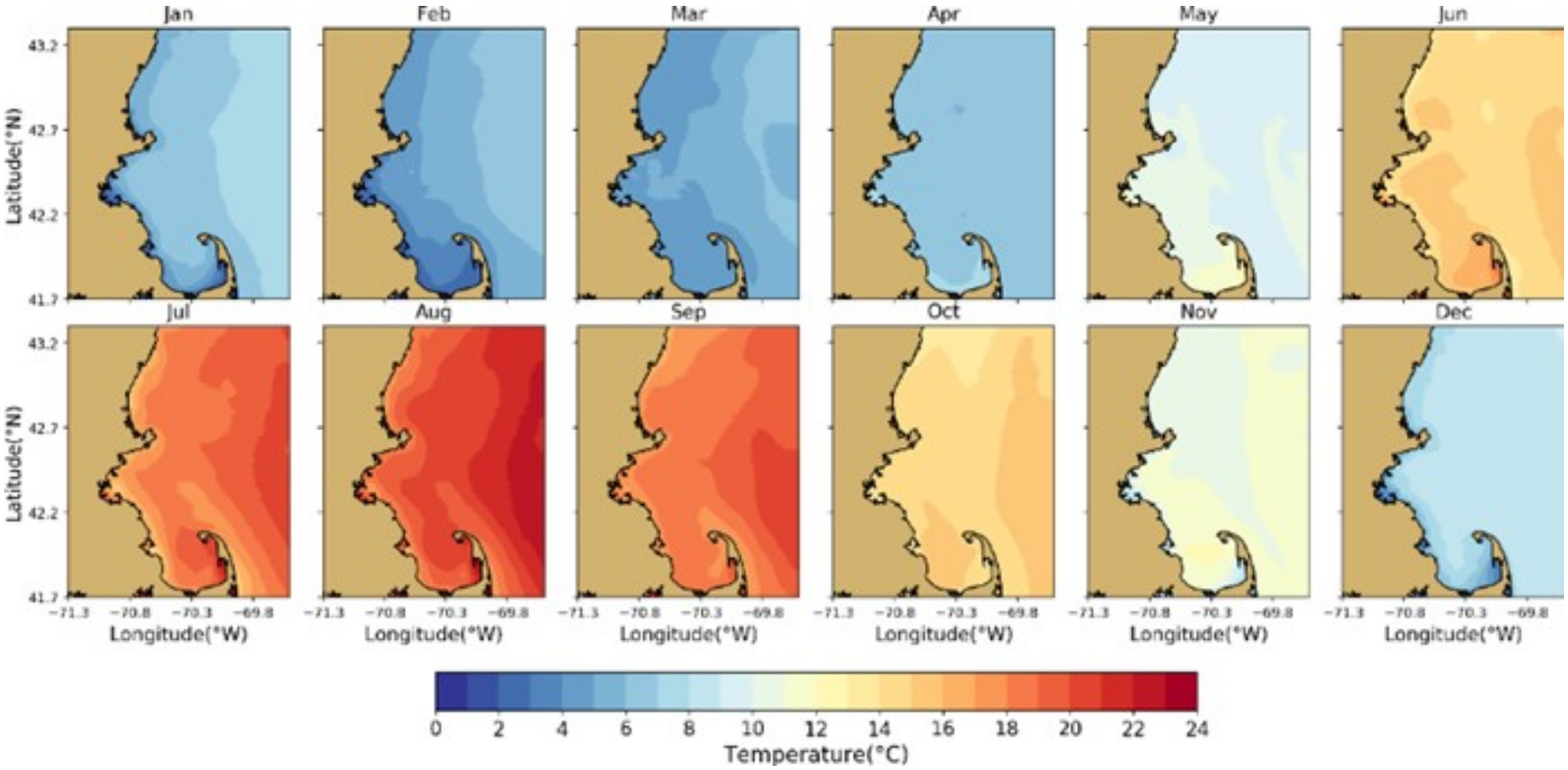

Figure 2-22 Updated BEM model monthly mean temperature at sea surface for 2016.

For seafloor temperatures (Figure 2-23 and Figure 2-24 for former and updated BEM, respectively), both models show comparable seasonal and spatial structures, with coastal seafloor temperatures at their minimum in February and highest in August, and surrounding waters in the Bay showing warmest temperatures in October. It is noteworthy that in the updated BEM, the presence of Stellwagen Bank is visible, showing warmer seafloor temperatures than its deeper surroundings. Additionally, the former BEM results are smoother at the bottom, while more detailed spatial structure is visible in the updated BEM results.

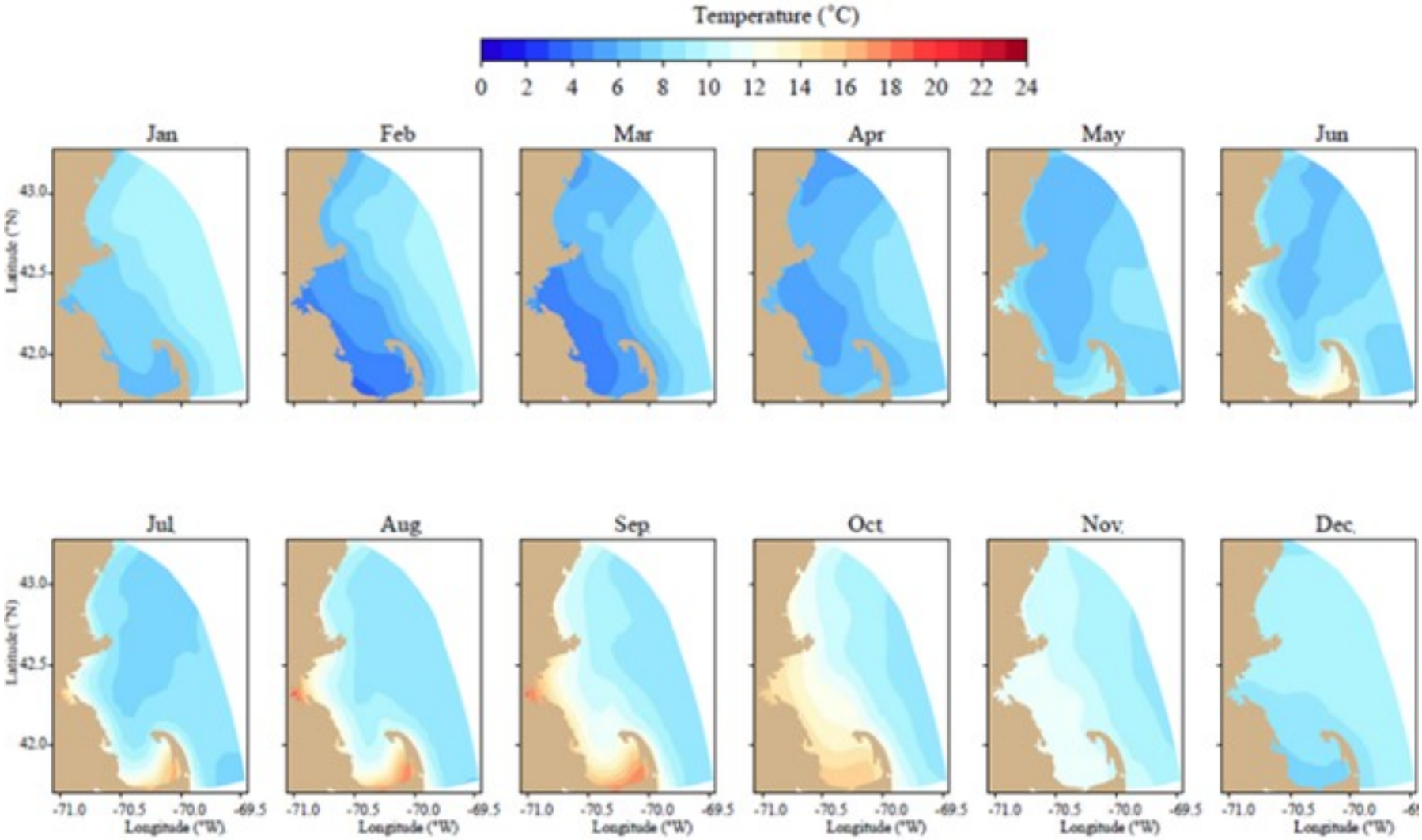

Figure 2-23 Former BEM model monthly mean temperature at seafloor for 2016 (Zhao et al. 2017, Figure 4-7b).

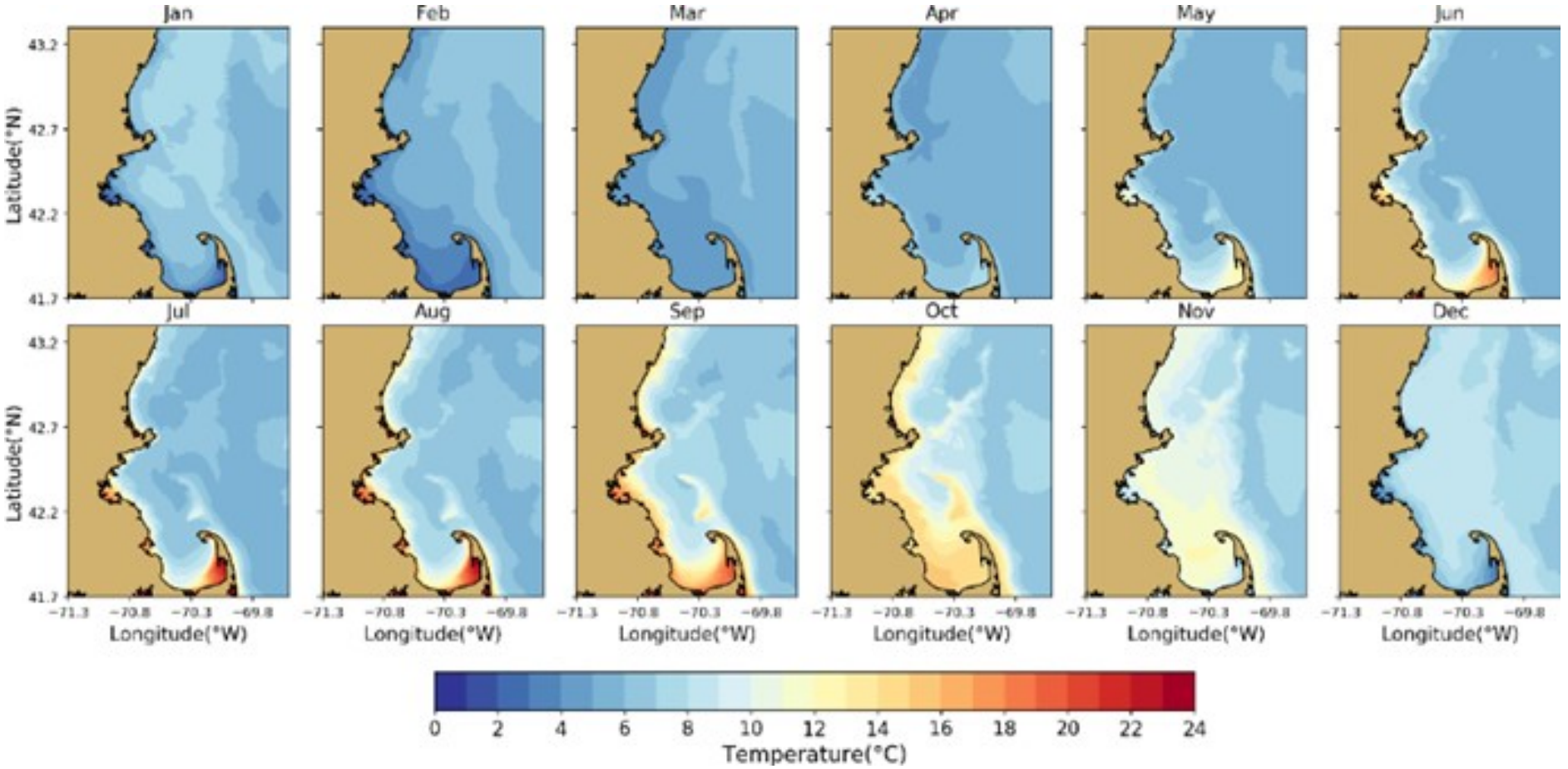

Figure 2-24 Updated BEM model monthly mean temperature at seafloor for 2016.

2.3.2 Salinity

Figure 2-25 and Figure 2-26 show the modeled monthly-mean fields for surface salinity for the former and updated BEM, respectively. As for temperature, due to the different methods (as explained in Zhao et al. 2017) the former BEM plots (Figure 2-25) are different than the corresponding spatial plots that were used for comparisons with observations (Figure 2-10) which showed fresher waters in Massachusetts Bay in comparison to values given in the plots below. In Figure 2-26, the river plume of the Merrimack and Piscataqua rivers (the latter defined as the sum of Exeter, Winnicut, Lamprey, Isinglass and ungauged Piscataqua discharges) is evident year-round and widest from May to August. The presence of rivers in the Boston Harbor is also evident from the former BEM surface salinity plots, showing salinity values < 29 psu persistent throughout the year.

Regarding seasonality, surface salinities show decreasing salinities from April until June and increasing again until September. Given the small seasonal variability in surface salinities and the chosen color scale limits and step, relatively uniform fields are obtained. When using the same color scale for the updated BEM, the resulting surface fields appear even more uniform.

Additionally, the freshwater plumes near rivers seem in general less evident in the updated BEM. For the Piscataqua River, the river plume predicted by the former BEM seems at least as prominent as the river plume due to the Merrimack River. Furthermore, the rivers within Massachusetts Bay and Cape Cod Bay are significant enough to result in salinity values in their discharge bays (Boston Harbor and Plymouth Bay) below 29 psu. In the updated BEM, only the Merrimack plume is identifiable in the plots, and within the Bay the Boston Harbor rivers are somewhat visible only during winter and spring.

Similar to the surface temperature plots, some boundary effects are visible in the former BEM salinity plots. In this case, the freshwater plume attached to the southern Gulf of Maine abruptly stops in the vicinity of the boundary. This means the boundary conditions at the coastal section of the open boundary in the former BEM did not predict these fresh waters. Despite the lack of fresh water coming from the open boundaries, the former BEM has a more pronounced presence of fresh water near the Merrimack and Piscataqua rivers.

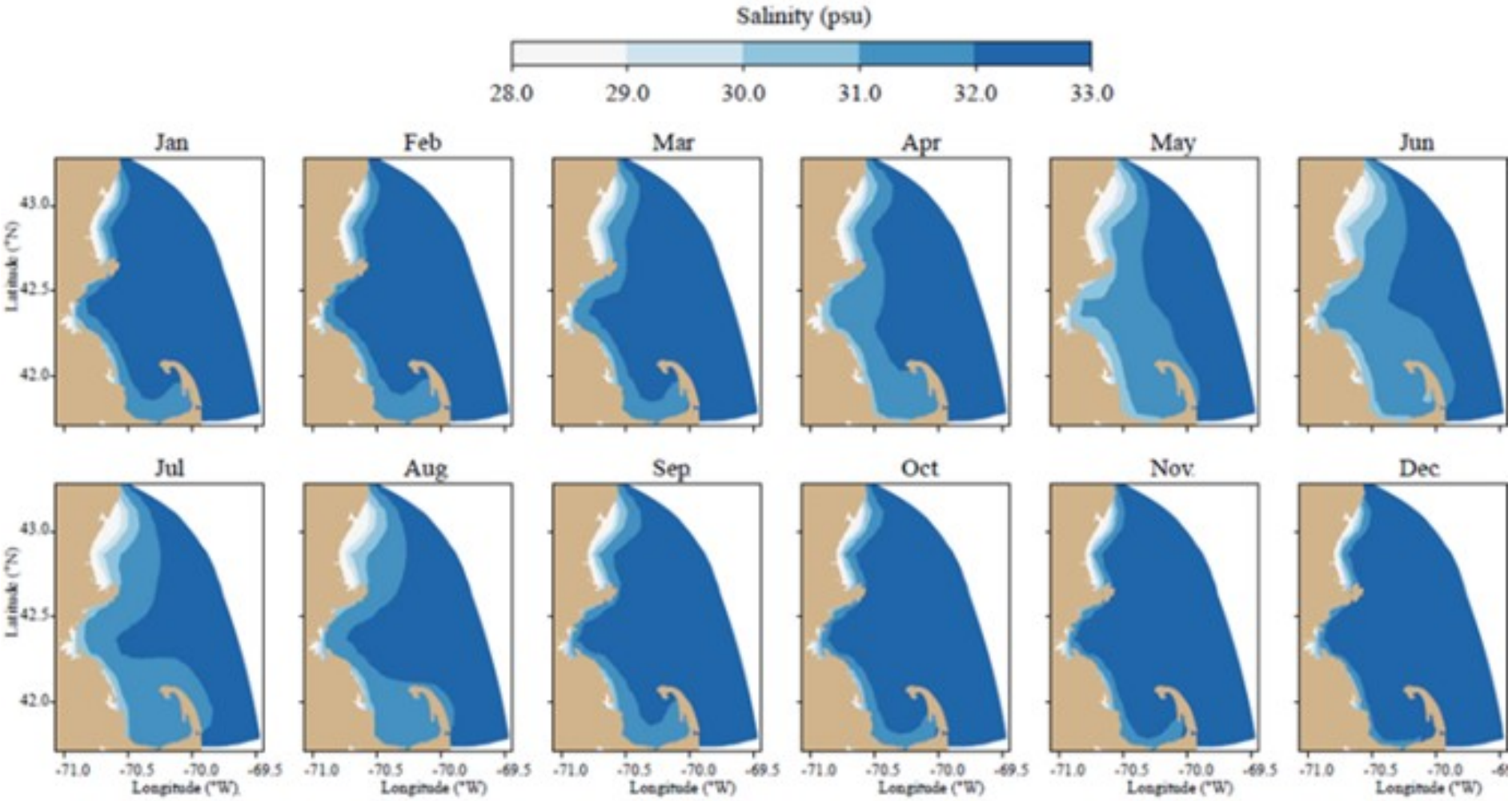

Figure 2-25 Former BEM model monthly mean salinity at sea surface for 2016 (Zhao et al. 2017, Figure 4-8a).

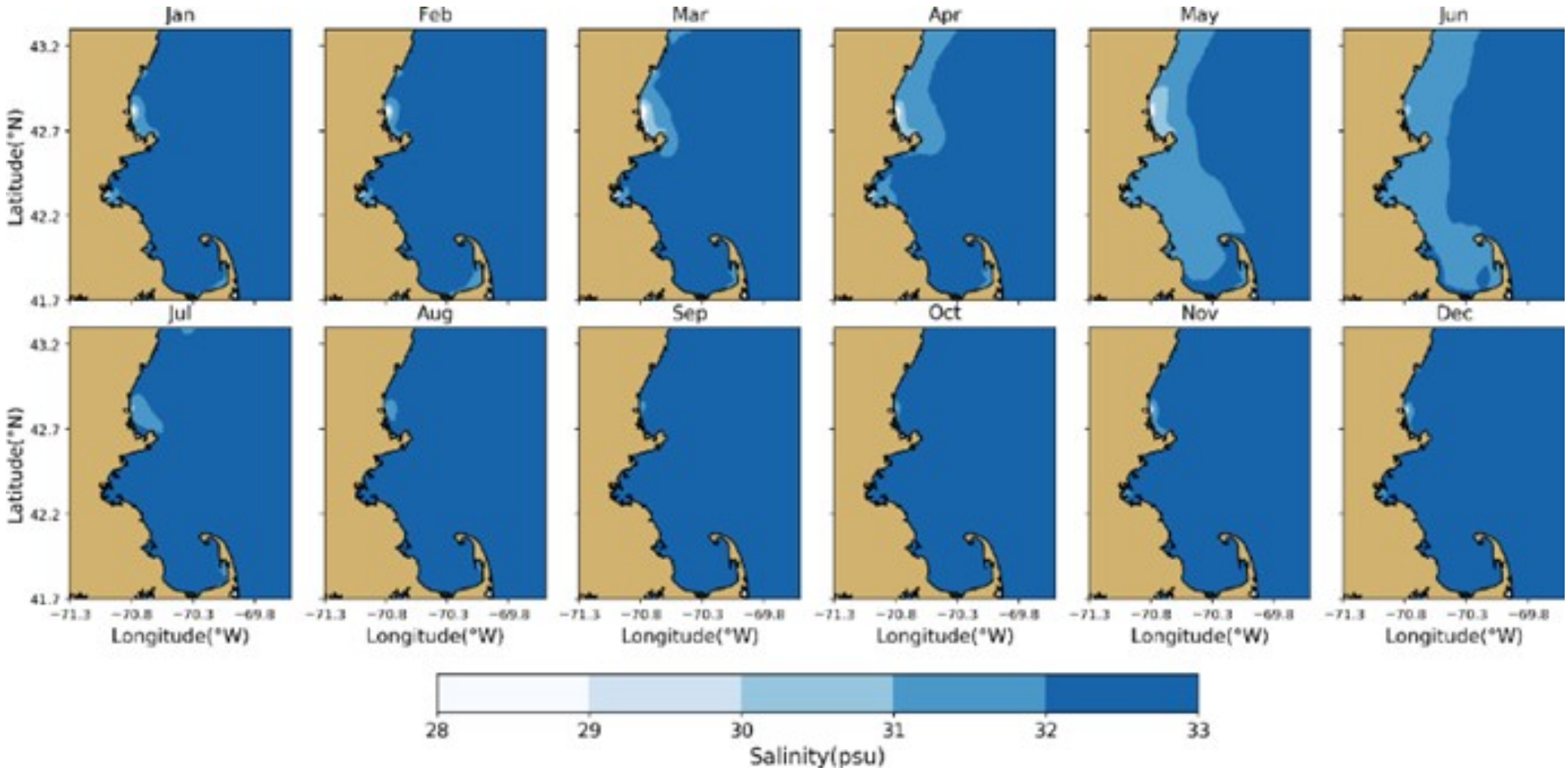

Figure 2-26 Updated BEM model monthly mean salinity at sea surface for 2016.

The seafloor monthly-mean fields for both former and updated BEM (Figure 2-27 and Figure 2-28 respectively) show quasi-uniform fields given the color scale used. The former BEM shows a year-round thin and fresher coastal band, most pronounced between Piscataqua and Merrimack rivers and somewhat wider during spring and summer. Except for minor bottom-water freshening in some months in Boston Harbor and eastern Cape Cod Bay, the updated BEM shows no spatial variability with this color scale for seafloor salinities.

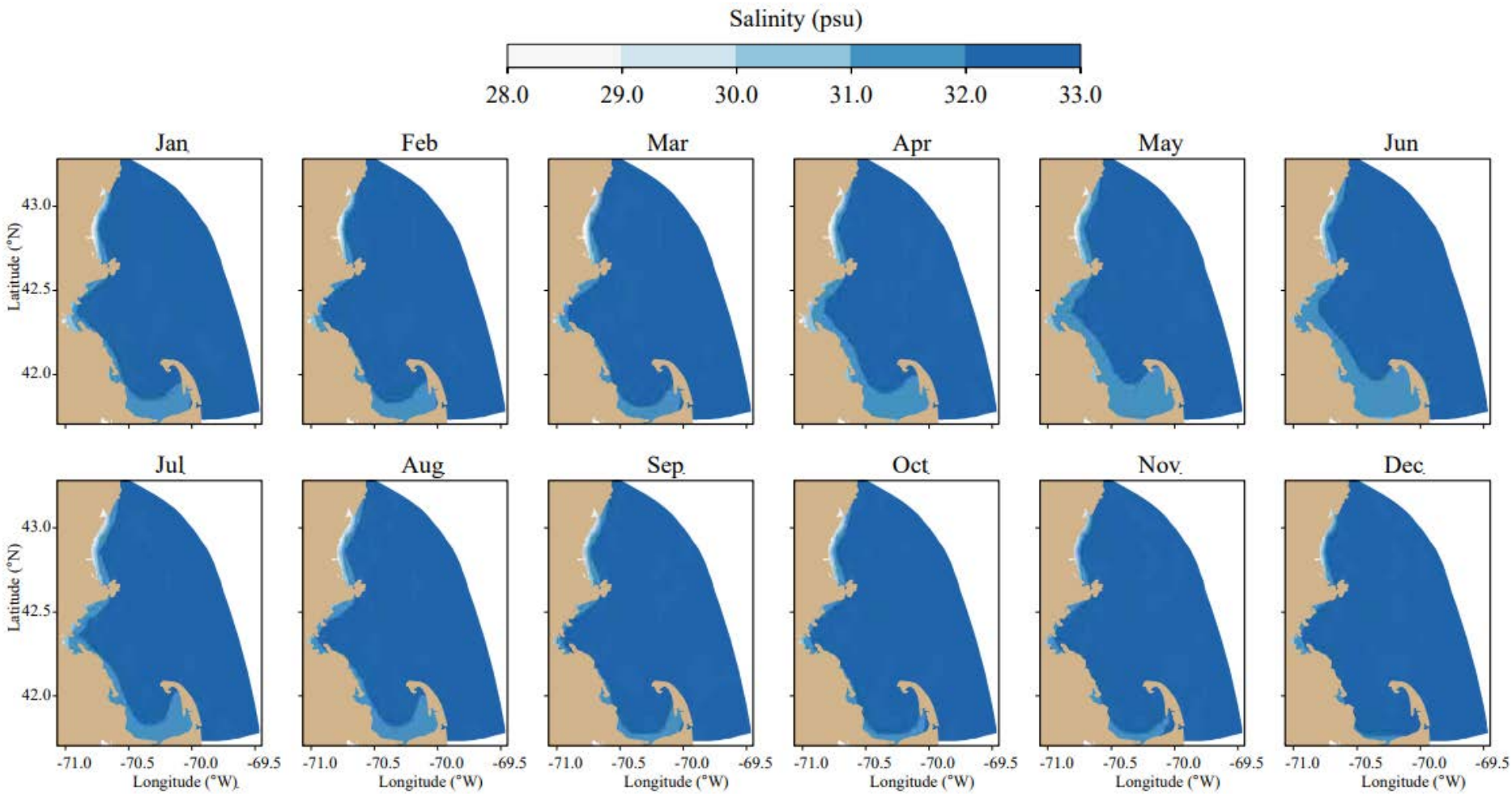

Figure 2-27 Former BEM model monthly mean salinity at seafloor for 2016 (Zhao et al. 2017, Figure 4-8b).

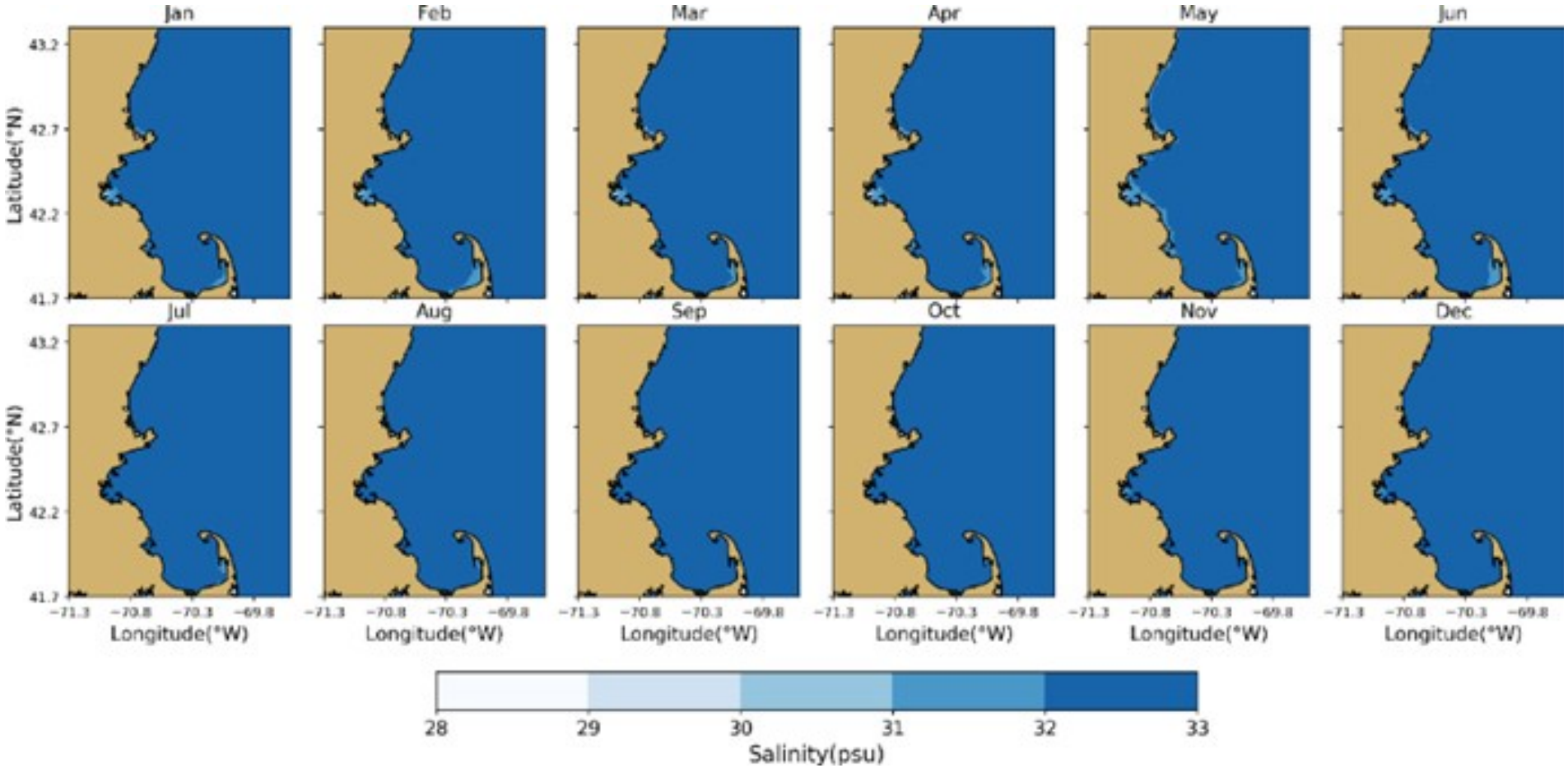

Figure 2-28 Updated BEM model monthly-mean salinity at near the seafloor for 2016.

2.3.3 Residual currents

In this section, the monthly residual currents at the surface and at 15m depth for the former and updated BEM are compared and evaluated. For guidance, Figure 1-1 from the previous 2016 simulation report (Zhao et al., 2017) is included, which shows the general mean circulation around and within Massachusetts Bay and Cape Cod Bay (Figure 2-29). A key feature in the circulation pattern is the Western Maine Coastal Current (WMCC).

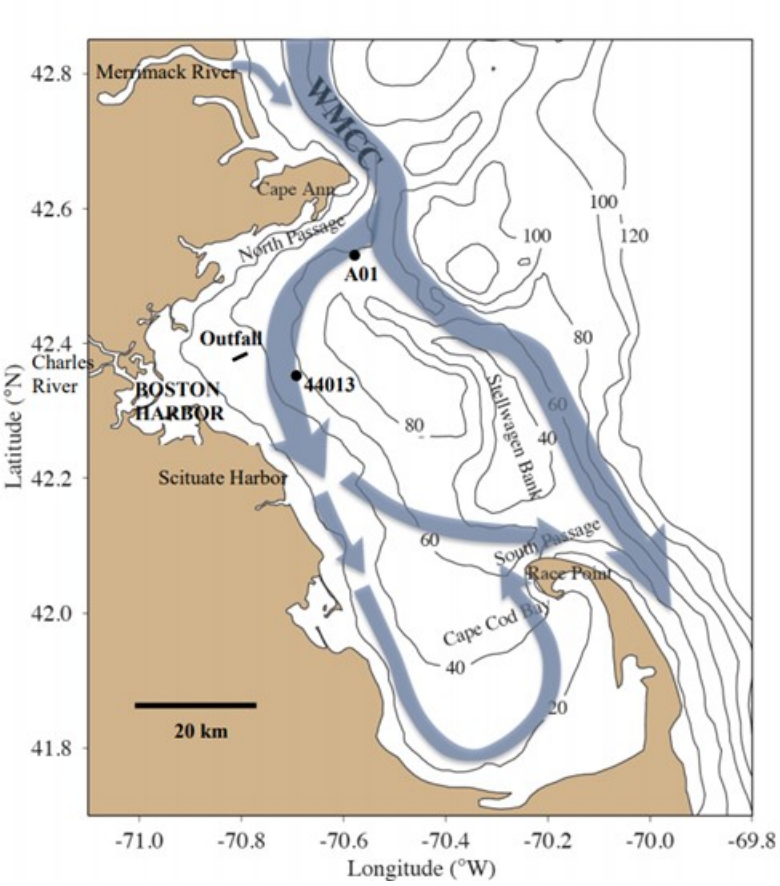

Figure 2-29 Schematic long-term mean circulation (Zhao et al. 2017, Figure 1-1). WMCC: Western Maine Coastal Current.

Figure 2-30 and Figure 2-31 show monthly mean surface currents for the former and updated BEM, respectively. In line with the description of the surface current structures provided in Zhao et al. (2017), the former BEM produces weaker currents within the bays in the period September-January, which is generally also true for the updated BEM. The former BEM produced the strongest coastal current within the bays (running southwards between Boston and Cape Cod) in December, while the updated BEM produces its maximum in January, albeit with lower magnitude. The former BEM showed evident flow into Massachusetts Bay south of Cape Ann between February and August, with stronger magnitudes between March and June, as is expected from the increased Merrimack River discharges in this period. The intrusion of the WMCC into the

Massachusetts Bay is also most evident in the updated BEM during the spring months, although it is also considerable in the months of November and December.

The former BEM produces a clockwise circulation in the northern Massachusetts Bay between March and June, which bifurcates southwards in the summer months creating a counter clockwise flow in the middle between the two bays, which loops offshore to merge again into the main branch of the southward flowing WMCC (between Cape Ann and Cape Cod). The updated BEM shows no clear evidence of northern clockwise circulation until May, and it also shows the development of the bifurcation which loops back offshore in the summer months, although this one develops a bit further east than in the former BEM. Zhao et al. (2017) reports strongest WMCC main branch currents between October and December, although currents of similar magnitude are visible in May and January. The updated BEM generally also predicts strongest mean currents in the late autumn/early winter period, and during May, but the magnitudes seem lower than the 30-40 cm/s reported for the former BEM. In general, the updated BEM produces lower mean current magnitudes than the former BEM, which is in line with the comparison against A01 currents shown previously. Moreover, the updated BEM seems to produce more consistent, southeastward mean currents outside the bays and offshore than the former BEM.

Both the former and updated BEM produce 15m deep mean currents of similar patterns to the surface currents but of considerably lower magnitudes (Figure 2-30 and Figure 2-31). A noteworthy difference is the pronounced northward flow between June and September around Cape Cod visible in the updated BEM, which bifurcates from the pronounced southward inflow of the WMCC into the bays and loops back around Stellwagen Bank to rejoin the WMCC main branch.

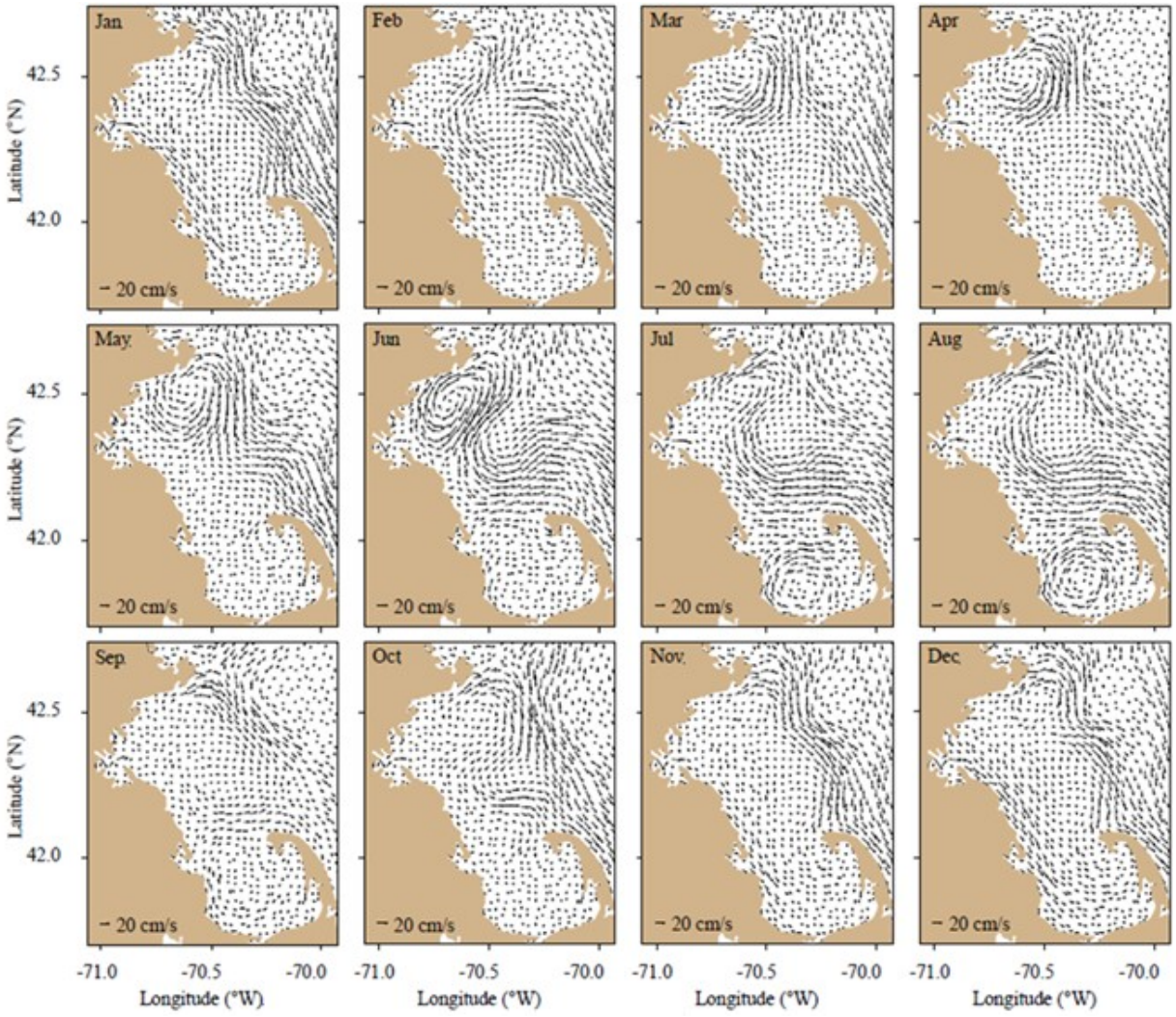

Figure 2-30 Former BEM model monthly-mean currents at sea surface for 2016 (Zhao et al.2017, Figure 4-9a).

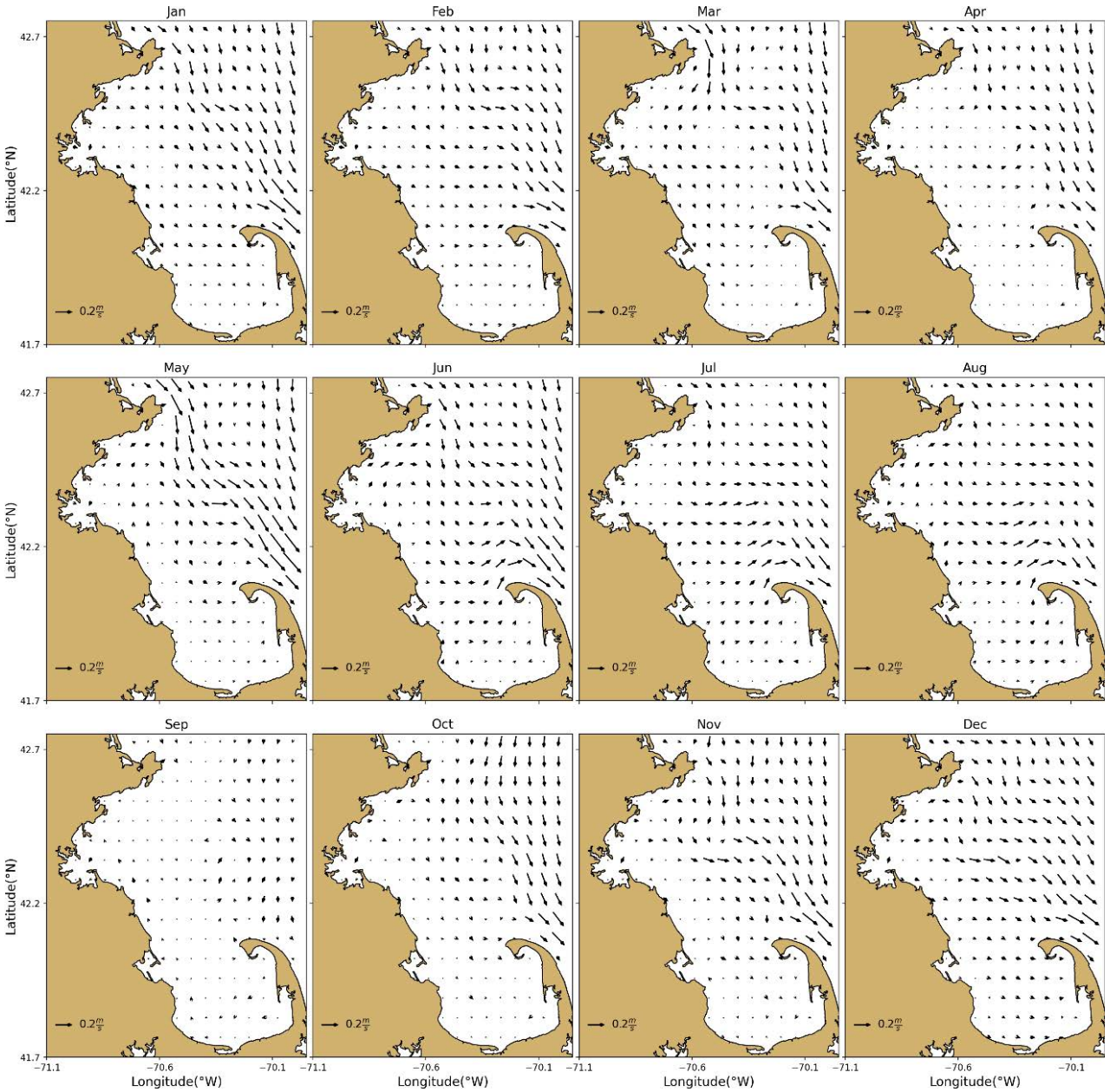

Figure 2-31 Updated BEM model monthly-mean currents at sea surface for 2016.

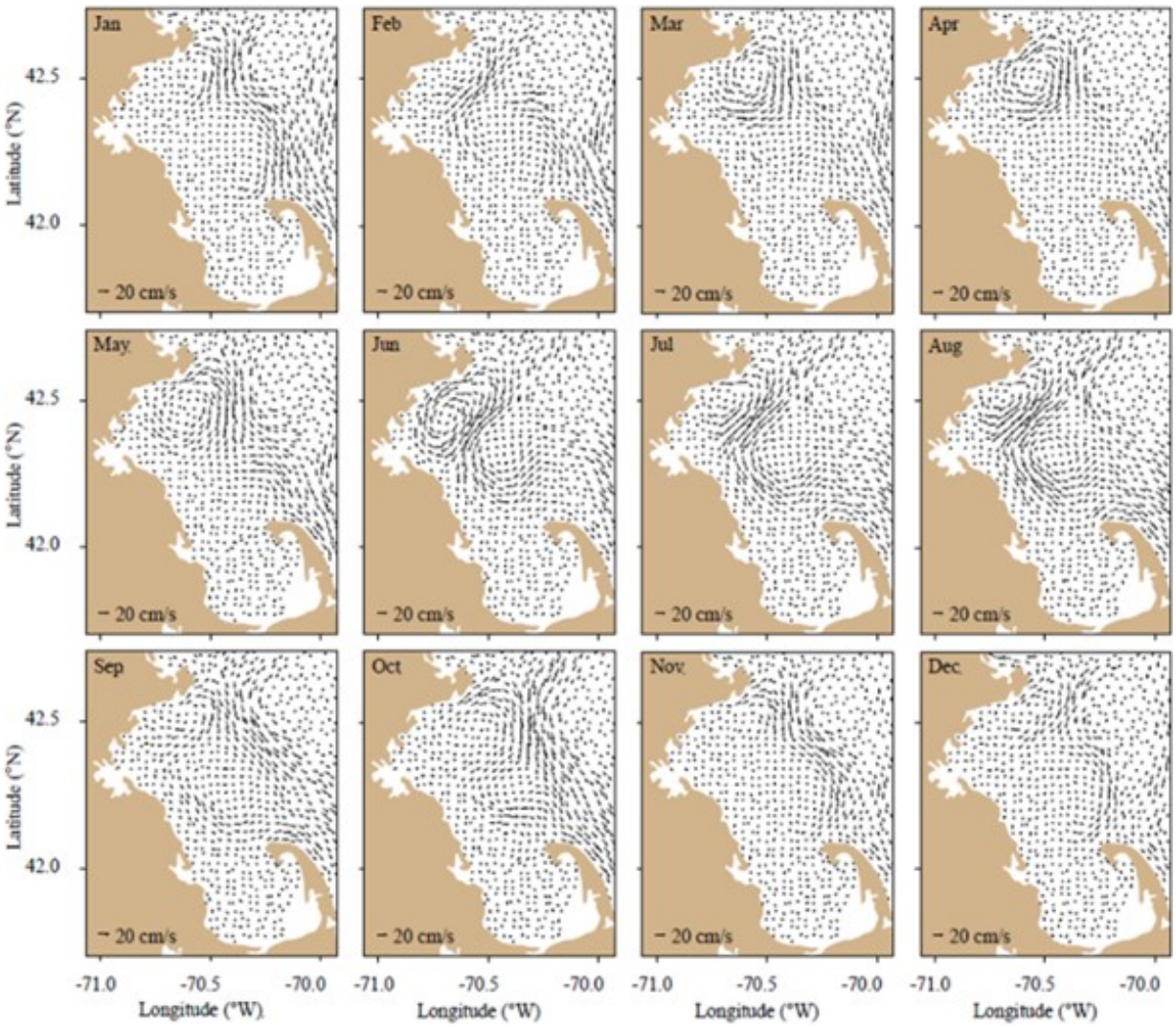

Figure 2-32 Former BEM model monthly-mean currents at 15 m depth for 2016 (Zhao et al.2017, Figure 4-9b).

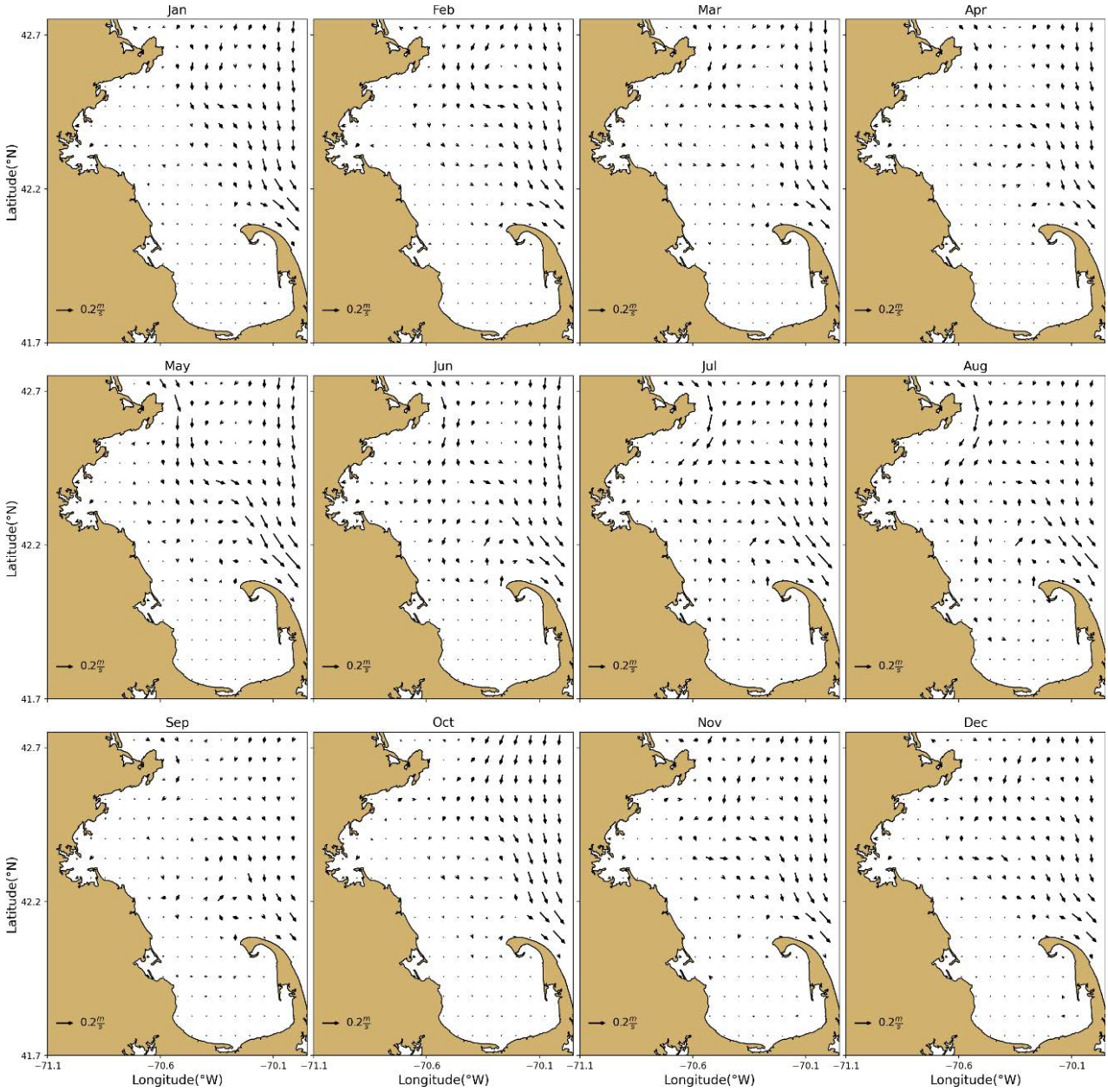

Figure 2-33 Updated BEM model monthly-mean currents at 15 m depth for 2016.

2.4 Conclusions on updated/former model comparisons for hydrodynamics

Based on the comparisons between the former and updated BEM it can be concluded that in general both models achieve a good agreement with measurements. The updated BEM shows more spatial variability and more natural looking gradients near the location of the former BEM open boundary. However, the salinity bias is somewhat larger in the updated BEM, especially at locations where salinity measurements are assimilated in the former BEM. Nonetheless, seasonal salinity stratification (as well as temperature stratification) is well represented in the updated BEM. This is of primary importance for a correct representation of the water quality in Massachusetts Bay.

The satisfactory quality of the updated BEM, in comparison with the former BEM, is notable in that this was achieved without the use of data assimilation (DA). The use of DA for salinity and temperature measurements in the case of the former BEM, decreases the difference between model results and observations for these quantities. However, DA may obscure inconsistencies in the representation of physical processes affecting salinity and temperature, such as residual horizontal and vertical transport due to advection and diffusion. As the processes driving salinity and temperature are also key for a correct representation of water quality, it was an explicit decision not to apply DA in the updated BEM. This means that by achieving similarly satisfactory model-observation comparisons for salinity and temperature in the updated BEM, there can be more confidence in the representation of physical processes affecting salinity, temperature and transport of water quality substances. Additionally, a better representation of the underlying physical process gives more confidence in the applicability of the hydrodynamic model for subsequent water quality modeling and for conducting scenario studies, such as assessing the impact of load changes.

3 Water Quality

In this section, the updated BEM water quality model is evaluated in comparison to the former BEM. As done for the hydrodynamics, the results from both models are compared for a series of plots, as published in Zhao et al. (2017). These plots show regressions and time series, as well as vertical transects, for several water quality parameters, including nutrients, chlorophyll and dissolved oxygen. In some of the plots, observations are also shown, allowing an assessment of the relative performance of the models with respect to the observations.

On top of these graphical comparisons, additional analysis, including mass balances, are carried out to gain a deeper understanding of system functioning in terms of transport and dominant water quality processes. For the updated BEM, mass balances are available as a standard feature of the software used. Mass balances were produced for three areas: Mass Bay North (MBN), Mass Bay South and Cape Cod Bay (MBS-CCB) and the offshore region (OFF), as shown in Figure 3-1. The combination of Massachusetts and Cape Cod bays (areas MBN and MBS-CCB) is referred to hereafter as the “study area” or “area of interest” and is approximately equivalent to the domain of the former BEM Water Quality model.

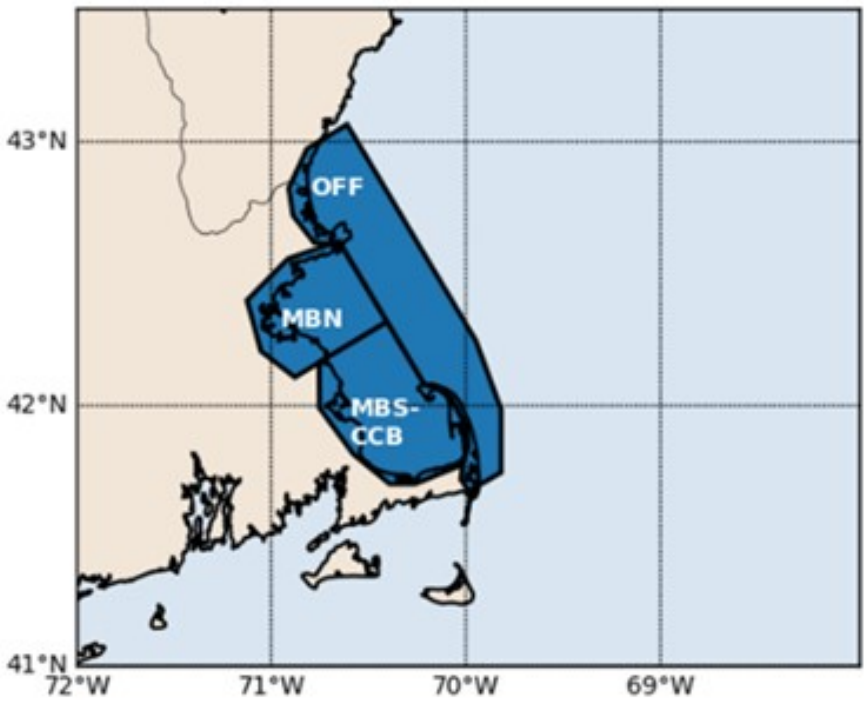

Figure 3-1 Zones over which mass balances are calculated in the updated BEM.

3.1 Distinctions between former BEM and updated BEM

This section discusses some design choices that make the updated BEM differ from the former BEM, as well as some other differences noticed during the setup and validation.

3.1.1 Location of the open boundary

The updated BEM has its open boundaries far away from the area of interest, mostly in deep off-shelf waters (Figure 3-2). The southern boundary runs from Pamlico Sound, North Carolina, toward the northeast. The eastern boundary runs from the eastern tip of Nova Scotia in a south-eastern direction.

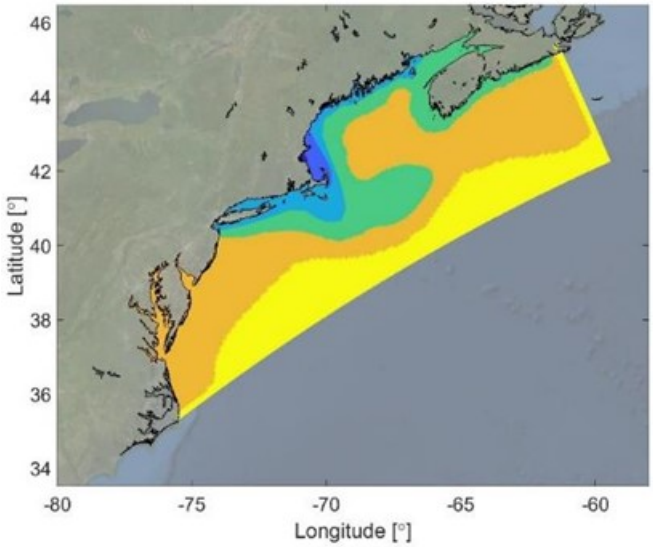

Figure 3-2 Extent of the updated BEM horizontal grid (colors indicate grid resolution: yellow=8km; orange=4km; green=2km; light blue=1km; royal blue=500m; dark blue=250m).

The ambition is not primarily to provide a realistic water quality model for this entire large domain. This approach is meant to provide a realistic estimate of the quality of the Gulf of Maine (GoM) waters entering the study area, and the variability thereof as affected by larger scale meteorological, hydrological and biogeochemical processes. For the much smaller domain of the former BEM (Figure 3-3), Zhao et al. (2017) mention (citing Hunt et al, 1999) that 7% of nitrogen influxes is from coastal sources and atmospheric deposition and the remaining 93% from the GoM. This makes Massachusetts Bay a strongly boundary dominated system (see also Section 3.3.1). The water quality boundary conditions of the former BEM "…*are specified using MWRA monitoring program observations…*" (Zhao et al., 2017). To this end, multiple stations well within the area of interest were used to derive boundary conditions, including stations that are later used for model validation. Using the same data for setting boundary conditions and for model validation is avoided in the updated BEM. In addition, the larger domain allows a more realistic representation of the inflow of the Merrimack River and its interaction with Massachusetts Bay.

The updated BEM simulates the concentration of GoM waters entering the study area rather than prescribing it. The 3D fields of different water quality variables at the boundary of the study area result from:

- boundary forcing at the open ocean, based on a separate, external, publicly-available, state-of-the-art, well-validated model simulation of North Atlantic conditions (see Appendix A),
- estimated loads and atmospheric forcing over the entire domain, and
- physical and biogeochemical processes (as represented in the Delft3D-FM code) over the entire domain.

As a logical consequence of the larger domain, and not using observations from multiple stations within the area of interest to derive the offshore boundary conditions, the updated BEM may not reproduce the observed water quality at the location of the former BEM's boundary as accurately as the former BEM.

3.1.2 Non-oceanic loads

As described in Zhao et al. (2017) and references therein, non-oceanic loads in the former BEM, besides the Deer Island Treatment Plant (DITP) outfall, include river inputs, combined sewer overflows (CSOs), atmospheric deposition and non-point sources originating from coastal rainfall runoff. The updated BEM includes river inputs and atmospheric deposition only, whilst other sources have been neglected. Boston Harbor CSOs have decreased significantly since the 1990s and other sources are not considered to be significant in comparison to the rivers and DITP outfall.

River loads in the updated BEM include all rivers discharging to the larger domain (Figure 3-2), insofar as they are expected to affect the GoM and thus the study area. Appendix A provides further details. River loads in the former BEM are limited to those inside the smaller model domain (Figure 3-3), while the others, including Merrimack River, are only indirectly included in the water quality model via the open boundary conditions.

3.1.3 Representation of biogeochemical processes

The Water Quality Model (WQM) configuration selected for the updated BEM deviates somewhat from the former BEM as described in Zhao et al. (2017) and references therein. In some cases, the formulations have been expanded, whereas in other cases they have been simplified. Initial design choices were checked during the development and calibration process and have been updated where necessary to make the updated BEM fit-for-purpose. Below, some key aspects of the selected configuration are briefly discussed. More details are provided in Appendix A.

3.1.3.1 Phytoplankton model

The phytoplankton sub-model of the updated BEM, called BLOOM, is functionally fully equivalent to the former BEM, although it uses a slightly different numerical approach. The model is flexible with respect to the number and nature of algae groups. Four functional groups of algae are included, all of them featuring variable nutrient to carbon and chlorophyll to carbon ratios. BLOOM is documented in peer-reviewed journal publications (Los et al., 2008; Blauw et al., 2009; Smits et al., 2013). It also has a long

track record in North Sea eutrophication models (Los, 2009; Chapter 8) and has been applied world-wide for the past two decades in models using Delft3D and Delft3D-FM.

3.1.3.2 Attenuation of light

The vertical attenuation of photosynthetically active radiation (PAR) in the water column is represented in the updated BEM by a linear extinction model. The total extinction coefficient (the fraction of PAR attenuated per unit of vertical path length) is composed of a small background contribution and contributions by phytoplankton, particulate organic matter, dissolved organic matter and inorganic suspended particles (silt, clay, fine sand). These contributions are all space and time dependent and directly linked to simulated state variables.

The former BEM used the same concept: the extinction coefficient was represented by a spatially variable background contribution and a space and time dependent contribution by the simulated phytoplankton. The background contribution represented contributions by inorganic and organic suspended and dissolved substances (other than phytoplankton). This led to a relatively stable simulated extinction coefficient.

To represent the contribution of inorganic suspended particles to light extinction in the updated BEM, a state variable was added to represent inorganic particles in the water column. A spatially variable amount of fine sediment particles, available for resuspension, was defined. These particles resuspend into the water column when and where conditions are suitable and slowly re-settle afterwards, temporally contributing to light extinction.

3.1.3.3 Representation of organic matter

The updated BEM represents organic matter by one dissolved and one particulate fraction, whereas the former BEM used 5 different fractions. In the updated BEM, the same state variables are used to represent both the organic matter from the discharge and detritus. This is considered feasible since the effluent has undergone treatment and shows relatively low concentrations of organic matter. The smaller number of state variables makes for shorter runtimes and easier calibration. This simplified approach was confirmed as fit-for-purpose during model validation (Appendix B).

3.1.3.4 Sediment processes

For the representation of sediment diagenesis (release of nutrients as a result of decomposition of settled (i.e. benthic) organic matter) in the updated BEM, there appeared to be no reason to deviate from the standard Delft3D approach used routinely in North Sea applications. This approach is a lot simpler than the Sediment Flux Model embedded in the former BEM. In the updated BEM, only settled organic particulates (C, N, P and Si) are represented by state variables. Porewater concentrations of dissolved constituents are not calculated. Regenerated nutrients are directly released back to the water column, and the oxygen consumed for the mineralization of benthic organic matter is directly drawn from the water column. This simplified approach was confirmed as fit-for-purpose during model calibration (Appendix B).

3.2 Model-observation comparisons

As in Zhao et al. (2017), time series of former and updated BEM model results for key water quality variables are plotted, together with MWRA observations at a selection of 15 stations, grouped in three zones (Figure 3-3):

- Northern stations: F22, N01, N04, N21, N07
- Southern stations: F10, F06, F29, F01, F02
- Harbor stations: 024, 140, 142, 139, 124

Organic matter and dissolved oxygen results are plotted for the Northern and Southern stations only. Regression comparisons use all available data from the Massachusetts and Cape Cod bays (Northern and Southern stations, as well as N18, F13, F15 and F23). For comparison purposes, all plot scales are kept the same as in Zhao et al. (2017).

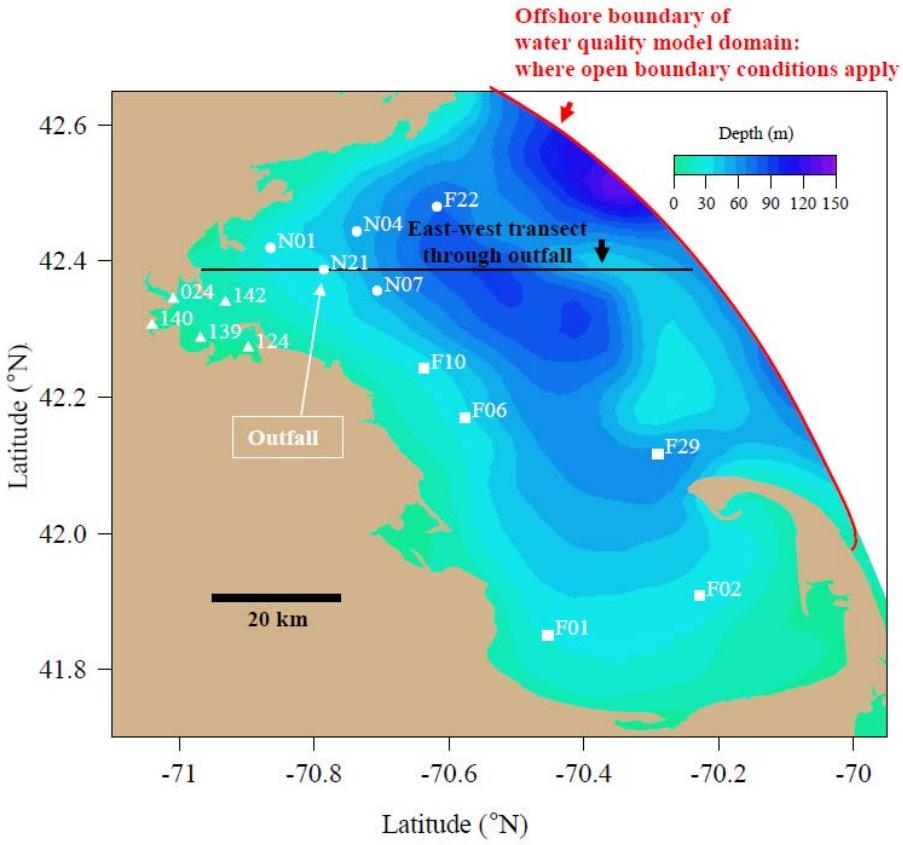

Figure 3-3 Water quality model domain of the former BEM. Red arc = Offshore boundary; Black line = East-west transect through outfall. Station groups: northern (circles), southern (squares), and harbor (triangles). (from Zhao et al. 2017, Figure 3-6).

In some of the figures comparing the updated BEM to former BEM there are differences between the observations shown in the plot frames. Some of the differences may be the result of updates and corrections to MWRA's long-term monitoring database, continuously implemented as part of quality assurance, which occurred between 2016 when measurements were provided for the former BEM plots and 2020 when they were

provided for the updated BEM plots. All observations in updated BEM frames have been confirmed as complete and correct, and none of the conclusions drawn are affected by these differences.

The water depths indicated on the time series plots for the updated BEM correspond to the maximum total depth reported at each station in the MWRA nutrient monitoring data; it is noted that station water depths in plots from Zhao et al. (2017) sometimes differ by small amounts from those in plots of updated BEM results.

In general, the updated BEM shows more high-frequency variability, which is expected and largely due to wind forcing. As the temporal resolution of the water quality component of the former BEM is 3 days, a 3-day running average transformation was applied to the updated BEM outputs in all time series comparisons.

3.2.1 Model-observation correlation analysis

Model-observation correlation and regression analyses are carried out for key water quality variables at all Massachusetts and Cape Cod bays stations (total of 14 stations). For the updated BEM, each observation was linked to the nearest daily model output. For the former BEM, Zhao et al. (2017) do not describe how model and observation values were matched, but it can be presumed to be similar.

As for the former BEM (Figure 3-4), results from the updated BEM show no relevant correlation with MWRA measurements of near-surface chlorophyll, silicate, or ammonium (Figure 3-5), while model-observation correlations are high for surface NO_3 and bottom oxygen.

While the surface chlorophyll in the former BEM shows very little variability (concentrations between 1 and 3 µg L^{-1} for all stations over the entire year), the updated BEM captures some chlorophyll peaks but sometimes underestimates measured concentrations.

Correlations of silica and NH_4 concentration results with measurements remain poor in the updated BEM but the range of values is well represented.

As for the former BEM, NO_3 concentrations simulated with the updated BEM are well correlated with measurements, with a regression line approaching the 1:1 line. The whole range of concentrations is well represented, including the lowest values (< 1 µM) for which results from the former BEM seem more scattered.

Finally, the model-observation correlation for bottom oxygen concentration is very high in both BEMs (0.90 in former BEM and 0.89 in updated BEM). The correlation for bottom oxygen percent saturation is significantly better in the updated BEM (0.83 compared to 0.67).

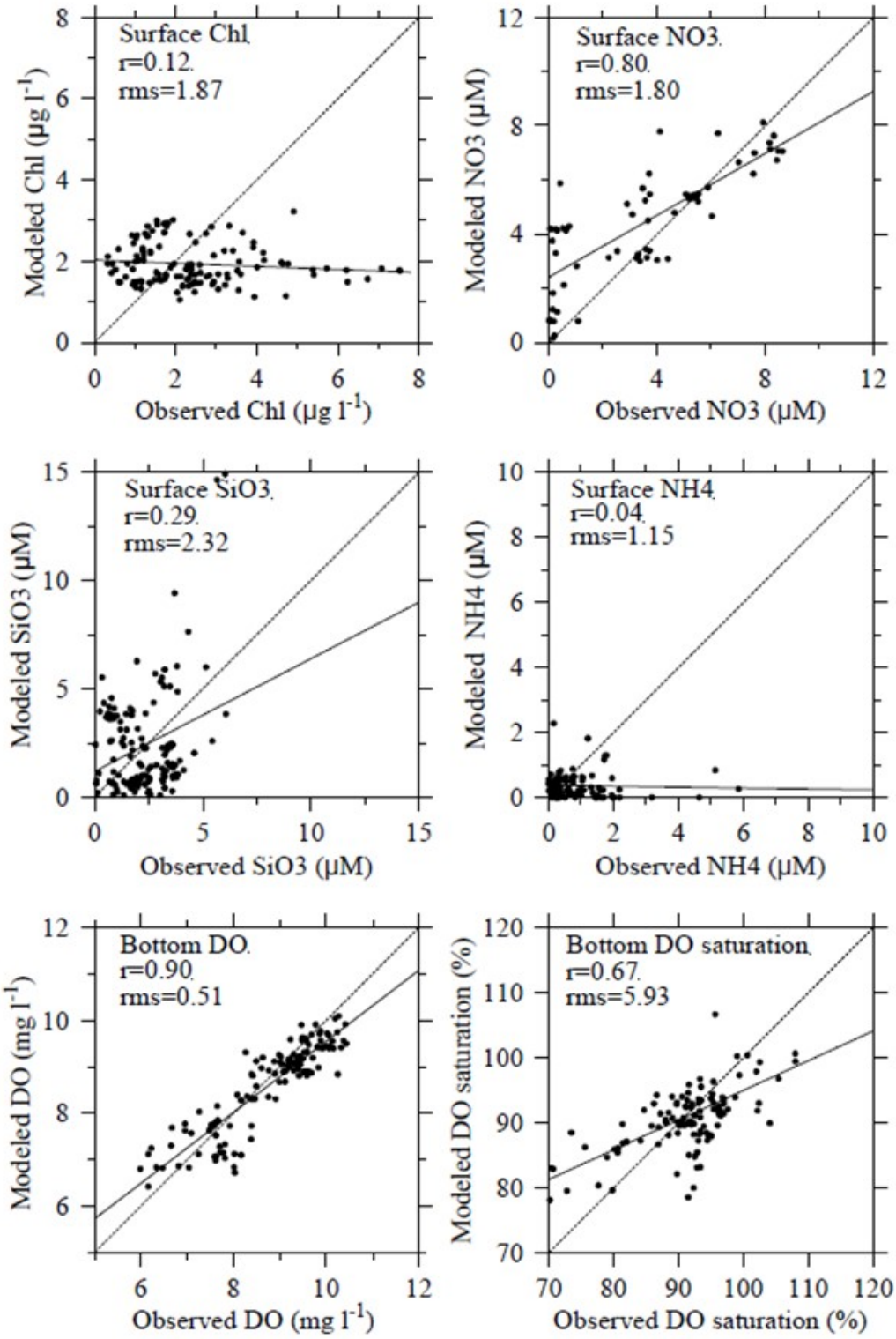

Figure 3-4 Model-observation correlation/regressions of key water quality parameters for 2016 for the former BEM. All stations outside Boston Harbor; regressions are solid lines, dashed lines indicate equality between observed and model results (Zhao et al. 2017, Figure 5-1).

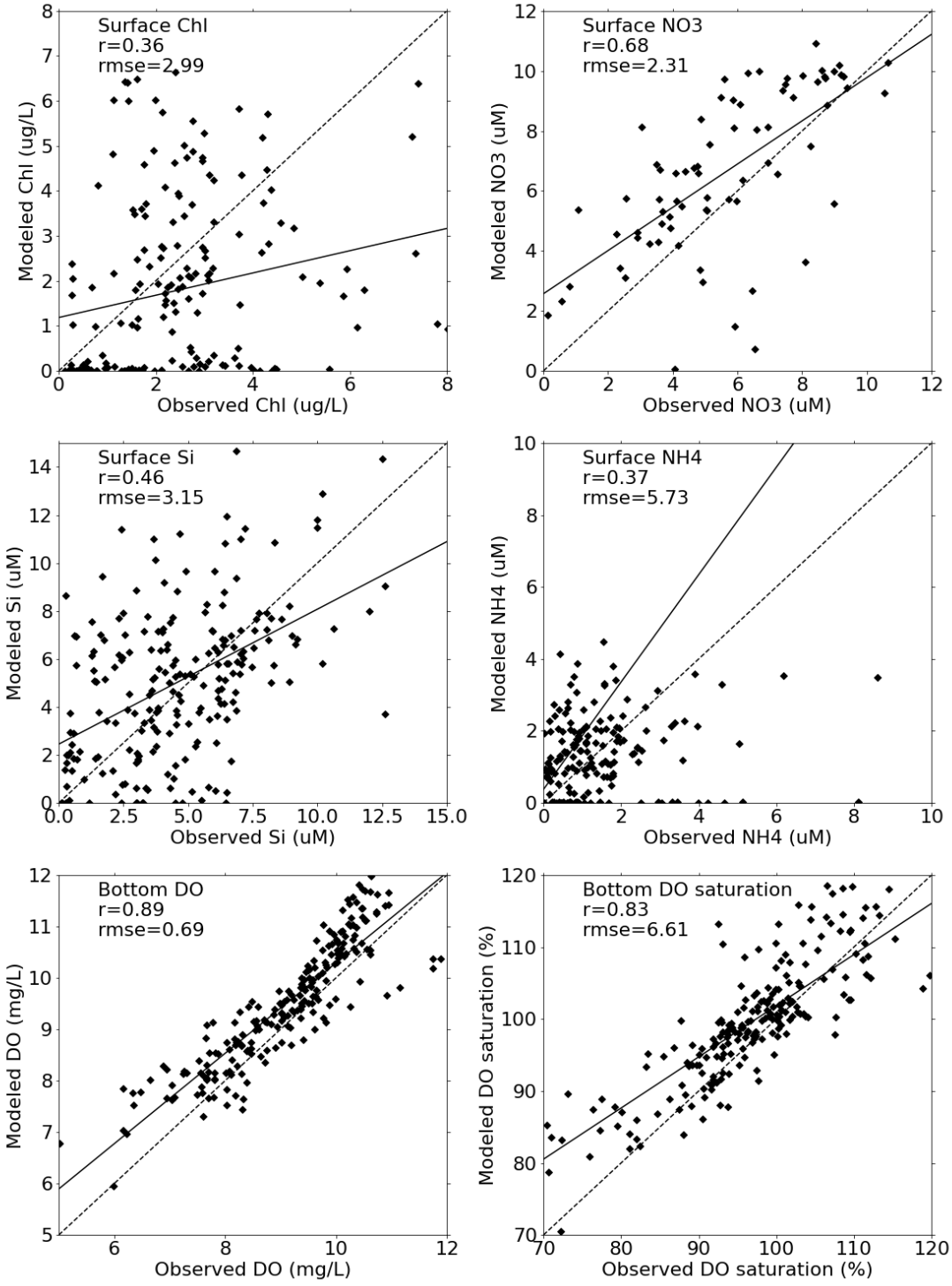

Figure 3-5 Model-observation regression plots for key water quality variables for 2016 for the updated BEM. The black line corresponds to the linear regression; the dotted line indicates equality between observations and model results.

3.2.2 Light climate

Comparison of model-observation plots of light extinction for the former and updated BEM at Northern (Figure 3-6 and Figure 3-7), Southern (Figure 3-8 and Figure 3-9) and harbor stations (Figure 3-10 and Figure 3-11) show that, while both models represent the average yearly extinction well, the updated BEM is better in reproducing temporal variability. In the former BEM, temporal variability of light extinction is underestimated at all stations, which leads to high model-observation differences especially at locations where the measured variability is highest (e.g. harbor station 140). At Northern and Southern stations, the updated BEM represents temporal changes in extinction very well, including peaks in spring and fall due to phytoplankton self-shading that were not captured by the former BEM. At the harbor stations, “base” extinction seems slightly underestimated by the updated BEM. In contrast to the former BEM, variability due to short resuspension events is mimicked by the updated BEM, even though the timing and magnitude of peaks in extinction do not always match those measured (e.g. station 139).

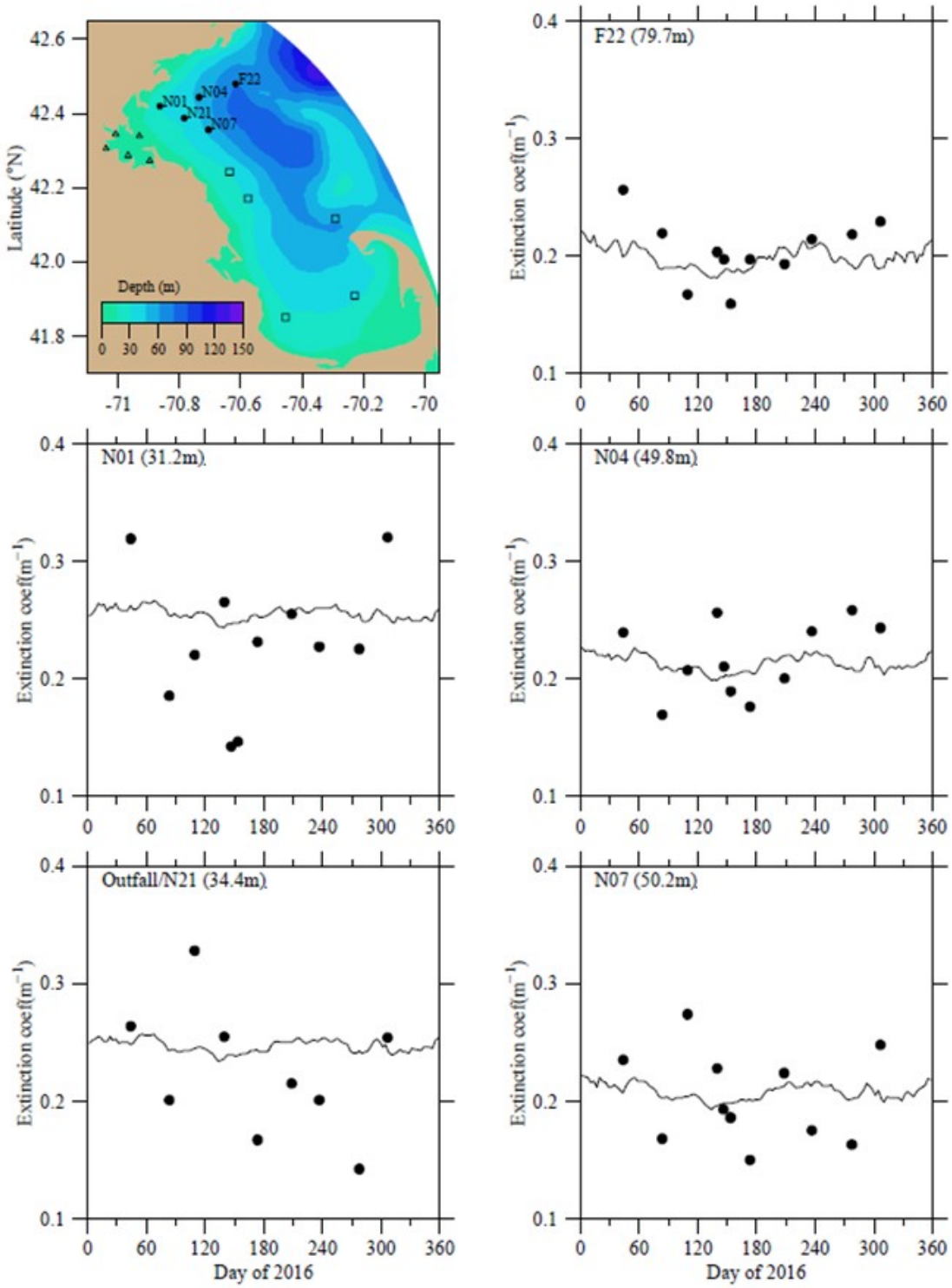

Figure 3-6 Light extinction at Northern stations for 2016. Line: Model results from former BEM. Symbols: Observations. In this and all similar plots to follow, upper left of frame shows "station name (bathymetric depth)" (Zhao et al. 2017, Figure 5-2a).

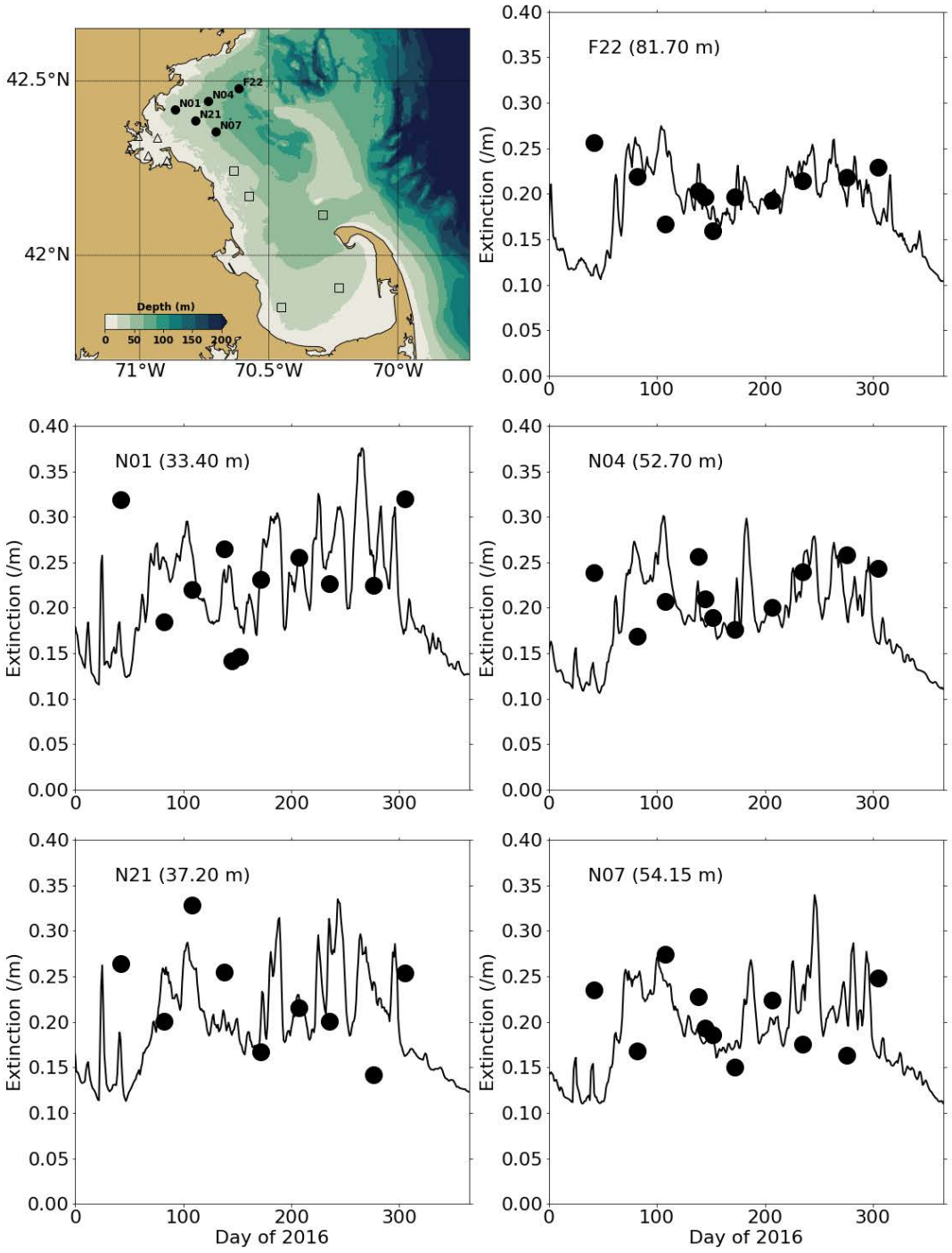

Figure 3-7 Light extinction at Northern stations for 2016. Line: Model results from updated BEM. Symbols: Observations.

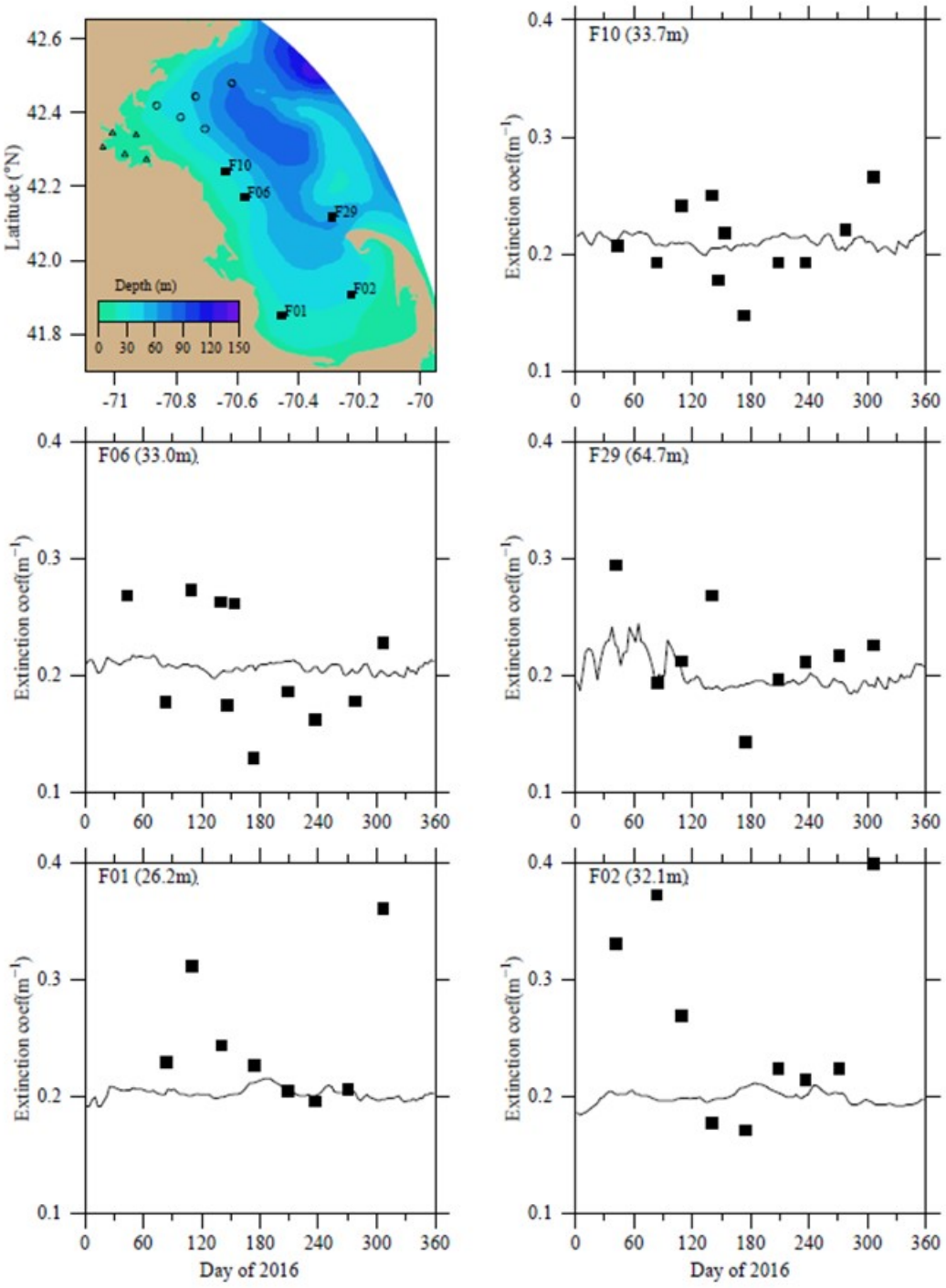

Figure 3-8 Light extinction at Southern stations for 2016. Line: Model results from former BEM. Symbols: Observations. (Zhao et al. 2017, Figure 5-2b).

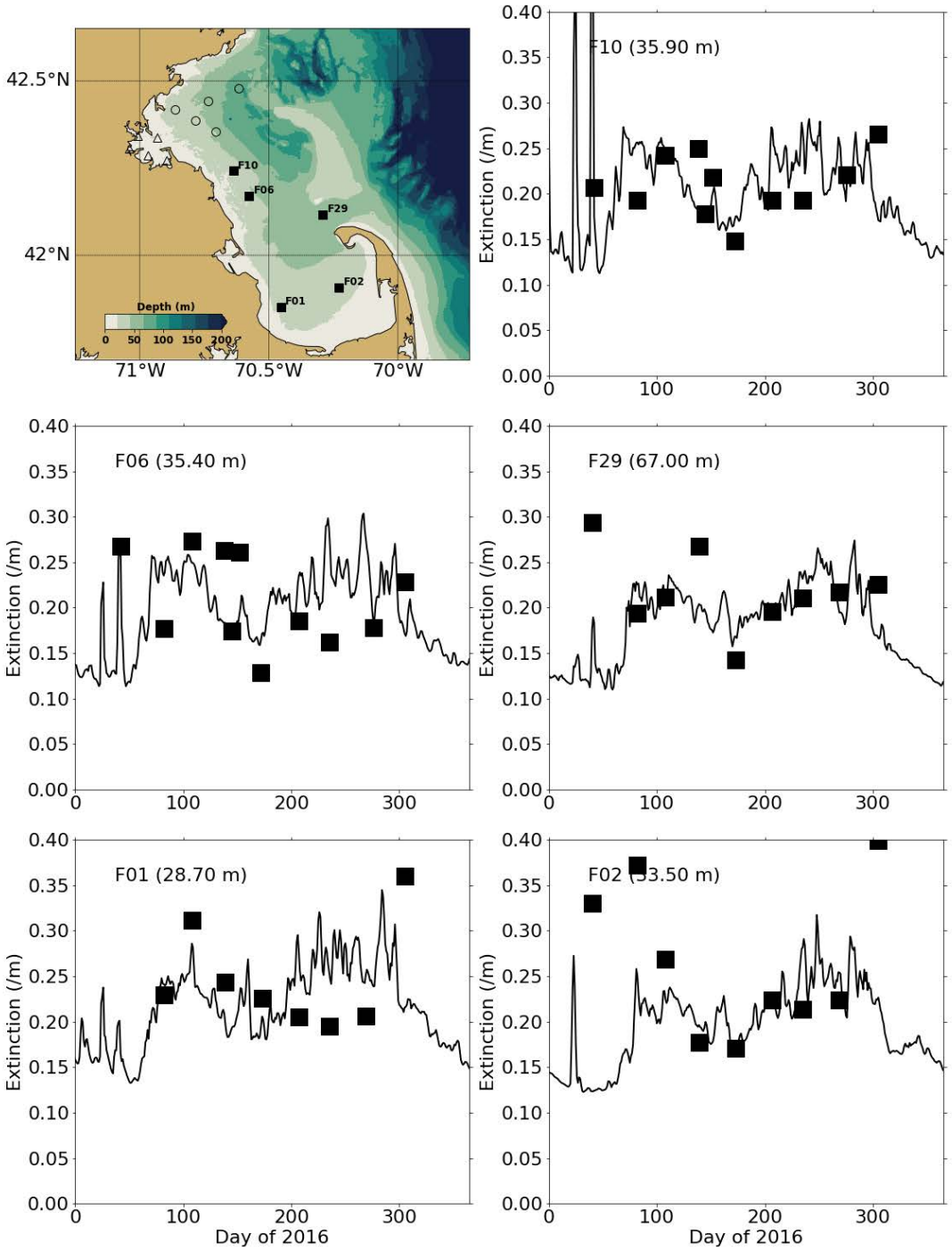

Figure 3-9 Light extinction at Southern stations for 2016. Line: Model results from updated BEM. Symbols: Observations.

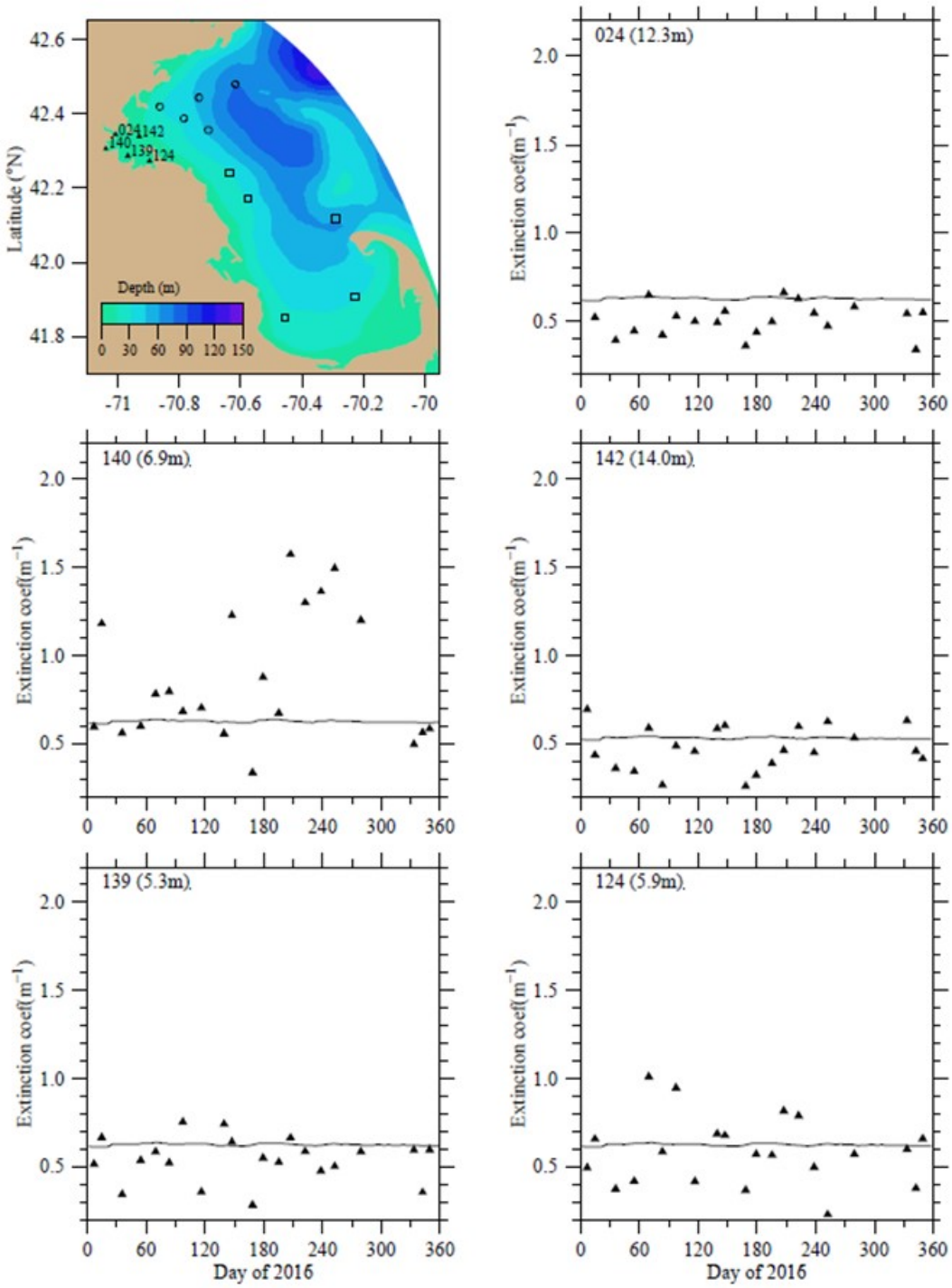

Figure 3-10 Light extinction at Harbor stations for 2016. Line: Model results from former BEM. Symbols: Observations. Note different y-axis scale than for bay stations in Figure 3-6 and Figure 3-8 (Zhao et al. 2017, Figure 5-2c).

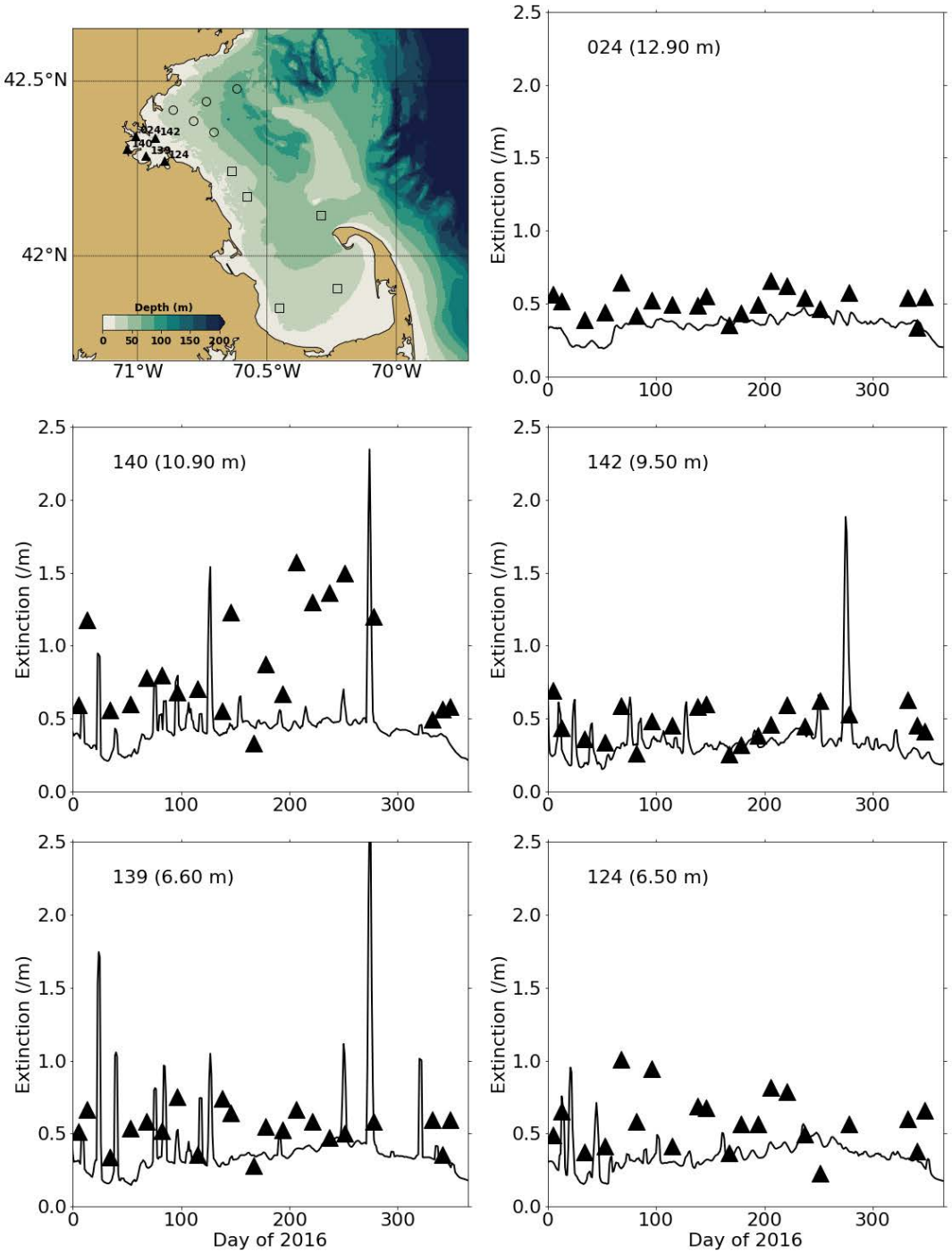

Figure 3-11 Light extinction at Harbor stations for 2016. Line: Model results from updated BEM. Symbols: Observations.

3.2.3 Dissolved Inorganic Nitrogen

Model-observation plots of dissolved inorganic nitrogen (DIN) are compared here for the former and updated BEM at Northern (Figure 3-12 and Figure 3-13), Southern (Figure 3-14 and Figure 3-15) and harbor stations (Figure 3-16 and Figure 3-17).

While the former BEM underestimated seafloor DIN concentrations at many Northern and Southern stations (e.g. F22), the updated BEM reproduces variations of DIN with depth very well. The updated BEM bottom DIN concentrations show an excellent match with measurements, except for stations F01 and F02, where they are overestimated at the end of the summer/early fall. For the updated BEM, simulated bottom concentrations at station N21, at the location of the outfall, are much higher than measurements. This is related to the model formulations and the precise position of station N21 relative to the outfall (see further detailed discussion in Section 3.3.2). Overall, both models reproduce winter surface concentrations well. In contrast to the former BEM, the updated BEM captures the higher concentrations observed at the surface above the DITP outfall. Finally, the decrease in surface DIN concentrations due to the phytoplankton spring bloom is faster in the updated BEM than in the measurements (and in the former BEM). However, the updated BEM performs better than the former BEM in simulating summer DIN depletion.

At harbor stations, the former BEM seems to slightly overestimate winter DIN concentrations, while the updated BEM slightly underestimates them. This is probably due to differences in the non-oceanic loads of the two models (see Section 3.1.2).

The comparison of vertical sections along an east-west transect through the outfall location (Figure 3-18 and Figure 3-19) confirms that the updated BEM shows much stronger changes in DIN concentrations with depth than in the former BEM from March to October. As in the former BEM, the signature of the outfall is visible all year round, leading to increased concentrations up to a distance of ~10 km. In the updated BEM, the signature of the outfall in winter near the surface is stronger than in the former BEM. This is consistent with time-series comparisons that show that the former BEM underestimated winter DIN concentrations near the surface at station N21. Finally, winter coastal DIN concentrations are lower in the updated BEM than in the former BEM, which agrees with the time-series differences at the harbor stations.

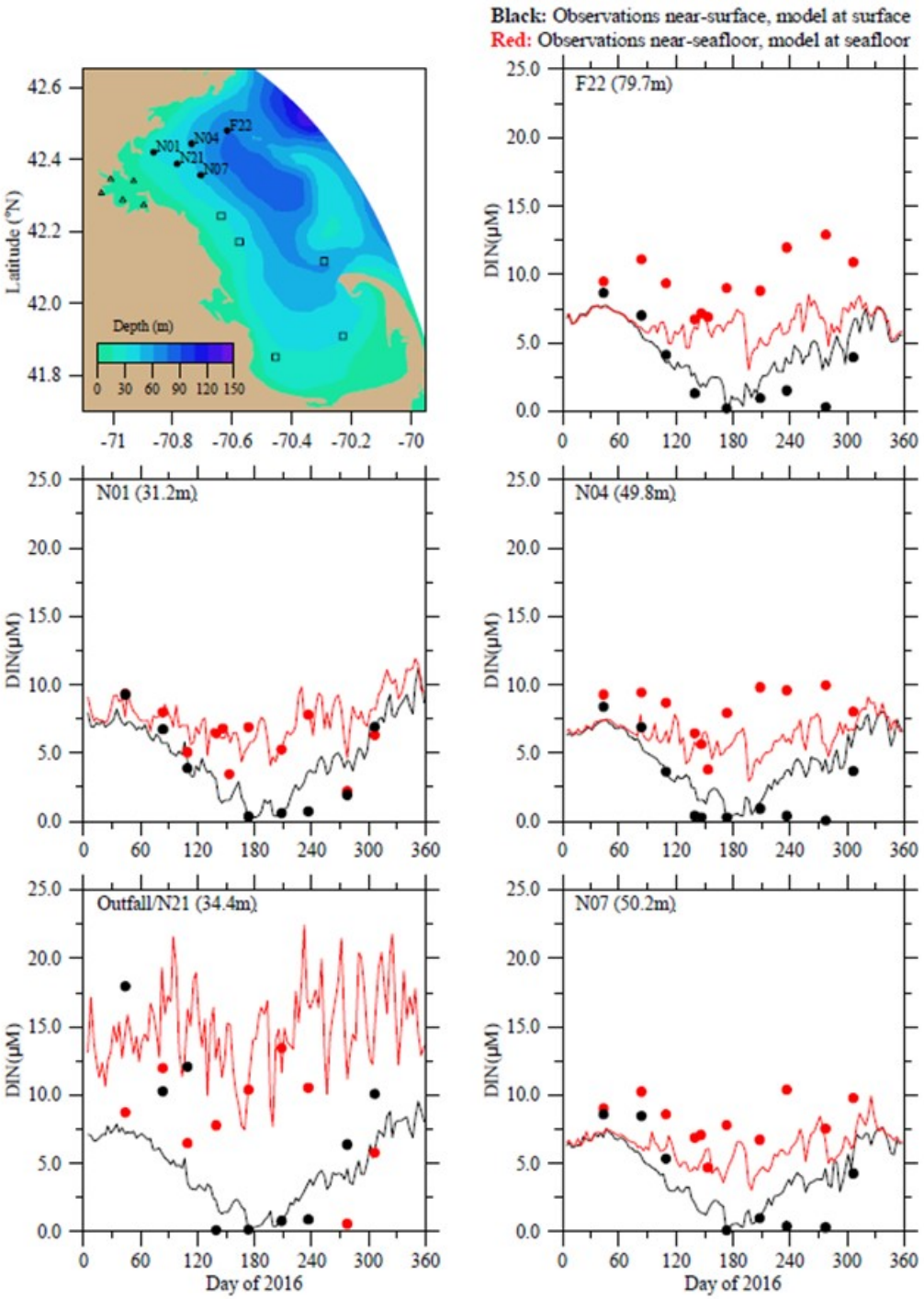

Figure 3-12 Dissolved inorganic nitrogen at Northern stations. Model-observation comparisons for 2016 for former BEM (Zhao et al. 2017, Figure 5-3a).

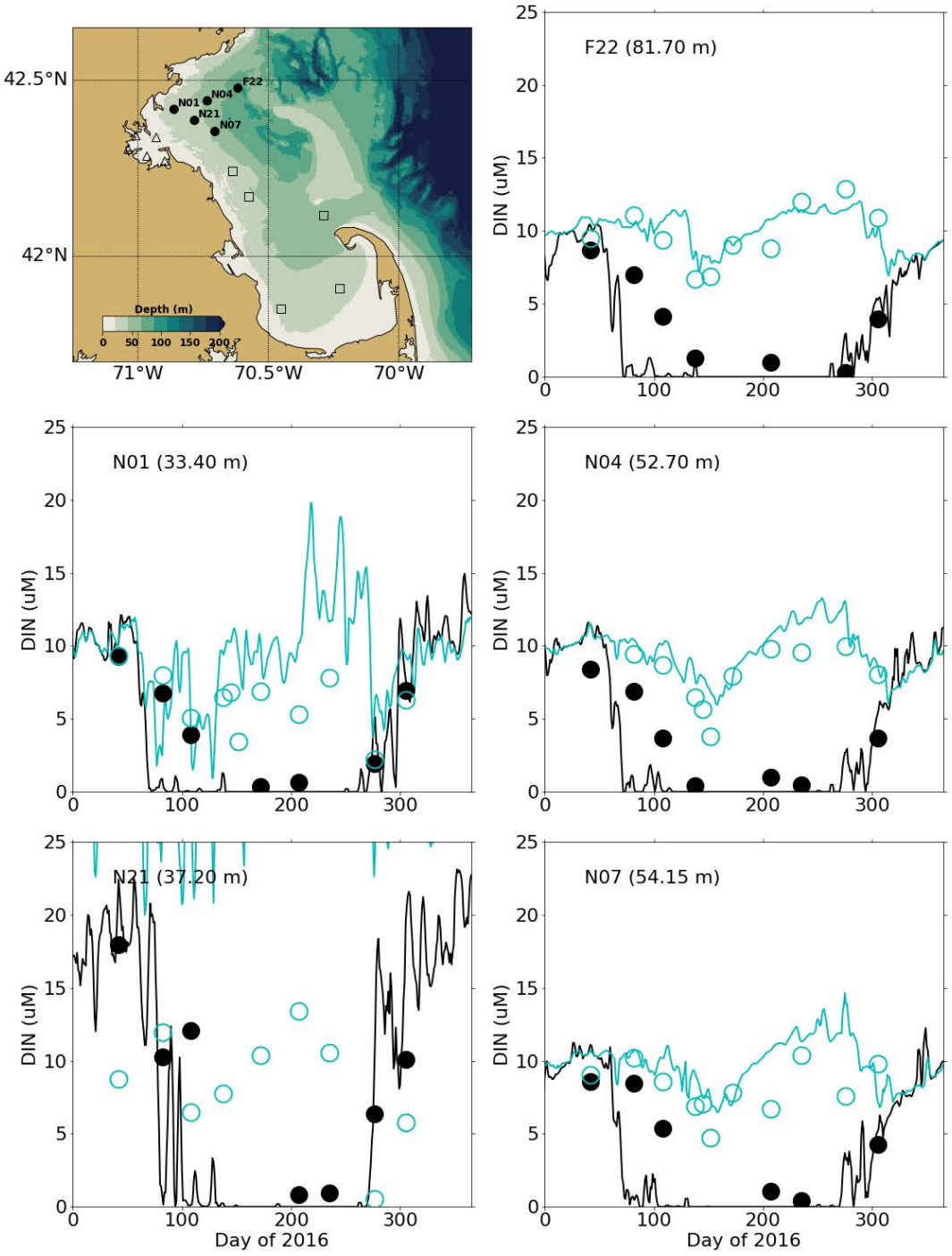

Figure 3-13 Dissolved inorganic nitrogen at Northern stations. Model-observation comparisons for 2016 for updated BEM. Black: observations near surface, model at water surface. Blue: observations near seafloor, model at bottom.

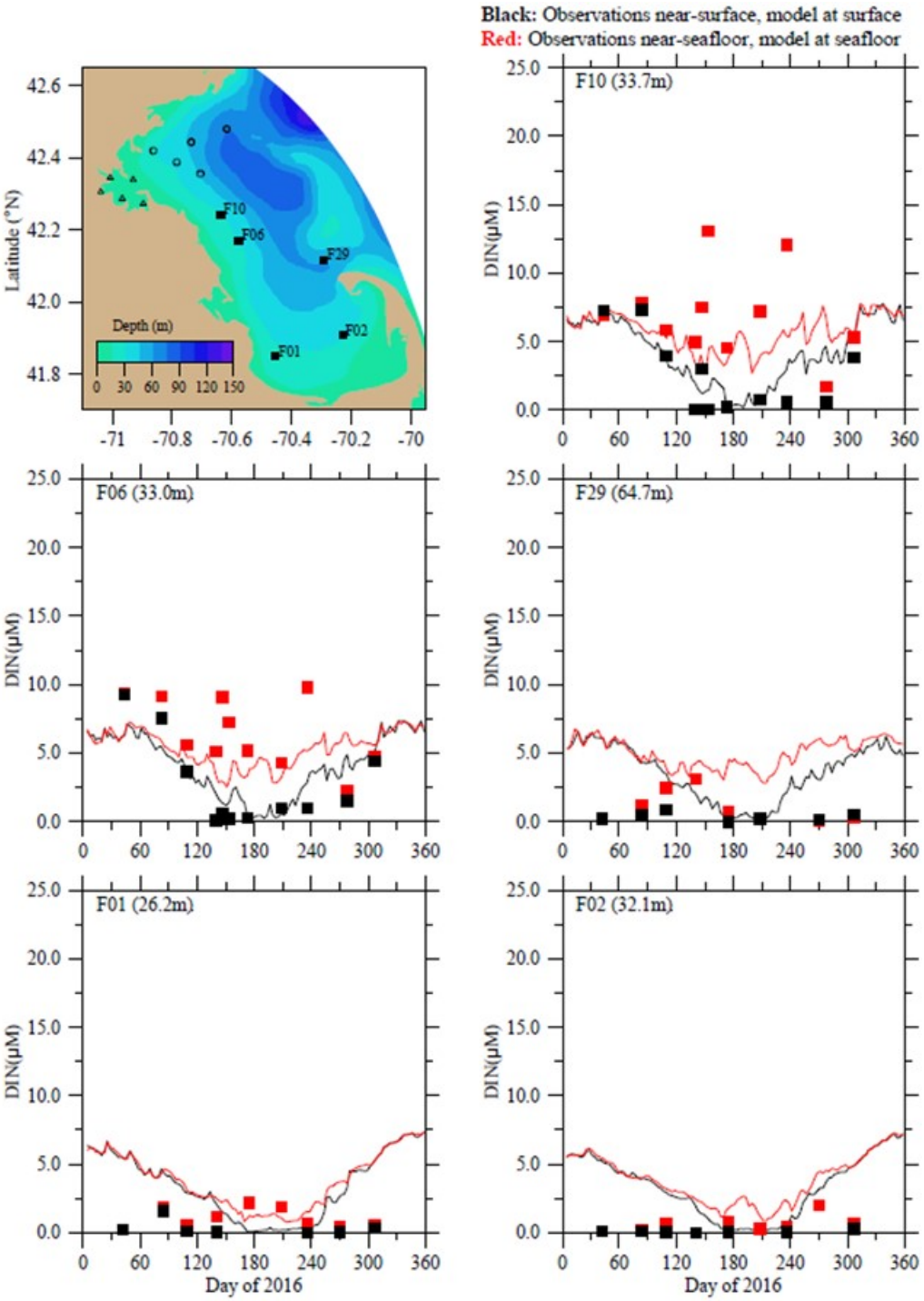

Figure 3-14 Dissolved inorganic nitrogen at Southern stations. Model-observation comparisons for 2016 for former BEM (Zhao et al. 2017, Figure 5-3b).

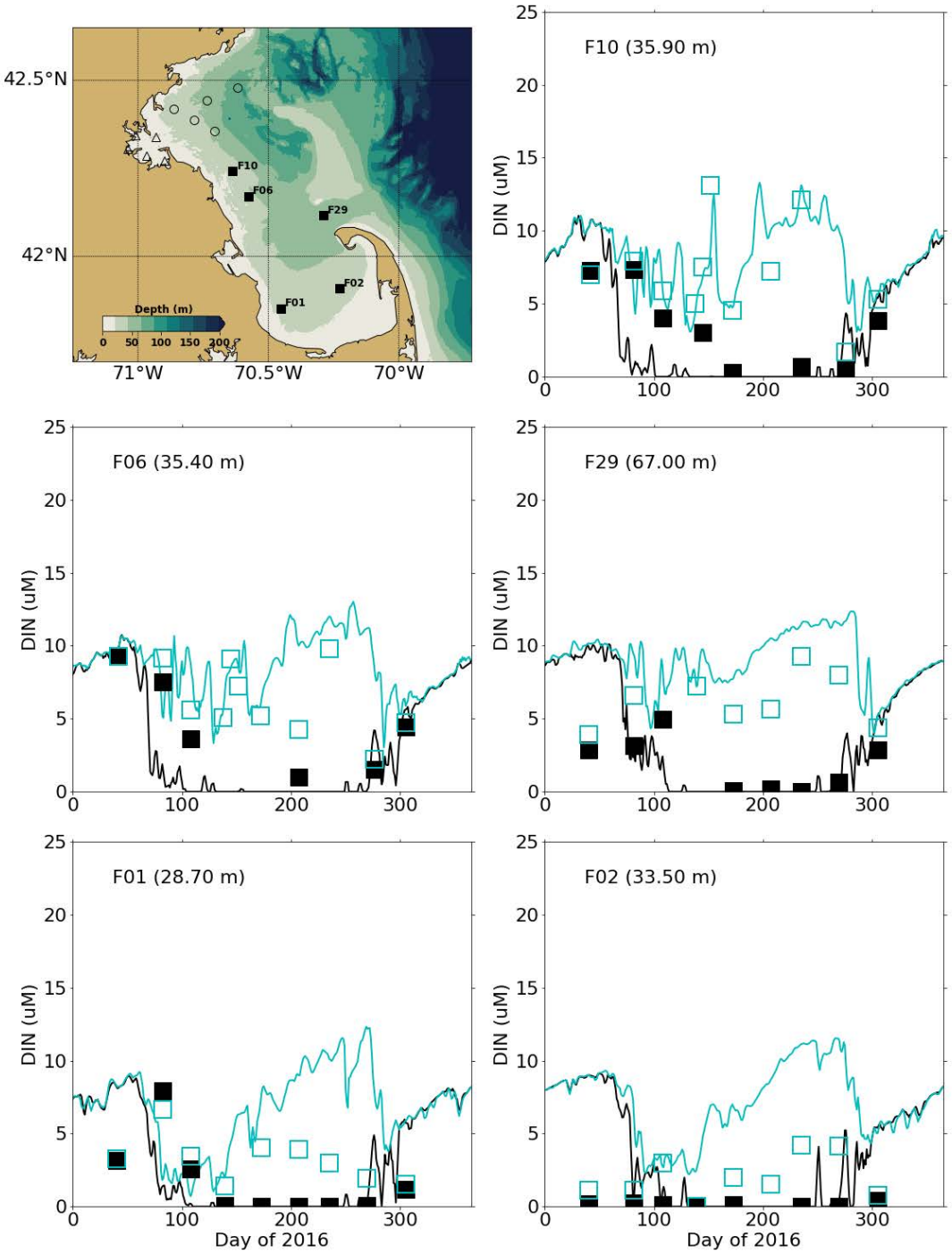

Figure 3-15 Dissolved inorganic nitrogen at Southern stations. Model-observation comparisons for 2016 for updated BEM. Black: observations near surface, model at water surface. Blue: observations near seafloor, model at bottom.

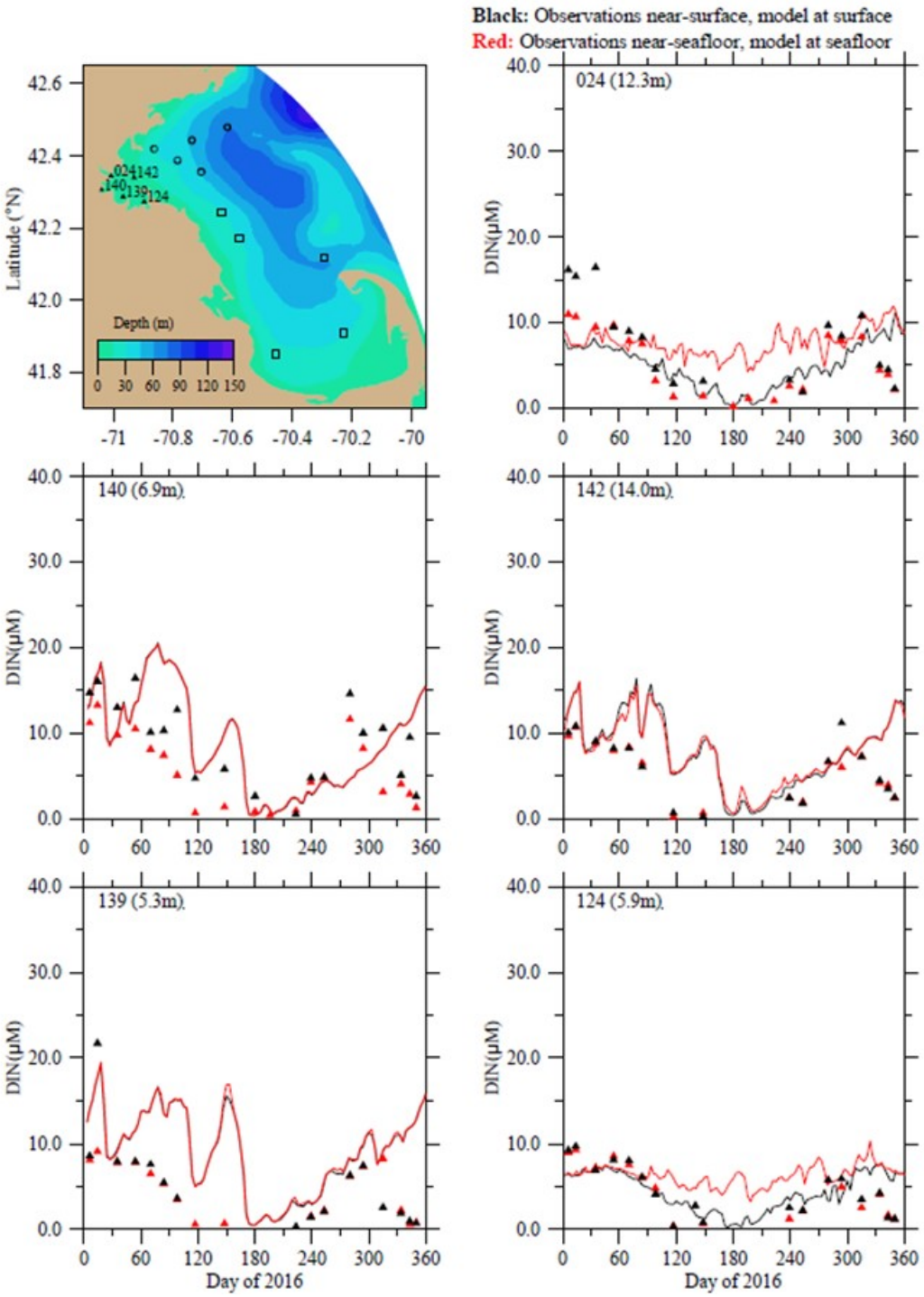

Figure 3-16 Dissolved inorganic nitrogen. Harbor stations. Model-observation comparisons for 2016. Note different y-axis scale than for bay stations in Figure 3-12 and Figure 3-14 (Zhao et al. 2017, Figure 5-3c).

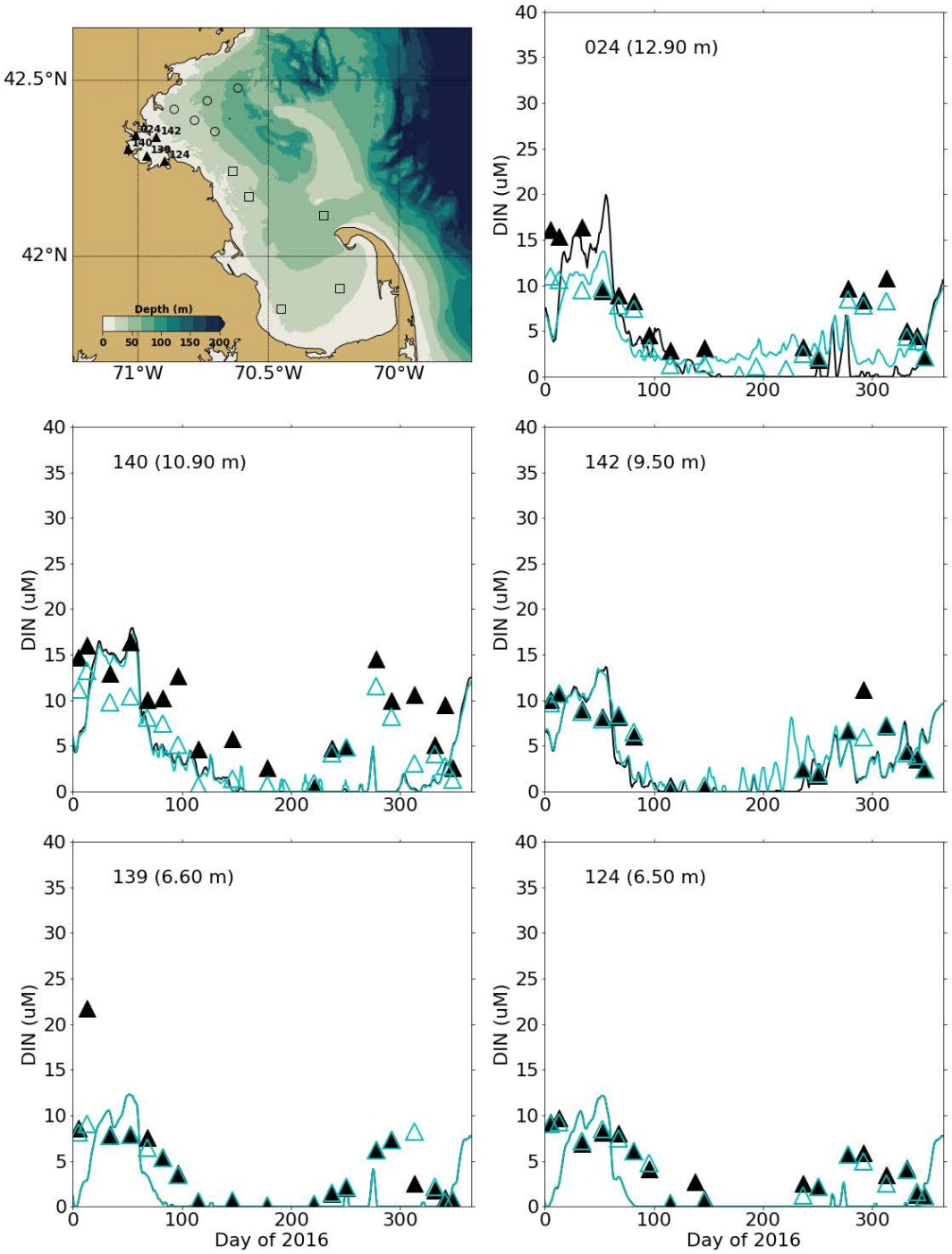

Figure 3-17 Dissolved inorganic nitrogen at Harbor stations. Model-observation comparisons for 2016 for updated BEM. Black: observations near surface, model at water surface. Blue: observations near seafloor, model at bottom.

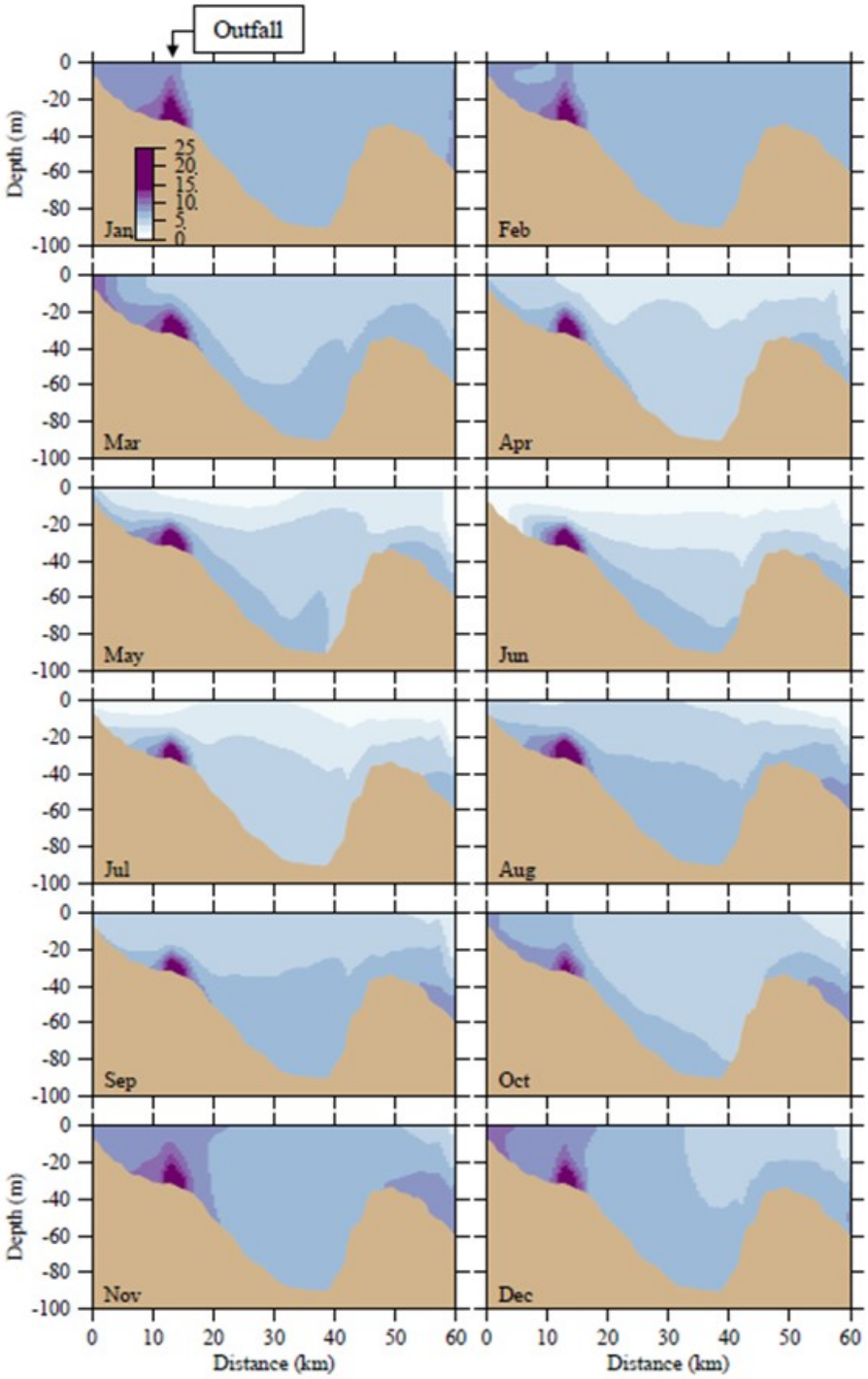

Figure 3-18 Dissolved inorganic nitrogen (µM). Former BEM results for 2016 along east-west transect (Figure 3-3). Horizontal axis is distance eastward from coast; outfall is on seafloor at approximately 13 km (Zhao et al. 2017, Figure 5-3d).

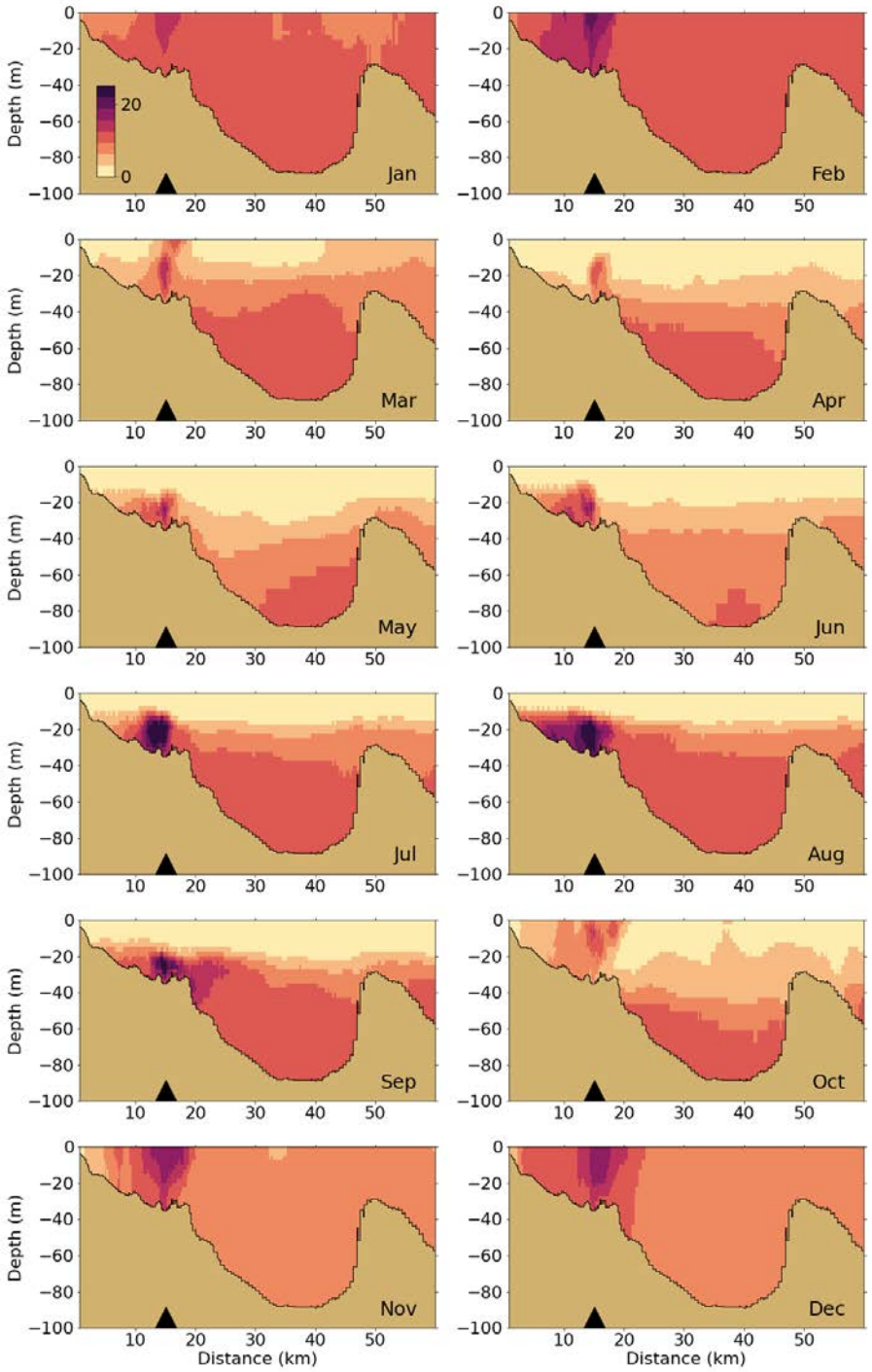

Figure 3-19 Dissolved inorganic nitrogen (µM). Updated BEM results for 2016 along east-west transect (Figure 3.1). Horizontal axis is distance eastward from coast; black triangle indicates the location of the outfall on seafloor.

3.2.4 Chlorophyll-a and primary productivity

Model-observation plots of chlorophyll are compared here for the former and updated BEM at Northern (Figure 3-20 and Figure 3-21), Southern (Figure 3-22 and Figure 3-23) and harbor stations (Figure 3-24 and Figure 3-25).

The former BEM chlorophyll concentrations show very little of the temporal variability observed in MWRA measurements and the model barely reproduces the observed differences between surface and seafloor values. In contrast, the updated BEM simulates strong seasonal variability of surface chlorophyll concentrations at the Northern and Southern stations, which matches well with the seasonal variations of the observations. Spring and fall peaks are well captured, while summer “base” concentrations tend to be slightly underestimated in the Northern stations (e.g., stations N04 and N07). The updated BEM captures the observed differences between upper and bottom layers of the water column, even though these differences tend be overestimated at some stations, where winter peaks are not captured (e.g., stations N07 and F22). The different behavior observed at station F02, where summer chlorophyll is higher at the bottom than at the surface, is not captured by either model.

In the harbor area, where the former BEM tends to underestimate chlorophyll concentrations, the updated BEM provides better average concentrations and variability. However, both models seem unable to reproduce the timing of the chlorophyll peaks (especially in December) that differs from those in the rest of the study area.

The vertical sections of chlorophyll concentrations along the east-west transect through the outfall show clear differences (Figure 3-26 and Figure 3-27). The former BEM calculates relatively high, vertically-uniform chlorophyll concentrations early in the year (January and February) and concentrations become lower from March-May, with a decreasing trend from the coast toward the open ocean. In the updated BEM, winter concentrations (November-February) are extremely low over the entire transect, except close to the coast. The highest concentrations are reached in March and April in the top 20 m of the water column. Both models estimate similar elevated concentrations in June-August in a subsurface layer, but the updated BEM shows higher vertical gradients. Finally, the former BEM shows high chlorophyll concentrations at the far east side of the transect that are not present in the updated BEM and that probably correspond to the boundary condition.

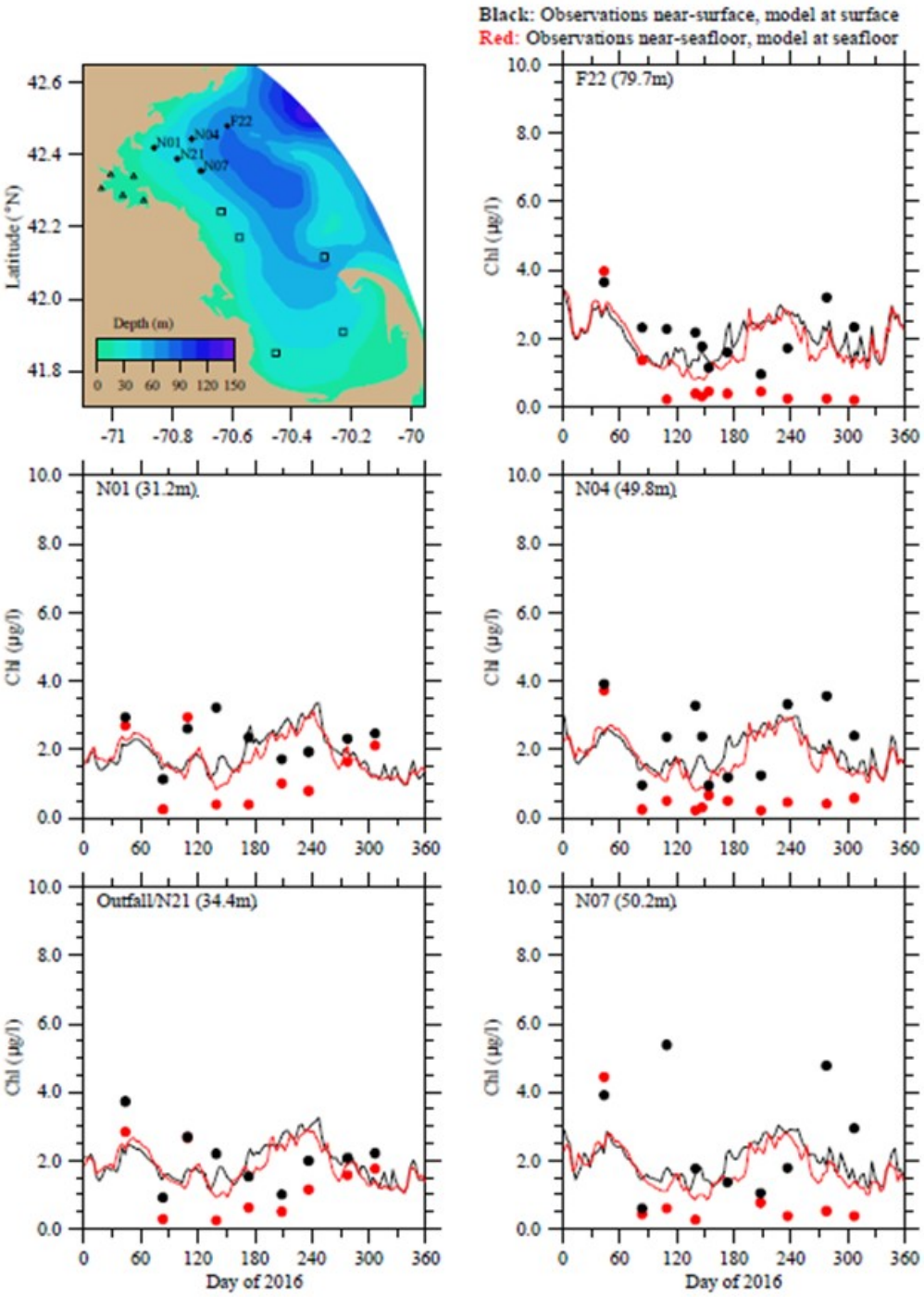

Figure 3-20 Chlorophyll at Northern stations. Model-observation comparisons for 2016 for former BEM (Zhao et al. 2017, Figure 5-4a).

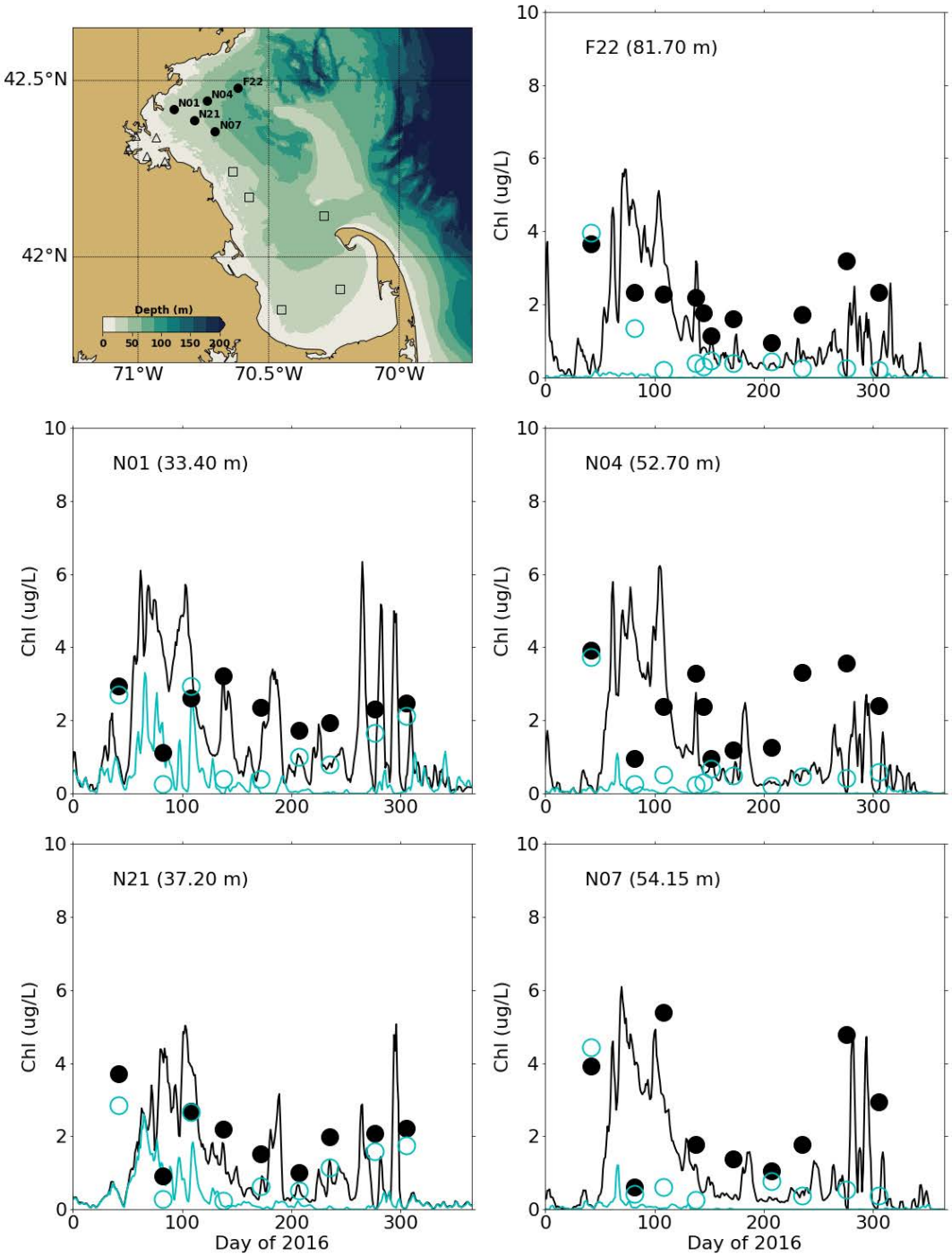

Figure 3-21 Chlorophyll at Northern stations. Model-observation comparisons for 2016 for updated BEM. Black: observations near surface, model at water surface. Blue: observations near seafloor, model at bottom.

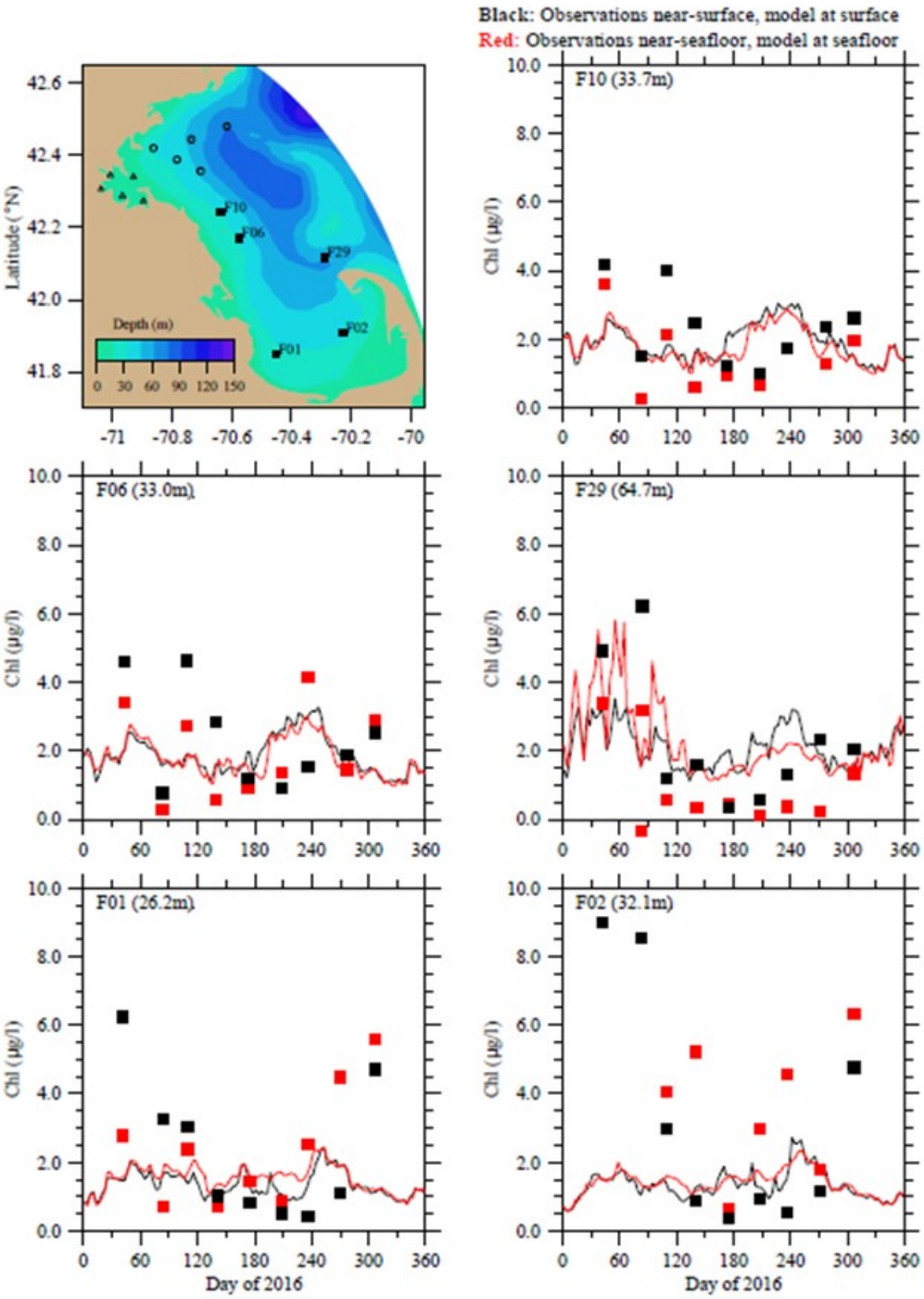

Figure 3-22 Chlorophyll at Southern stations. Model-observation comparisons for 2016 for former BEM (Zhao et al. 2017, Figure 5-4b).

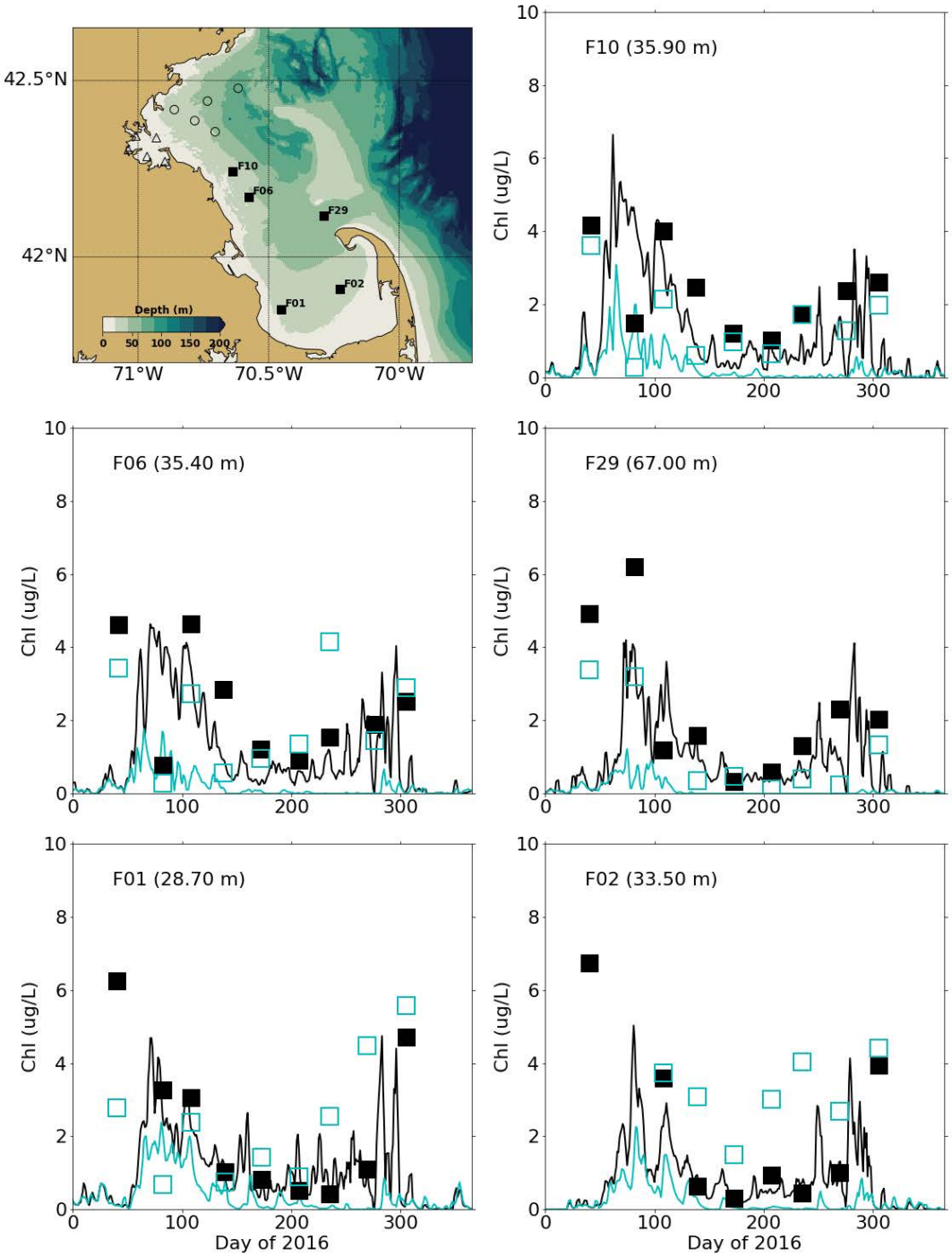

Figure 3-23 Chlorophyll at Southern stations. Model-observation comparisons for 2016 for updated BEM. Black: observations near surface, model at water surface. Blue: observations near seafloor, model at bottom.

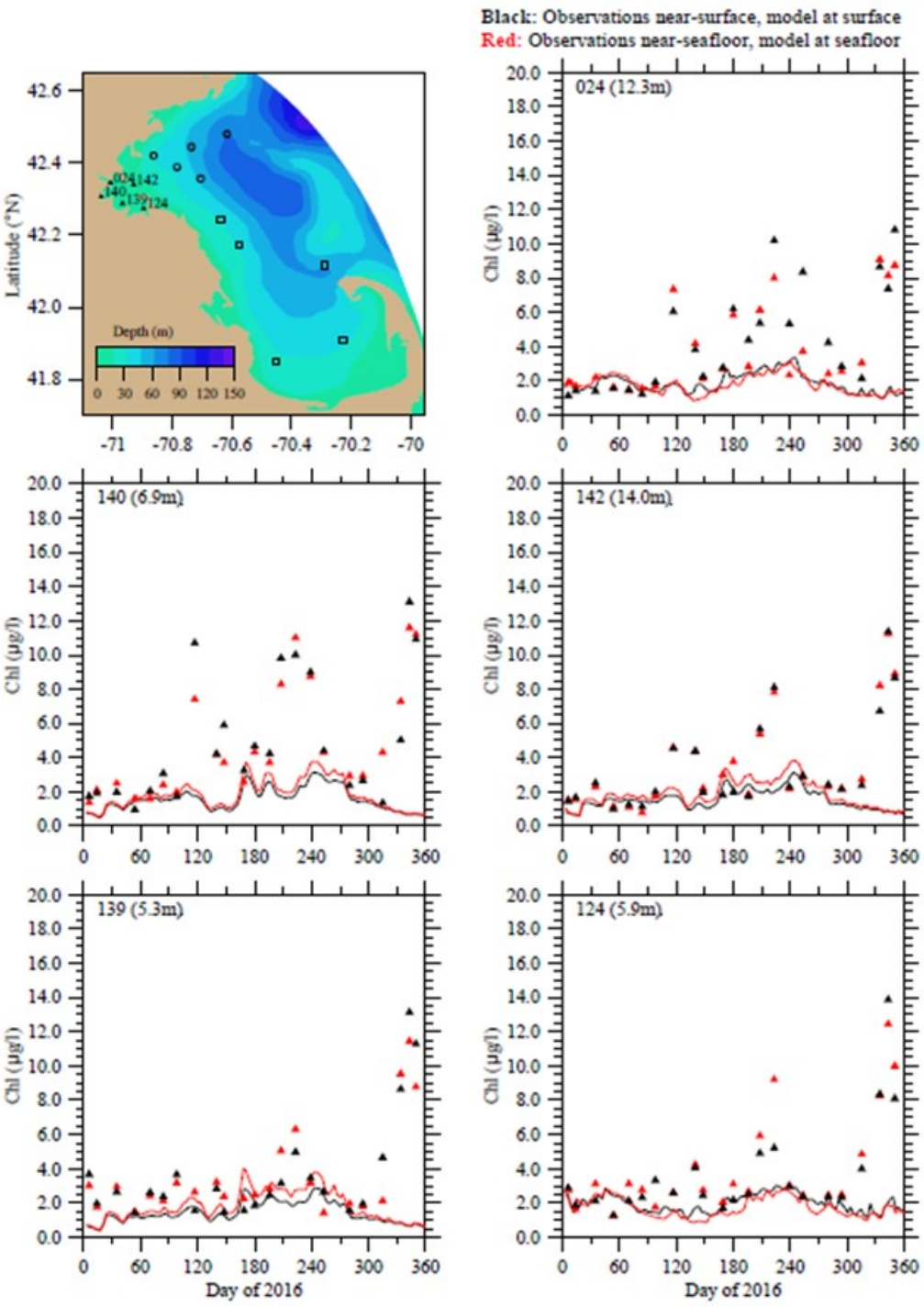

Figure 3-24 Chlorophyll at Harbor stations. Model-observation comparisons for 2016 for former BEM (Zhao et al. 2017, Figure 5-4c).

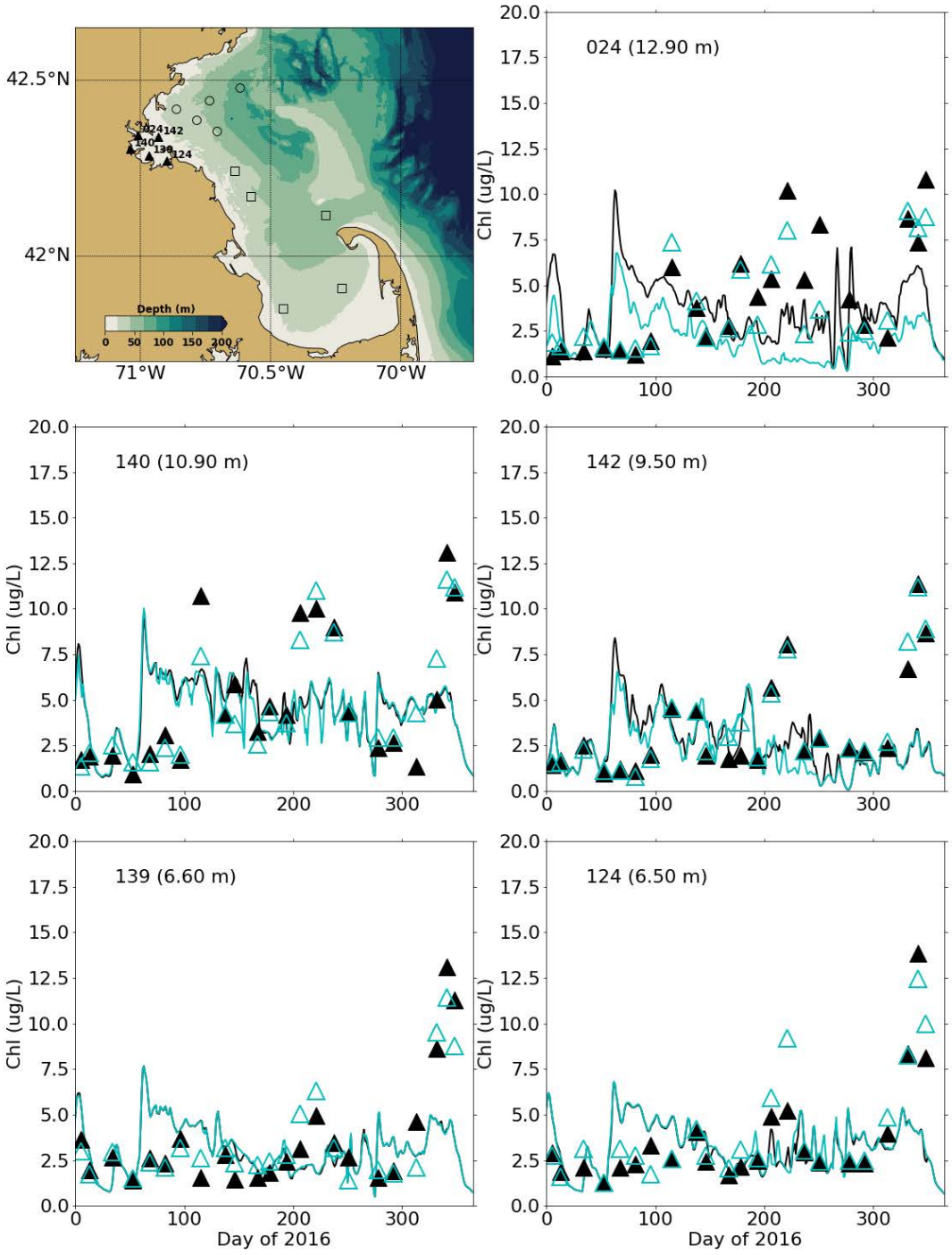

Figure 3-25 Chlorophyll at Harbor stations. Model-observation comparisons for 2016 for updated BEM. Black: observations near surface, model at water surface. Blue: observations near seafloor, model at bottom.

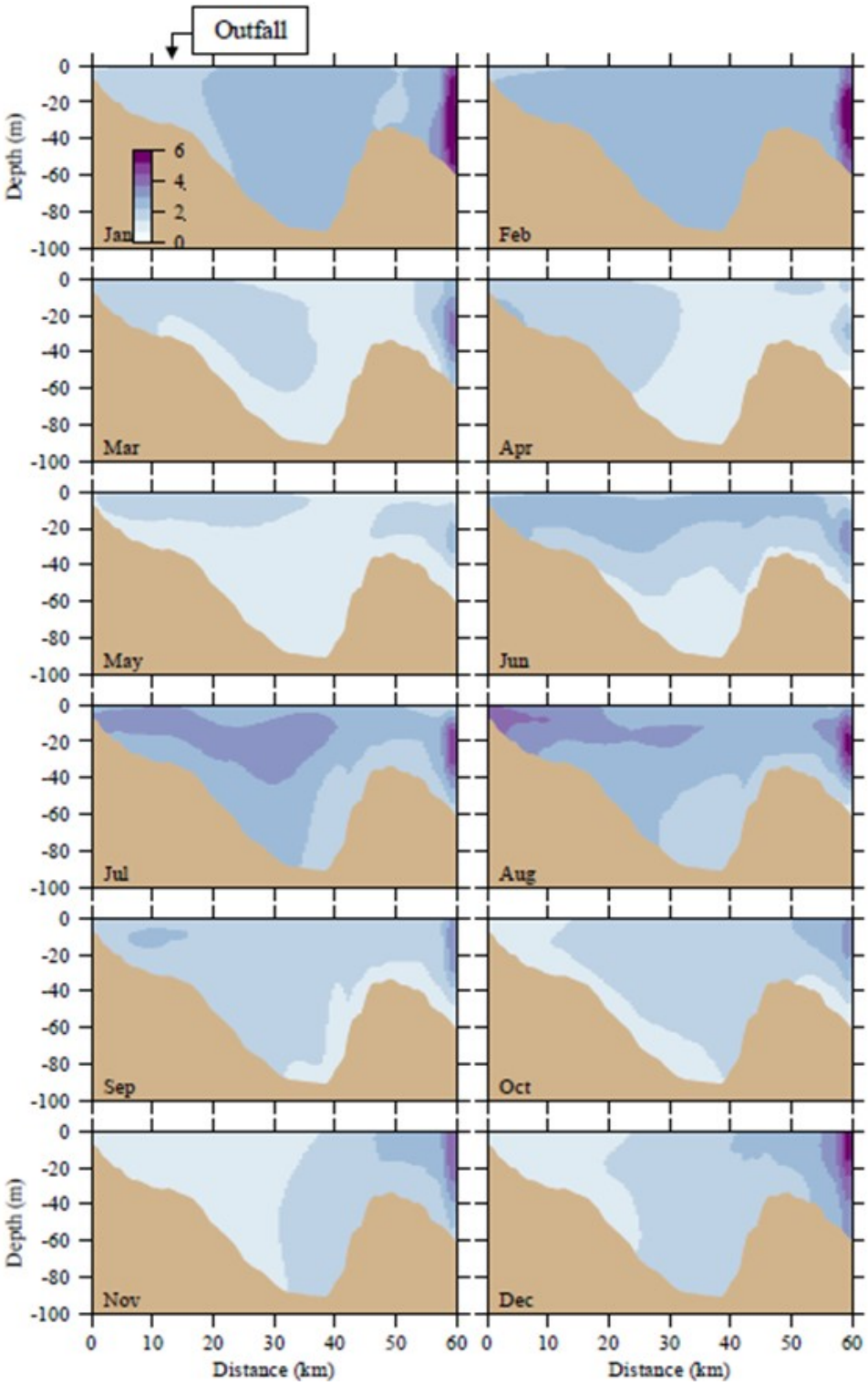

Figure 3-26 Chlorophyll (µg L^{-1}). Former BEM results along east-west transect for 2016 (Figure 3.1). Horizontal axis is distance eastward from coast; outfall is on seafloor at approximately 13 km (Zhao et al. 2017, Figure 5-3d).

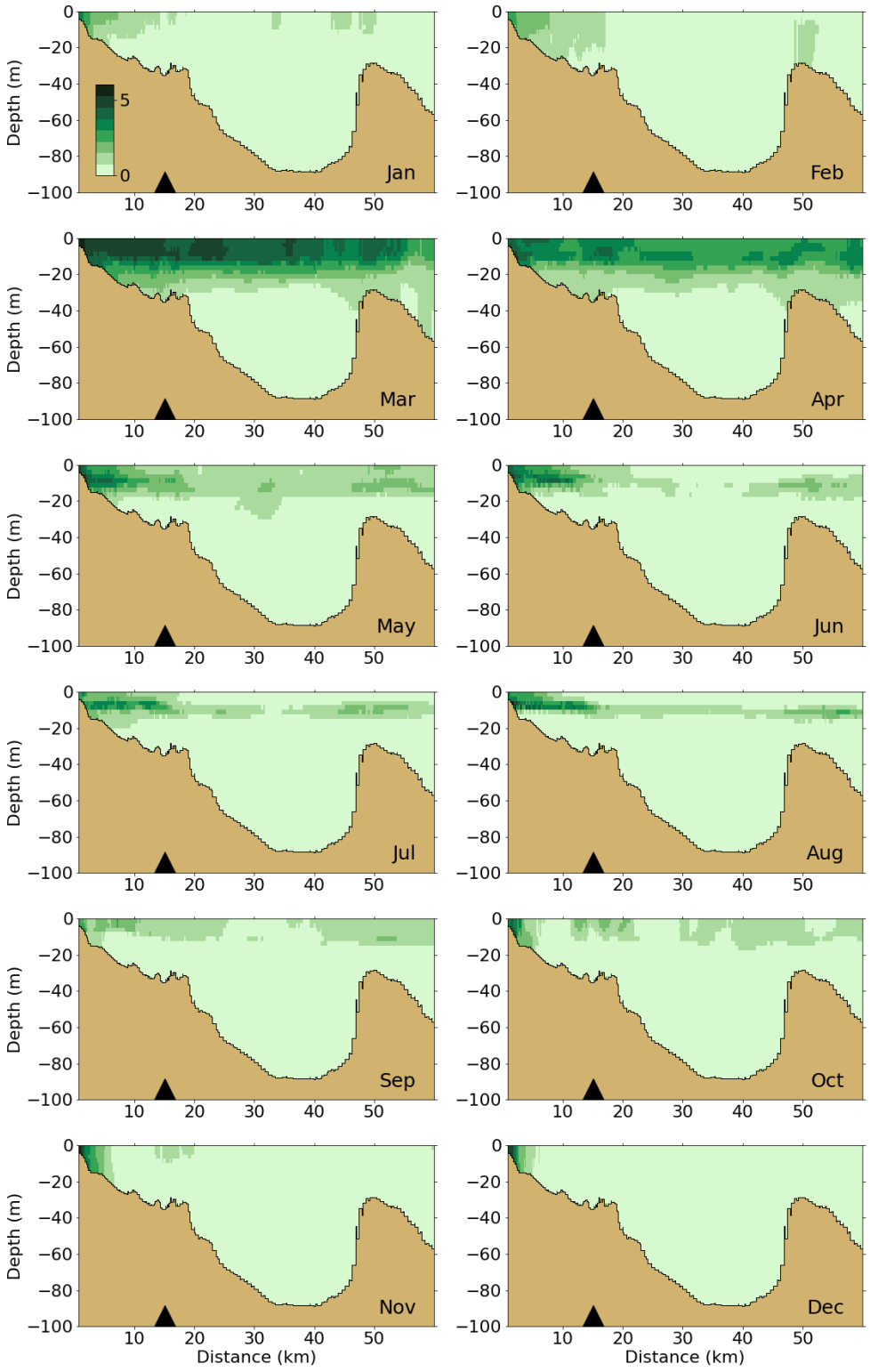

Figure 3-27 Chlorophyll (µg L^{-1}). Updated BEM results along east-west transect for 2016 (Figure 3.1). Horizontal axis is distance eastward from coast; black triangle indicates the location of the outfall on seafloor.

Net primary production time series from the former and updated BEMs are compared to observations from 1995-2010 using box-whisker plots (see Keay et al, 2012 and Zhao et al., 2017 for more details on the field methods; Figure 3-28 and Figure 3-29). Although the monitoring program for primary production ended in 2010, the observations are still relevant for indicating historical magnitude of production, as well as the geographic and seasonal patterns. Overall, primary production in the updated BEM is more variable than in the former BEM, and slightly higher. Values simulated with the updated BEM are in the range of historic observations, and seasonal variations are better reproduced than with the former BEM (i.e., higher values in spring and in fall). Both models predict a drop in primary production too early at the end the year, and underestimate winter values.

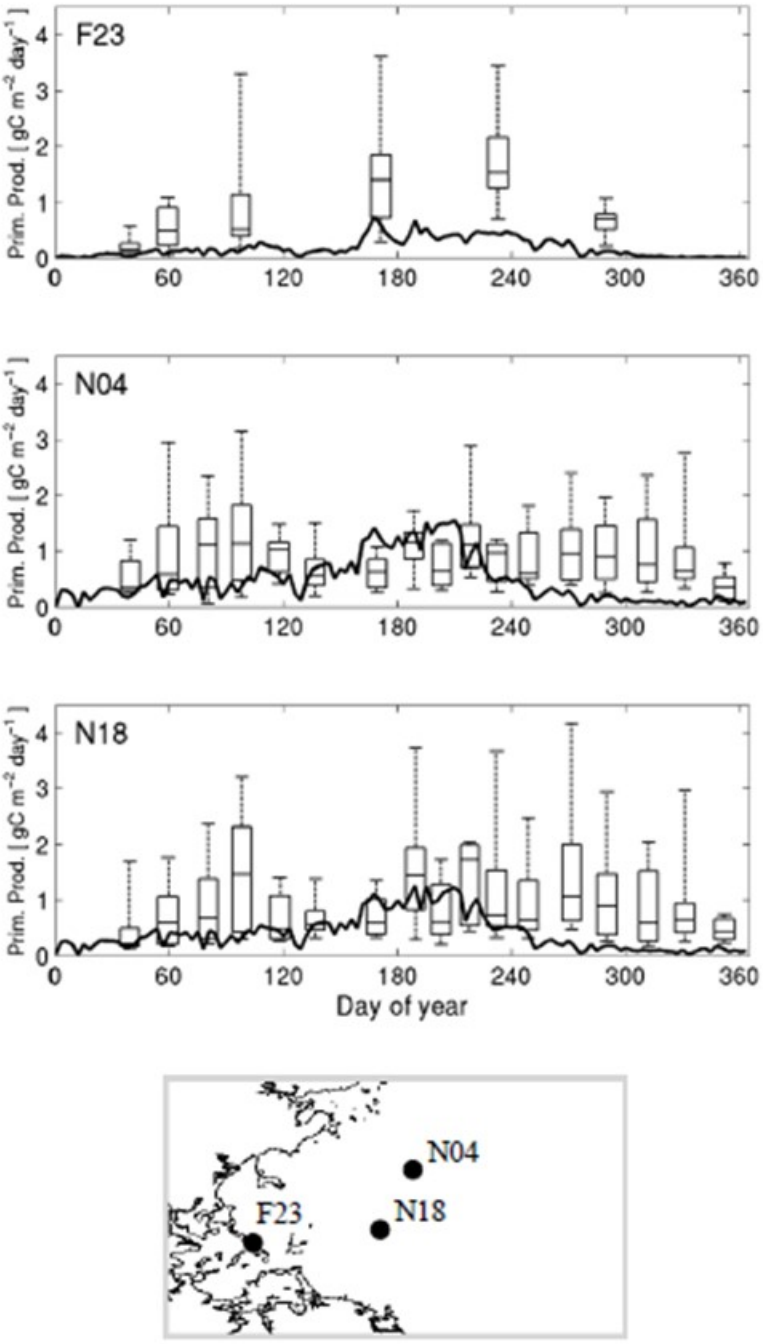

Figure 3-28 Primary production, vertically integrated, model-observation comparison for the former BEM. Line is 2016 model result. Box-whiskers are 1995-2010 observations; box shows 25th, 50th, 75th percentiles and whiskers are 9th and 91st percentiles (Zhao et al., 2017).

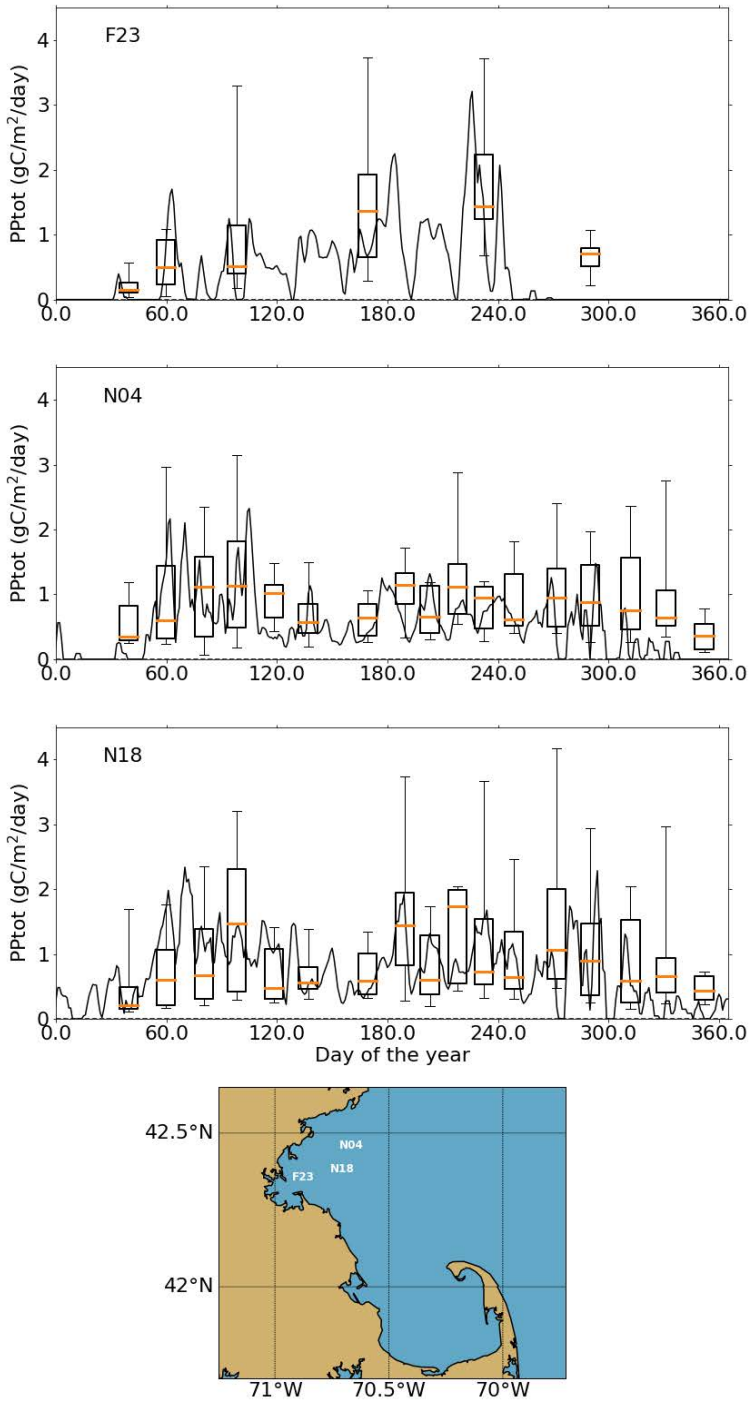

Figure 3-29 Primary production, vertically integrated, model-observation comparison for the updated BEM. Line is 2016 model result. Box-whiskers are 1995-2010 observations; box shows 25th, 50th, 75th percentiles and whiskers are 9th and 91st percentiles.

3.2.5 Dissolved and Particulate Organic Nitrogen

Comparison of model-observation plots of dissolved organic nitrogen (DON) concentrations for the former and updated BEMs at Northern (Figure 3-30 and Figure 3-31) and Southern stations (Figure 3-32 and Figure 3-33) show that, while the former BEM underestimates DON variability and tends to match only lowest observed values, the updated BEM reproduces DON variability well. Small differences between concentrations in the surface and bottom layers, which were not present in the former BEM, are better represented by the updated BEM. While the former BEM predicted similar concentrations at the outfall location as at other Northern stations, the updated BEM reproduces the slightly more elevated surface DON concentrations at station N21, but slightly overestimates concentrations near the bottom compared to measurements.

The vertical cross-section of DON concentrations from the former and updated BEMs along the east-west transect through the outfall shows some clear differences (Figure 3-34 and Figure 3-35). While DON concentrations show barely any vertical gradients in the former BEM, a clear decrease of DON concentrations from the surface toward the bed is visible in the updated BEM. The former BEM estimates low concentrations throughout the entire cross-section all year round, with slightly higher concentrations in October-December. The updated BEM has the highest values near the surface between July and October. Finally, in the updated BEM, DON concentrations are higher all year round close to the coast, which is not visible in the former BEM.

Comparison of model-observation plots of particulate organic nitrogen (PON) concentrations for the former and updated BEMs at Northern (Figure 3-36 and Figure 3-37) and Southern stations (Figure 3-38 and Figure 3-39) show that both models estimate average concentrations well. While the former BEM tends to underestimate PON variability, the updated BEM tends to overestimate it. The updated BEM reproduces differences between surface and bottom layers better.

The former BEM shows barely any vertical gradients in monthly PON concentrations over the east-west vertical cross-section through the outfall, except in June (Figure 3-40). The updated BEM shows clear vertical gradients from March to October (Figure 3-41), with highest concentrations near the surface (linked to high phytoplankton biomass). In both models, there is no evidence of the effect of the outfall on PON concentrations. Finally, PON concentrations in the updated BEM are higher near the coast all year round, which is not the case in the former BEM.

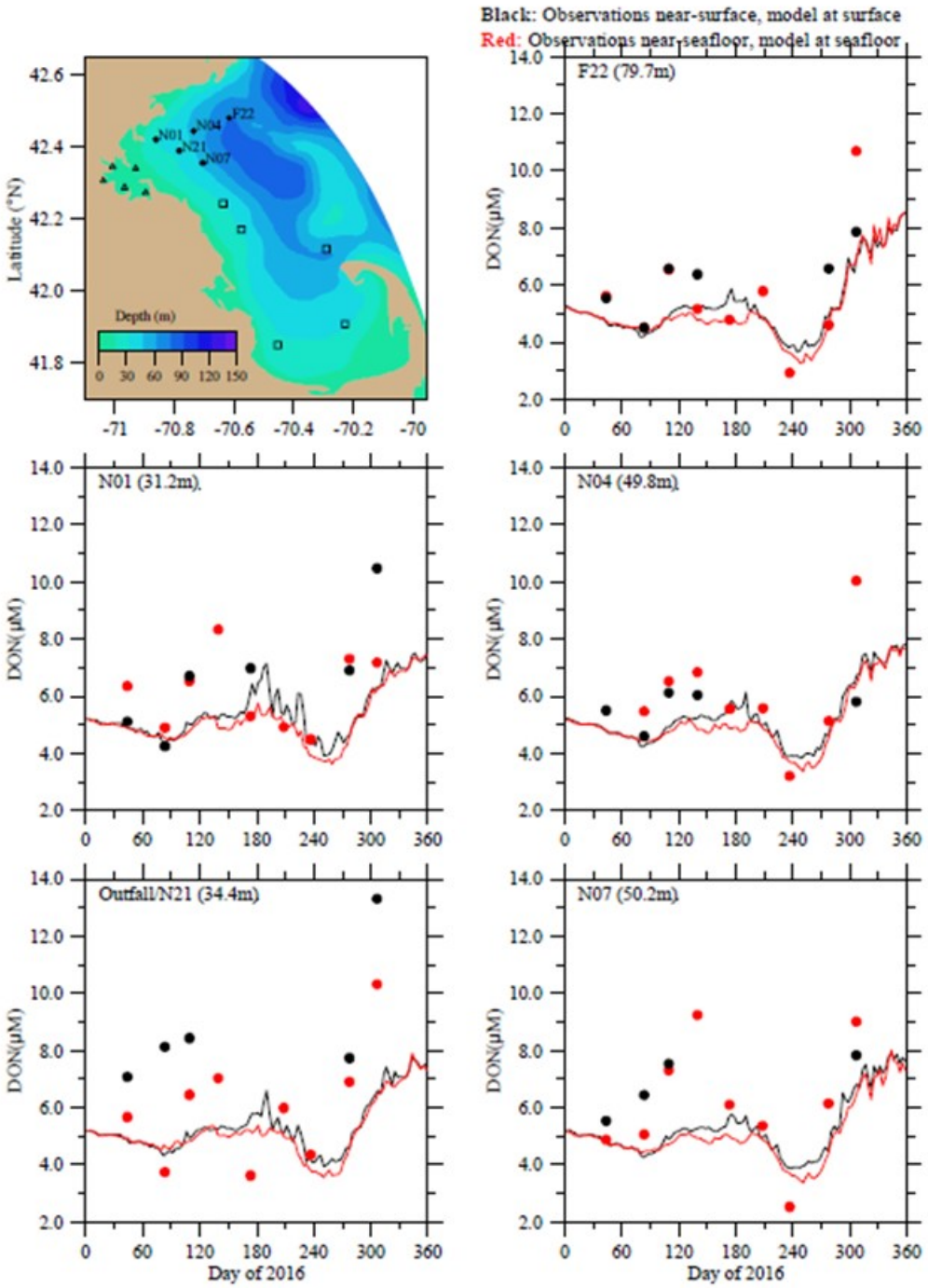

Figure 3-30 Dissolved organic nitrogen at Northern stations. Model-observation comparisons for 2016 for former BEM (Zhao et al. 2017, Figure 5-6a).

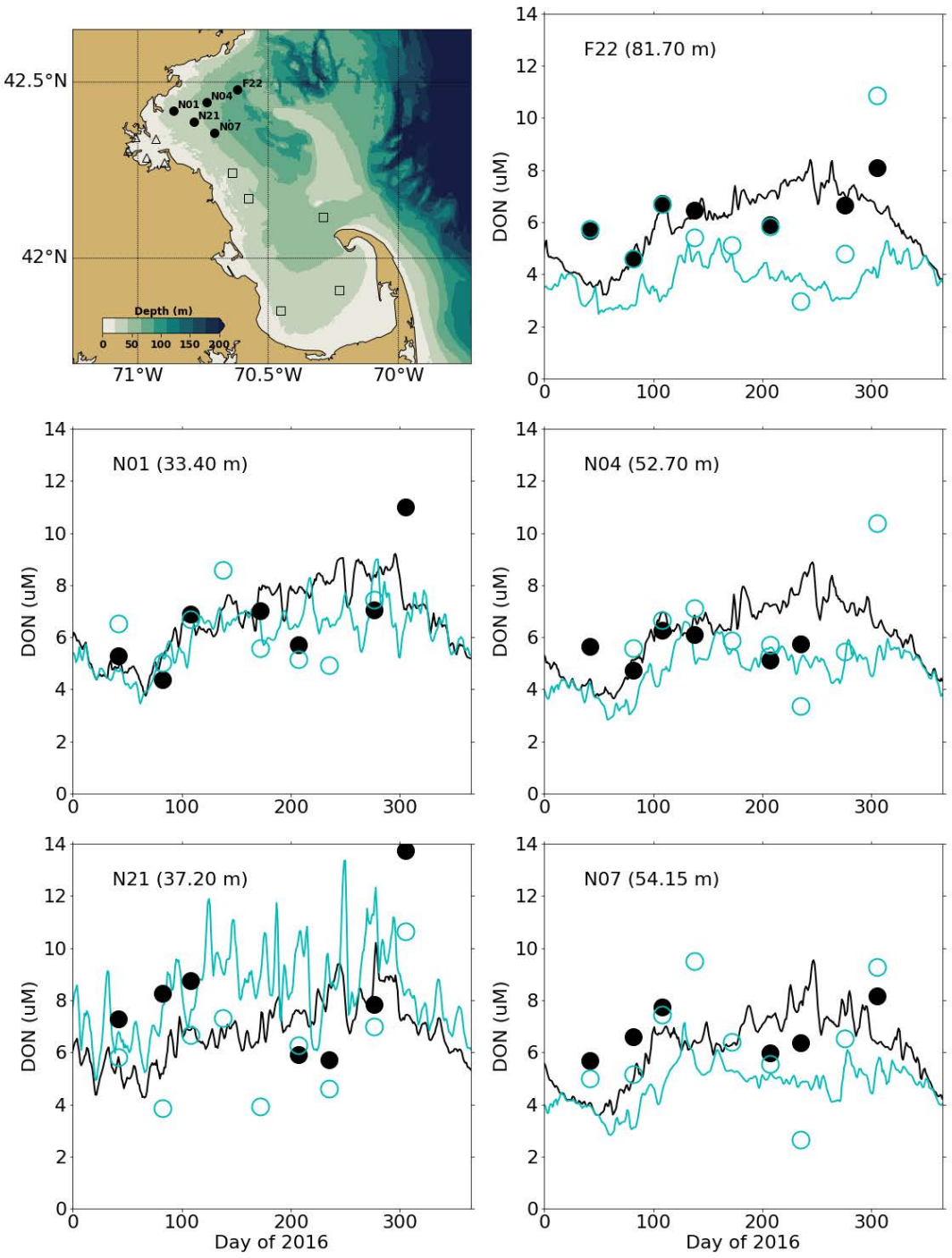

Figure 3-31 Dissolved organic nitrogen at Northern stations. Model-observation comparisons for 2016 for updated BEM. Black: observations near surface, model at water surface. Blue: observations near seafloor, model at bottom.

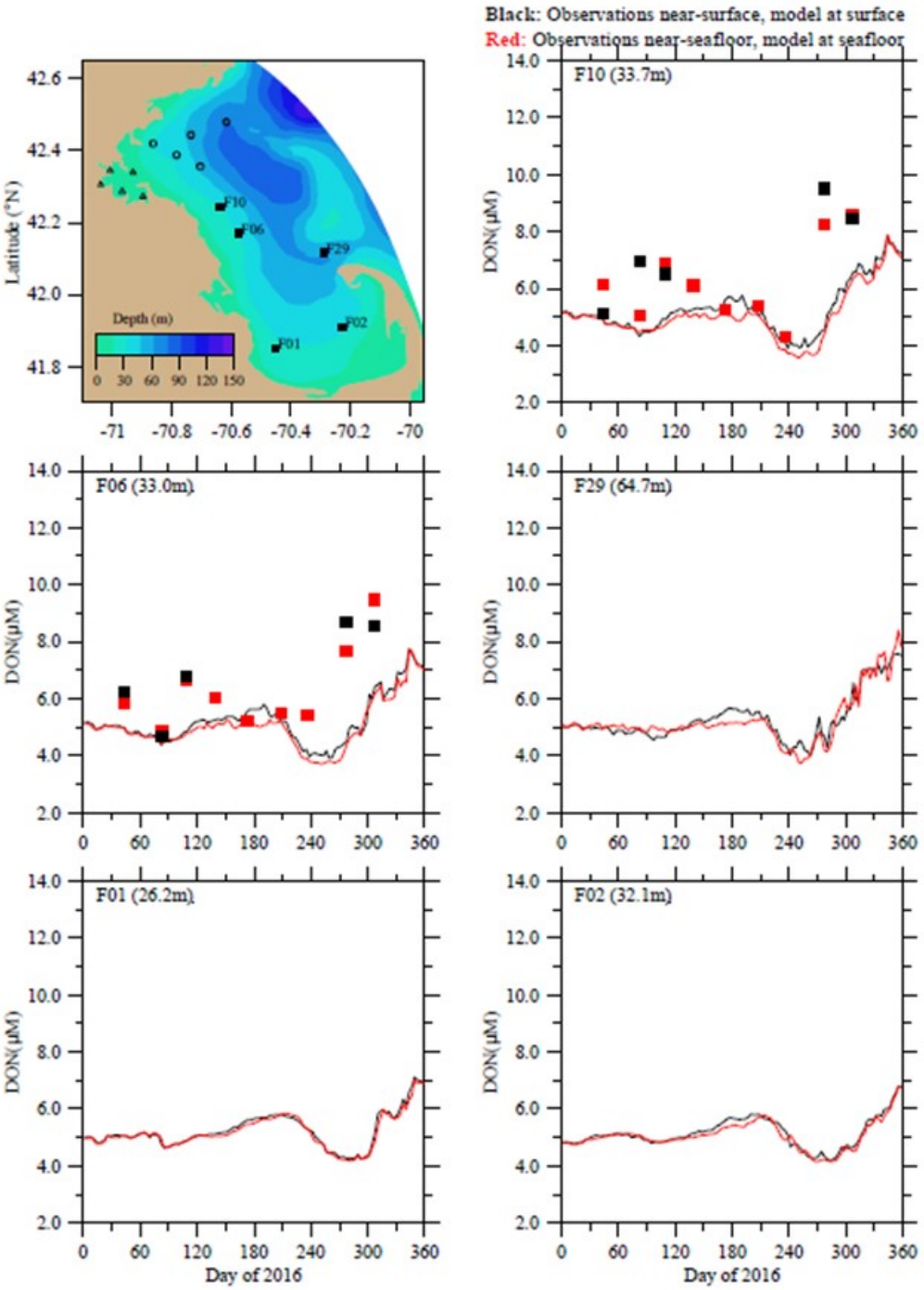

Figure 3-32 Dissolved organic nitrogen at Northern stations. Model-observation comparisons for 2016 for former BEM (Zhao et al. 2017, Figure 5-6b).

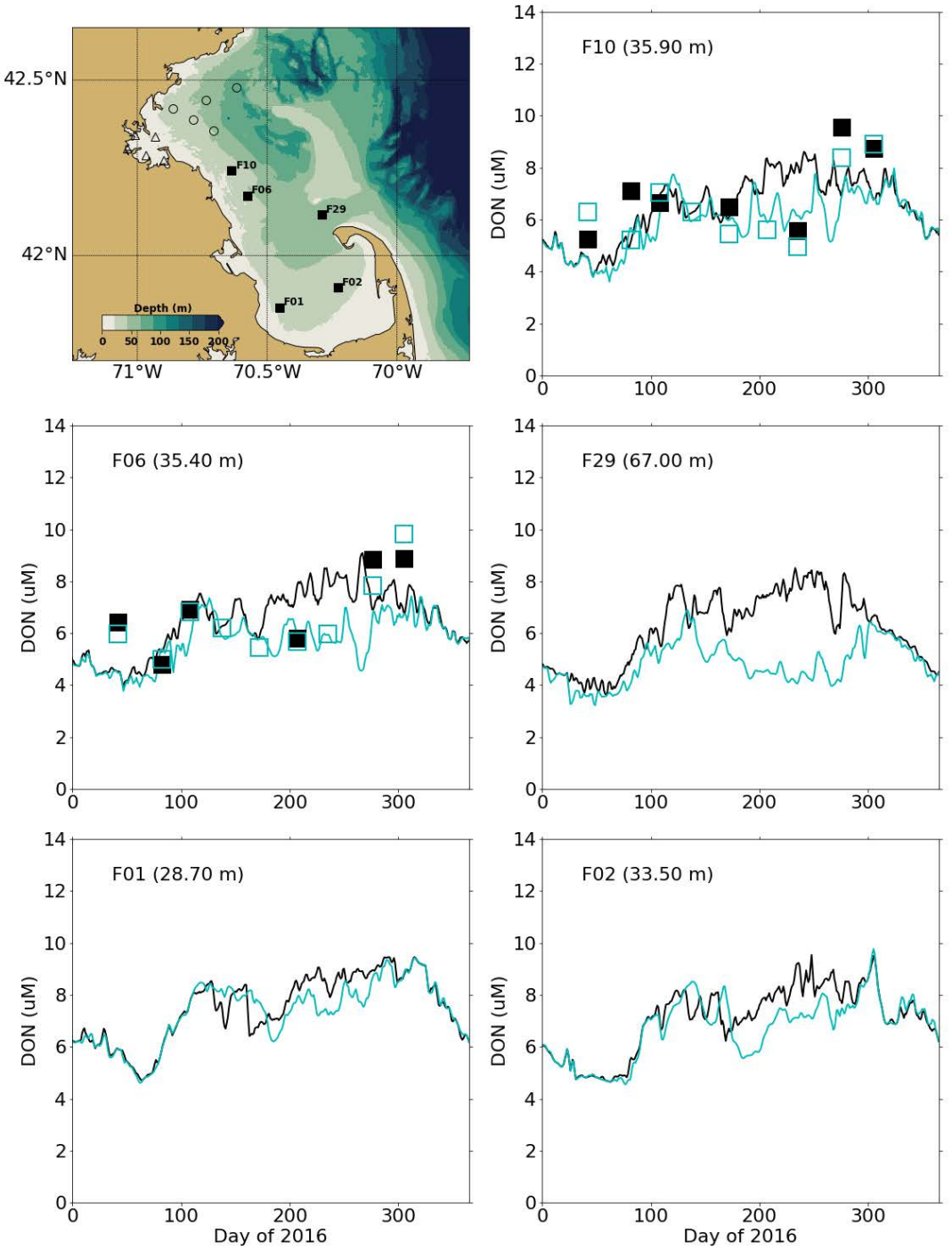

Figure 3-33 Dissolved organic nitrogen at Southern stations. Model-observation comparisons for 2016 for updated BEM. Black: observations near surface, model at water surface. Blue: observations near seafloor, model at bottom.

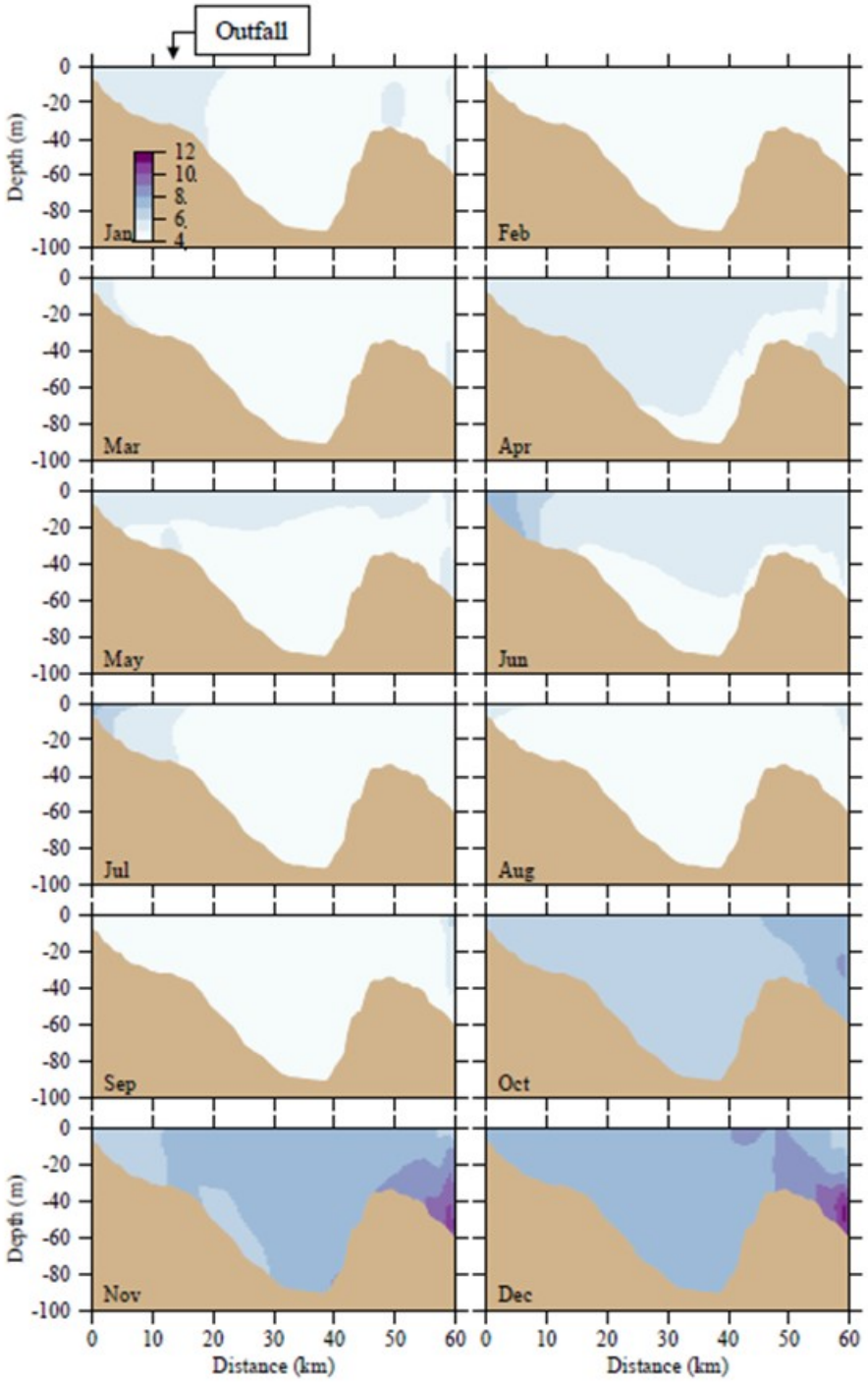

Figure 3-34 Dissolved organic nitrogen (µM). Former BEM results for 2016 along east-west transect (Figure 3.1). Horizontal axis is distance eastward from coast; outfall is on seafloor at approximately 13 km (Zhao et al. 2017, Figure 5-6c).

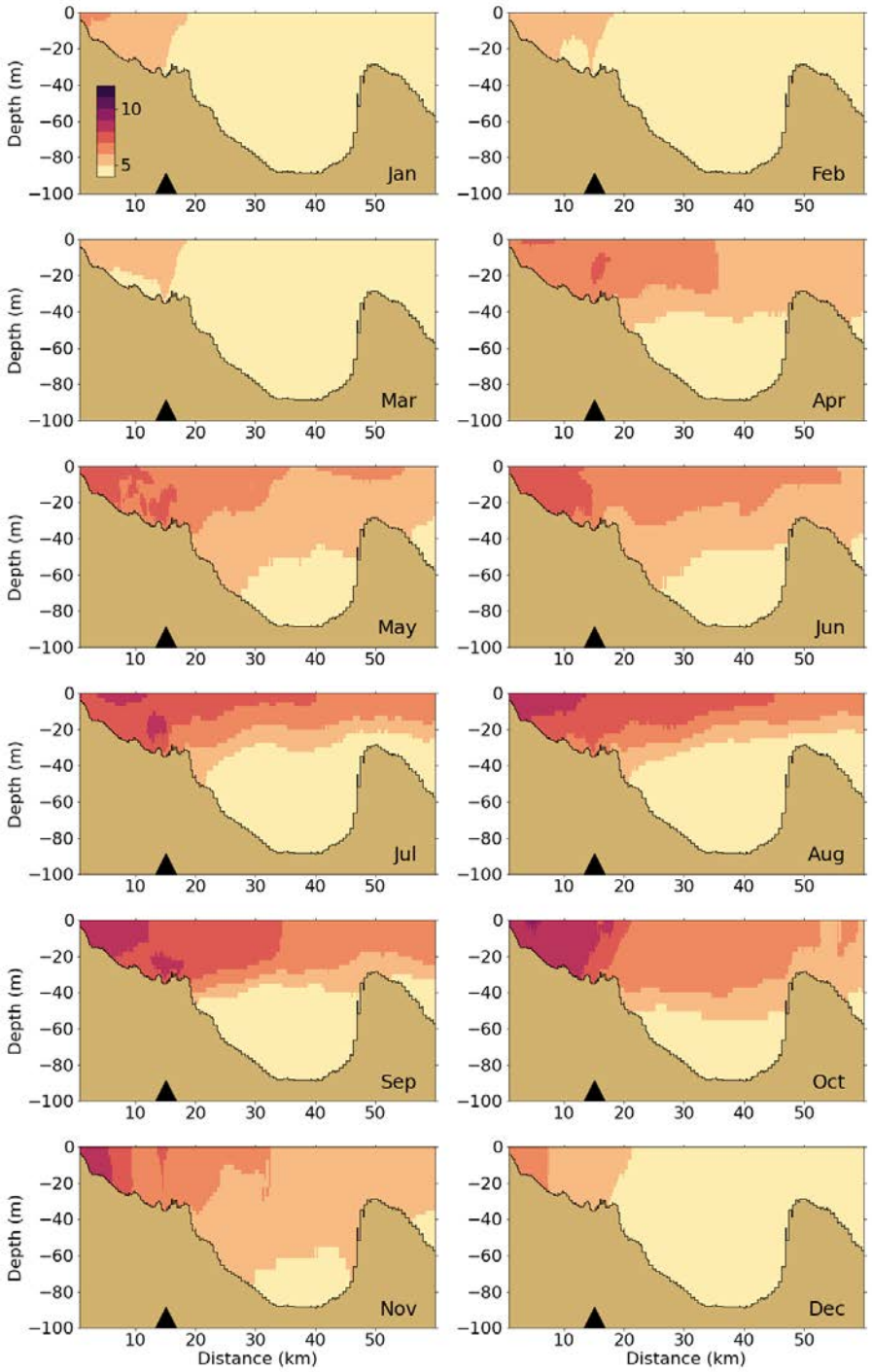

Figure 3-35 Dissolved organic nitrogen (µM). Updated BEM results for 2016 along east-west transect (Figure 3.1). Horizontal axis is distance eastward from coast; black triangle indicates the location of the outfall on seafloor.

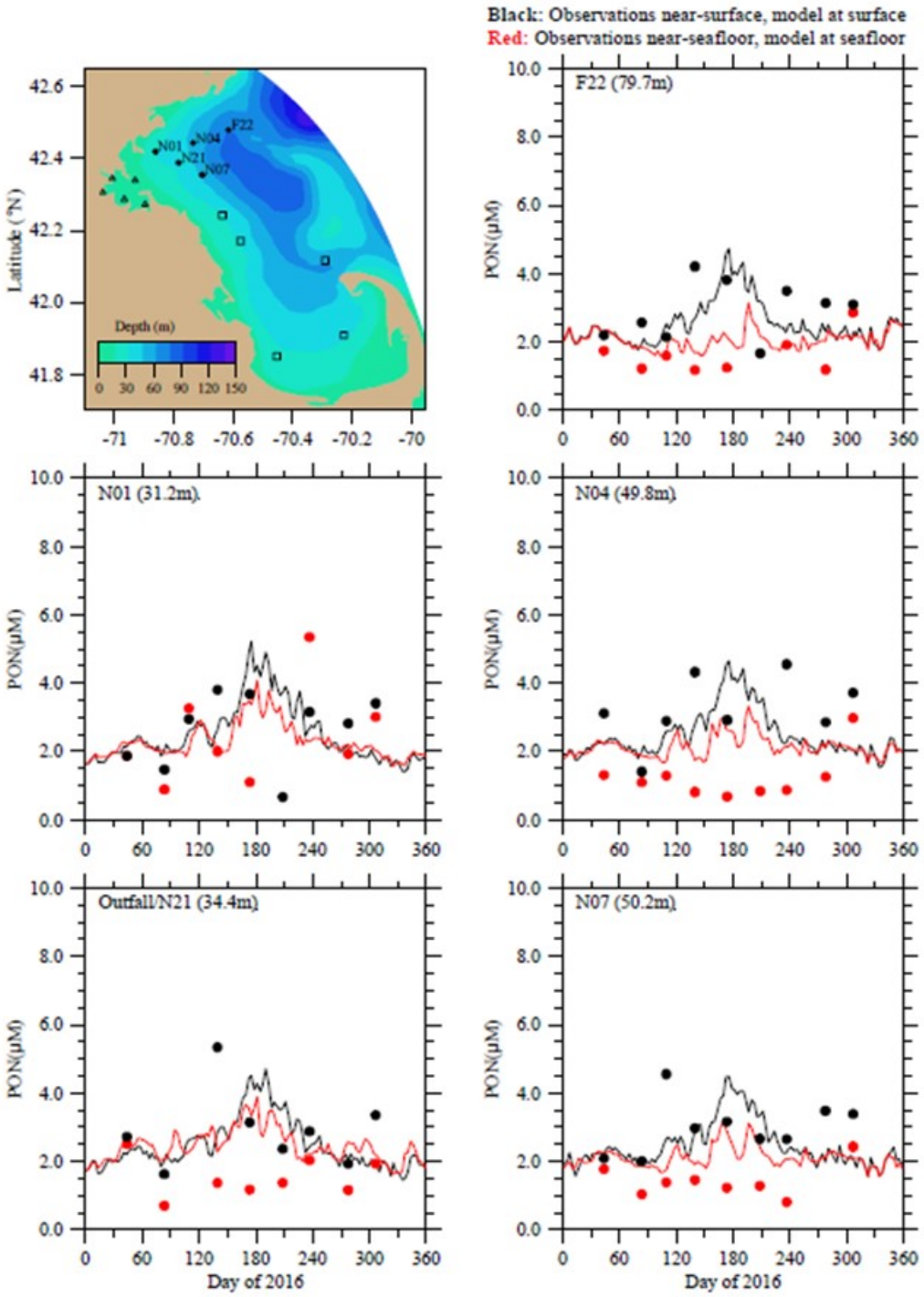

Figure 3-36 Particulate organic nitrogen at Northern stations. Model-observation comparisons for 2016 for former BEM (Zhao et al. 2017, Figure 5-7a).

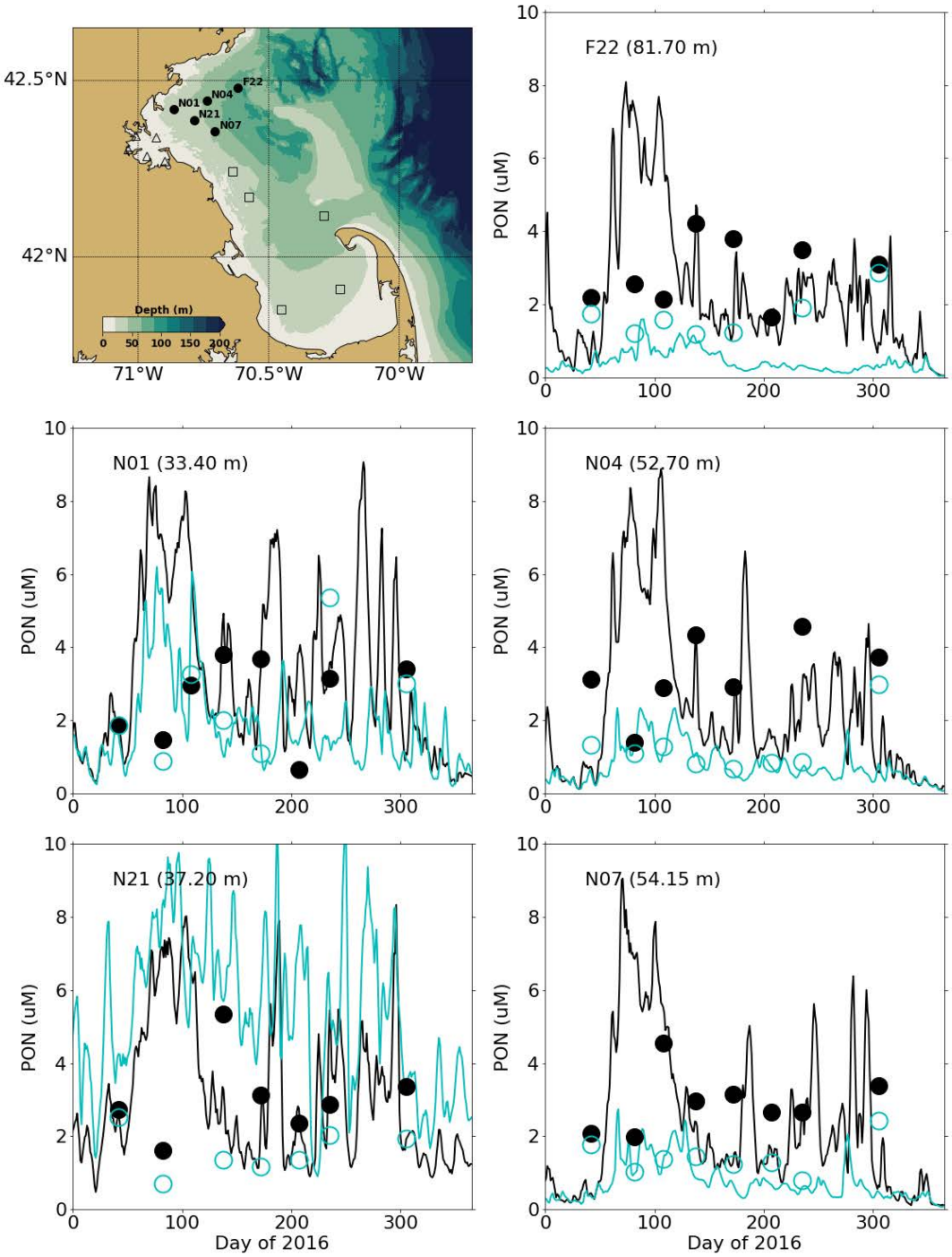

Figure 3-37 Particulate organic nitrogen at Northern stations. Model-observation comparisons for 2016 for updated BEM. Black: observations near surface, model at water surface. Blue: observations near seafloor, model at bottom.

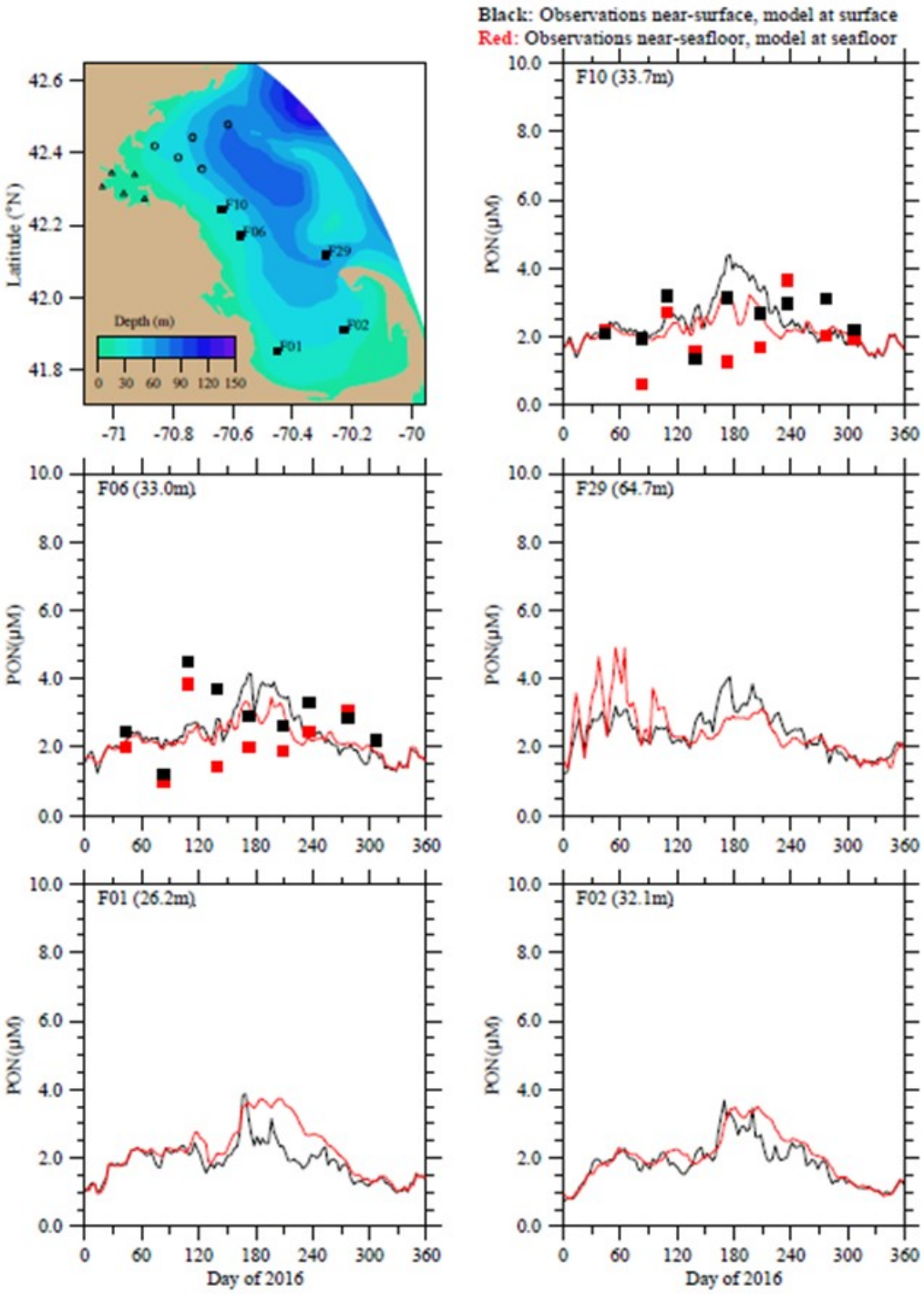

Figure 3-38 Particulate organic nitrogen at Southern stations. Model-observation comparisons for 2016 for former BEM (Zhao et al. 2017, Figure 5-7b).

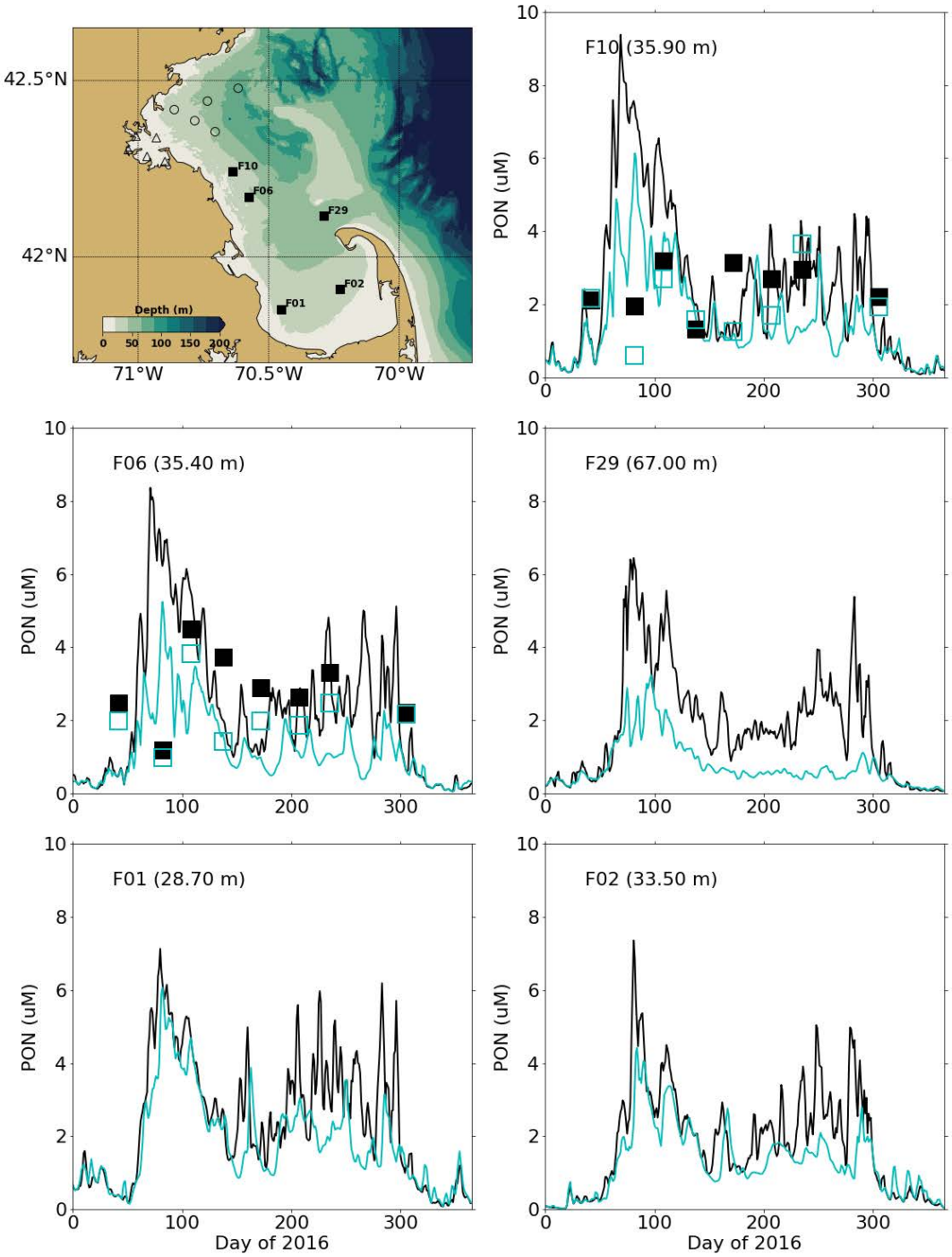

Figure 3-39 Particulate organic nitrogen at Southern stations. Model-observation comparisons for 2016 for updated BEM. Black: observations near surface, model at water surface. Blue: observations near seafloor, model at bottom.

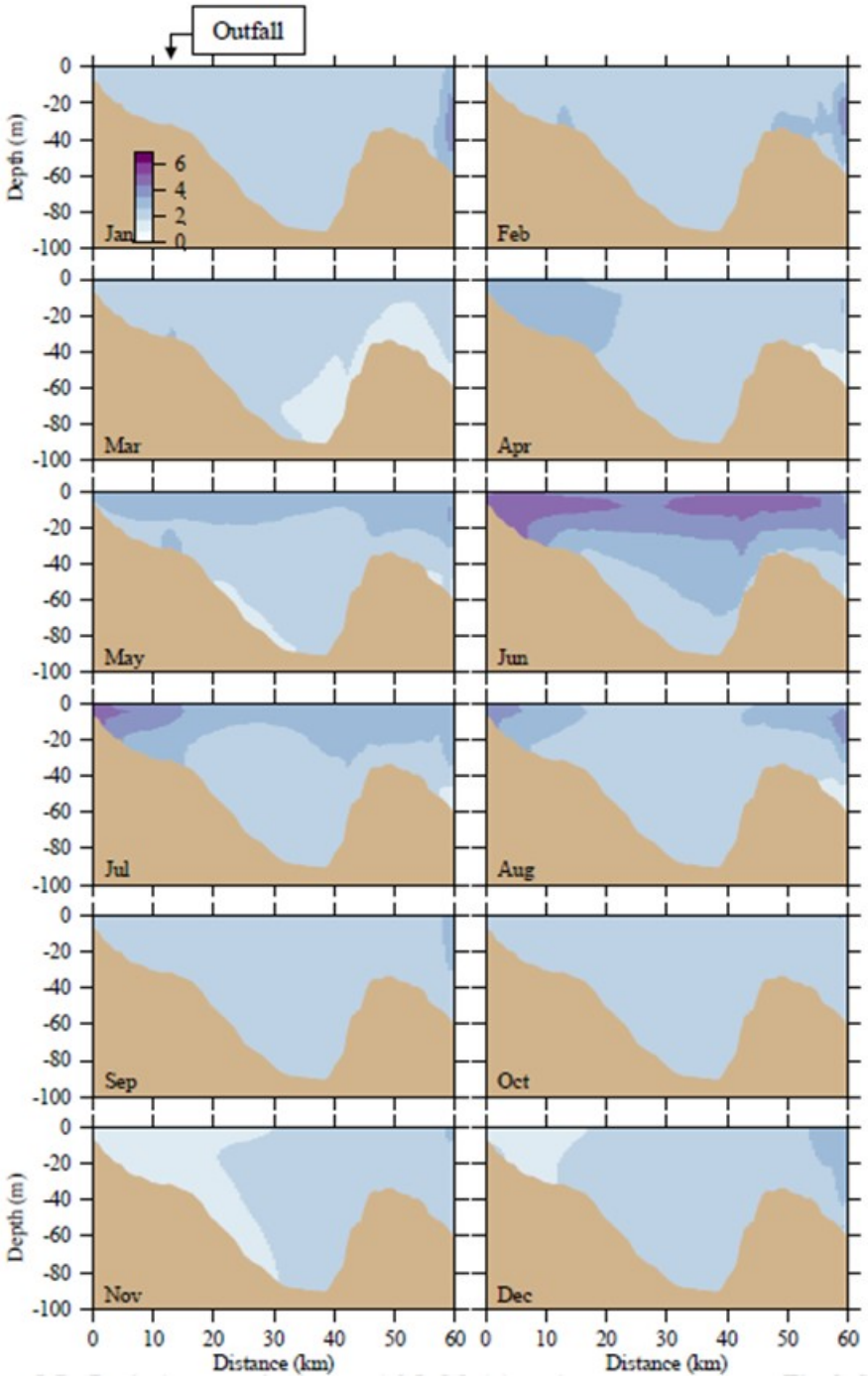

Figure 3-40 Particulate organic nitrogen (µM). Former BEM results for 2016 along east-west transect (Figure 3.1). Horizontal axis is distance eastward from coast; outfall is on seafloor at approximately 13 km (Zhao et al. 2017, Figure 5-7c).

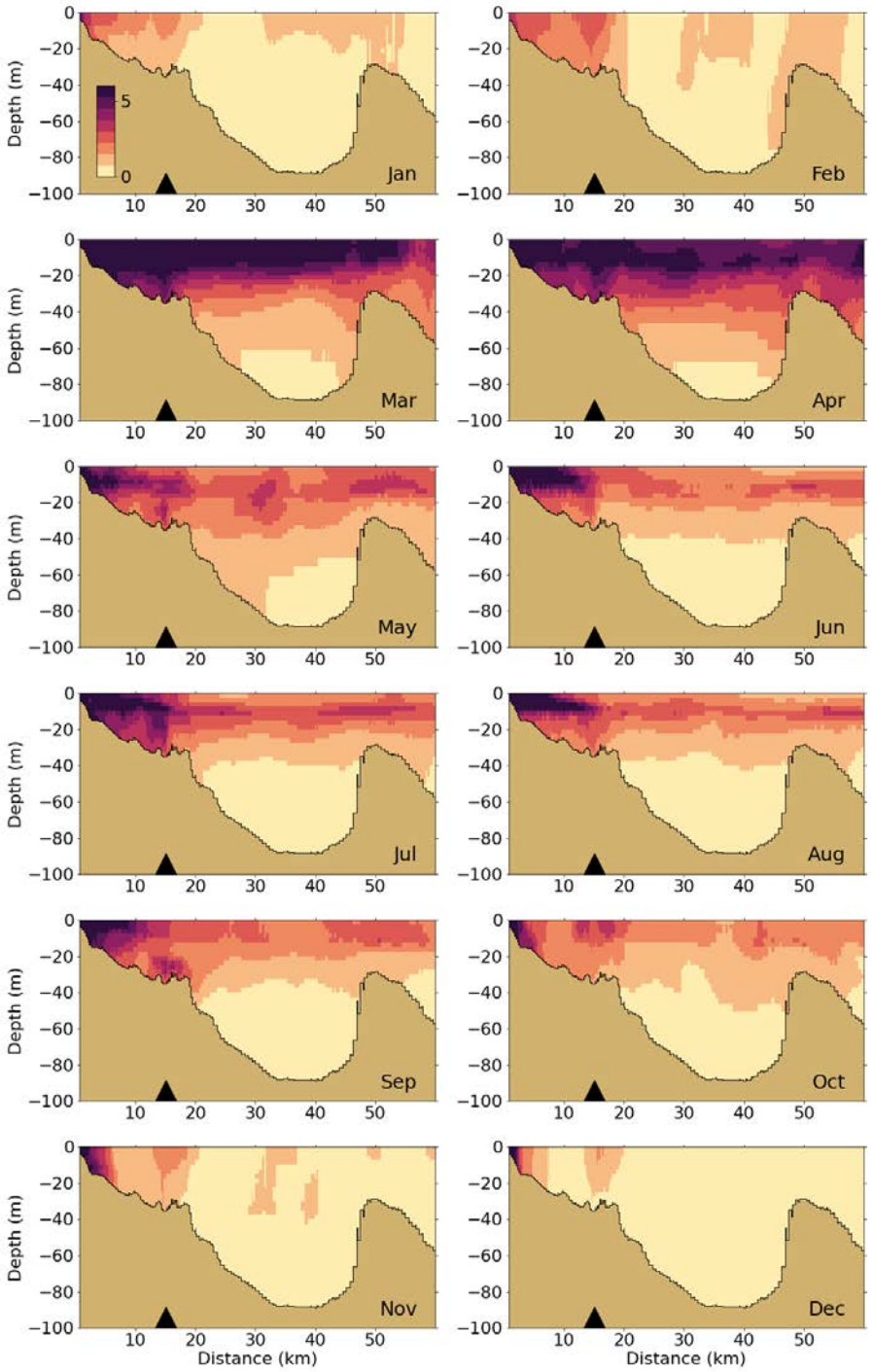

Figure 3-41 Particulate organic nitrogen (µM). Updated BEM results for 2016 along east-west transect (Figure 3.1). Horizontal axis is distance eastward from coast; black triangle indicates the location of the outfall on seafloor.

3.2.6 Particulate Organic Carbon

Model-observation plots of particulate organic carbon (POC) are compared here for the former and updated BEM at Northern (Figure 3-42 and Figure 3-43) and Southern stations (Figure 3-44 and Figure 3-45). Overall, the former BEM overestimates POC concentrations, especially in deeper layers. While observed concentrations are lower near the seafloor compared to near the surface, POC concentrations in the former BEM are higher in the bottom layers. The updated BEM usually underestimates POC, except during the spring bloom. Vertical differences in POC concentrations (i.e., higher concentrations at the surface compared to the bottom) are well reproduced by the updated BEM.

Along the vertical east-west transect through the outfall, the former BEM simulates low POC concentrations over the entire depth from October to March, and higher concentrations in April-September especially at the subsurface (Figure 3-46). In the former BEM, higher concentrations seem to originate from the eastern side of the transect, which is most likely the effect of boundary conditions. In the updated BEM, concentrations of POC over the vertical cross-section (Figure 3-47) show similar spatial and temporal patterns as for PON, with clear vertical gradients between March and October and the highest concentrations in March-April near the surface. No signal from the outfall is visible in the updated BEM, while a weak signal is perceptible in the former BEM results. Finally, as for DON and PON, the updated BEM estimates higher POC concentrations at the coast all year round.

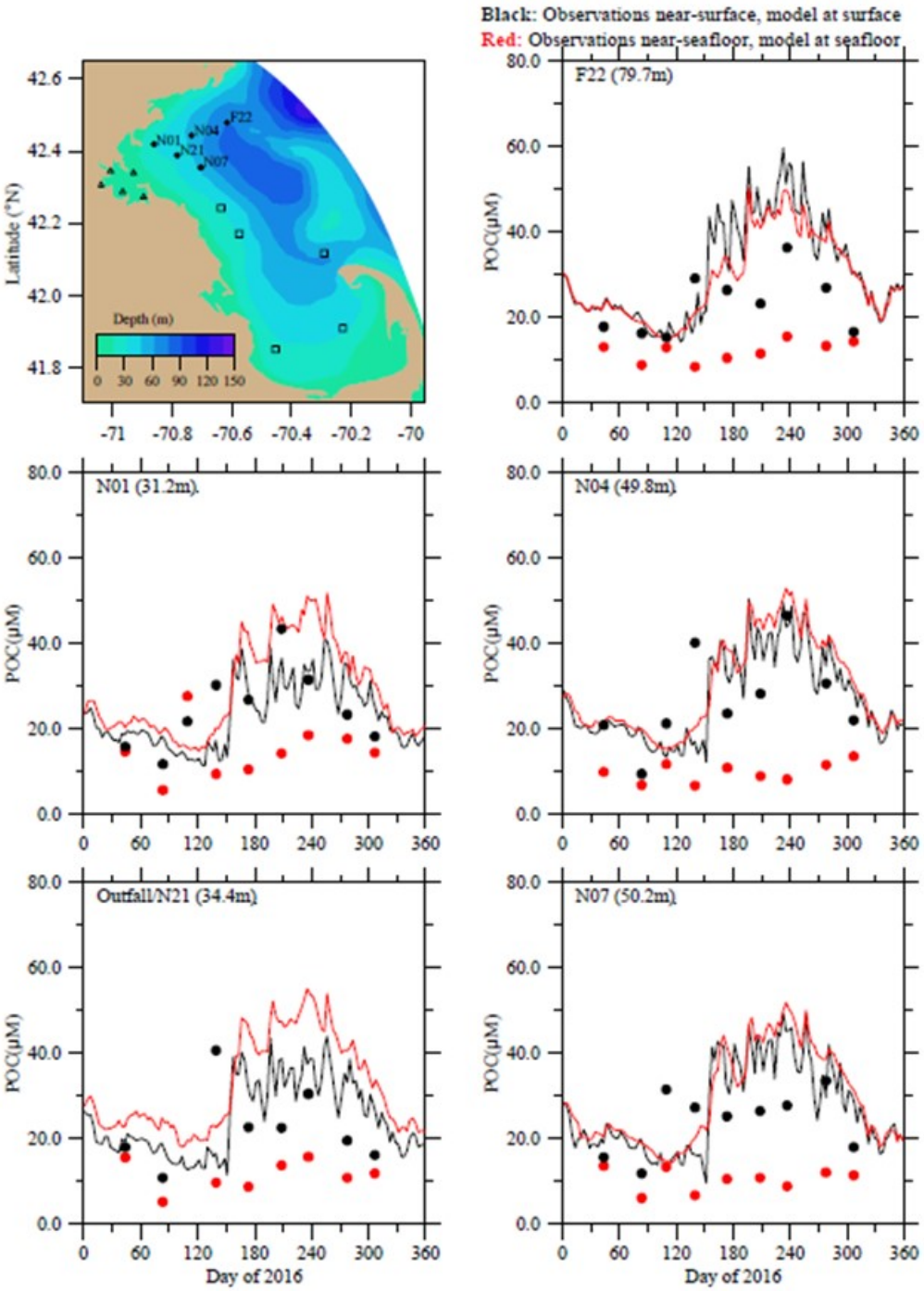

Figure 3-42 Particulate organic carbon at Northern stations. Model-observation comparisons for 2016 for former BEM (Zhao et al. 2017, Figure 5-8a).

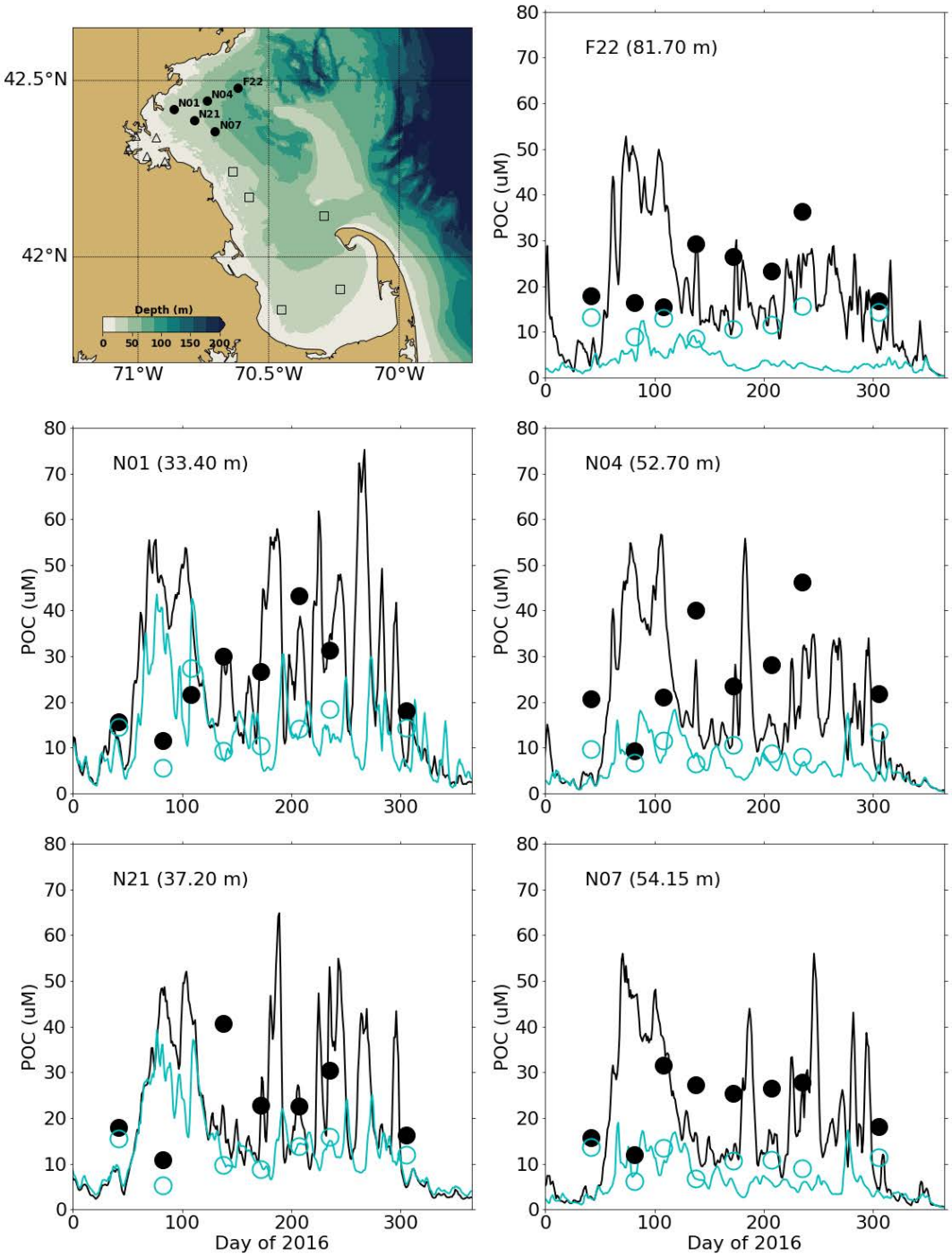

Figure 3-43 Particulate organic carbon at Northern stations. Model-observation comparisons for 2016 for updated BEM. Black: observations near surface, model at water surface. Blue: observations near seafloor, model at bottom.

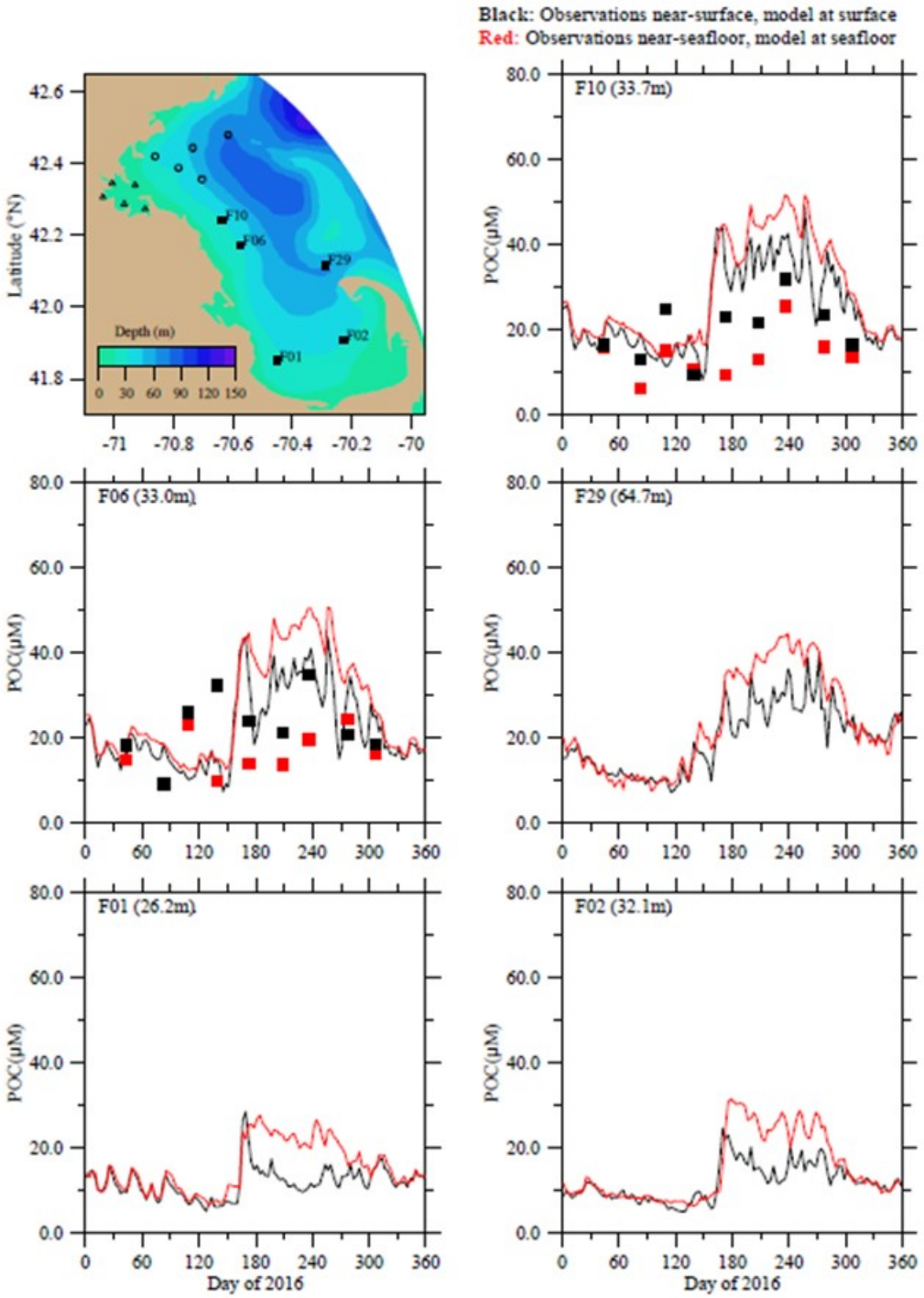

Figure 3-44 Particulate organic carbon at Southern stations. Model-observation comparisons for 2016 for former BEM (Zhao et al. 2017, Figure 5-8b).

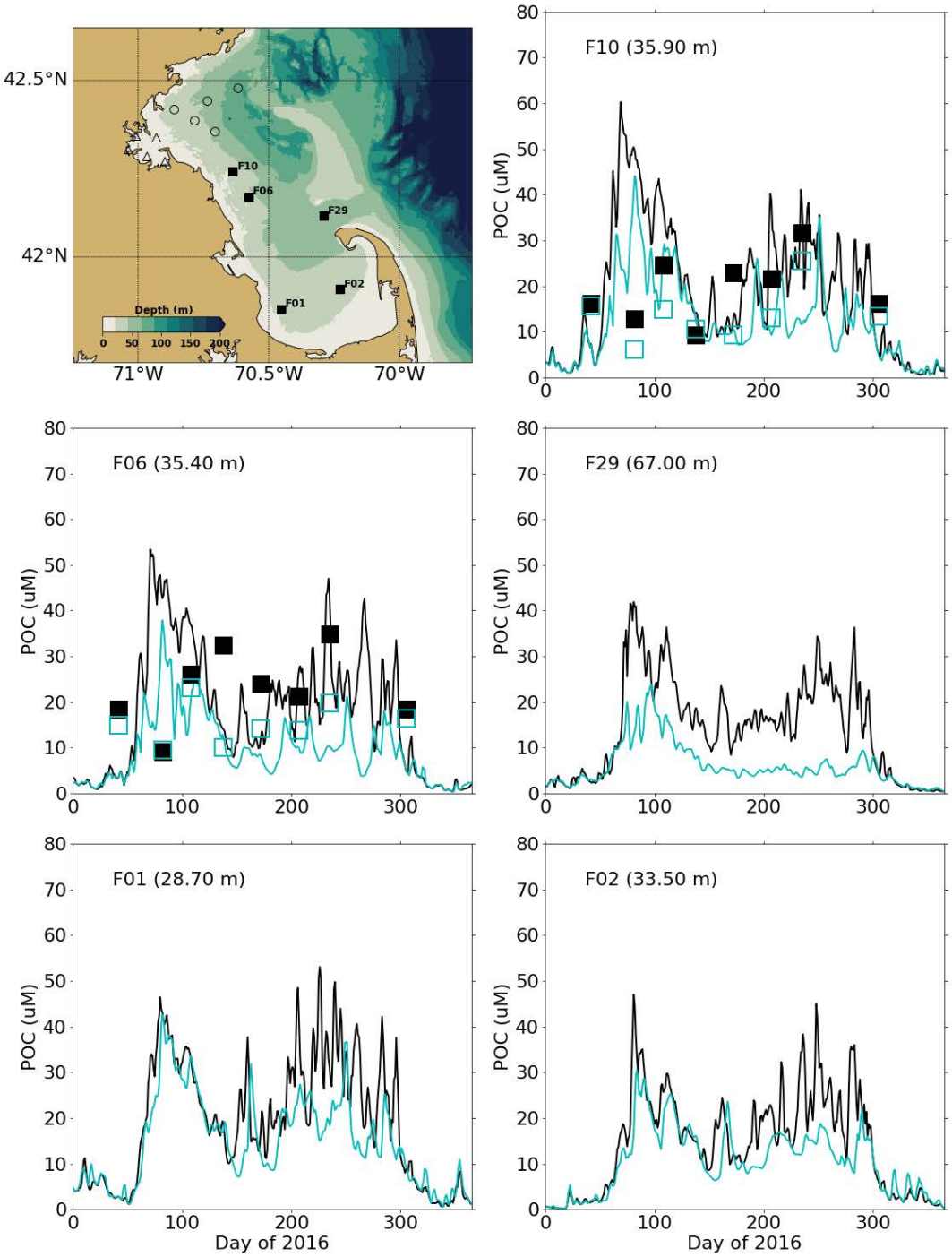

Figure 3-45 Particulate organic carbon at Southern stations. Model-observation comparisons for 2016 for updated BEM. Black: observations near surface, model at water surface. Blue: observations near seafloor, model at bottom.

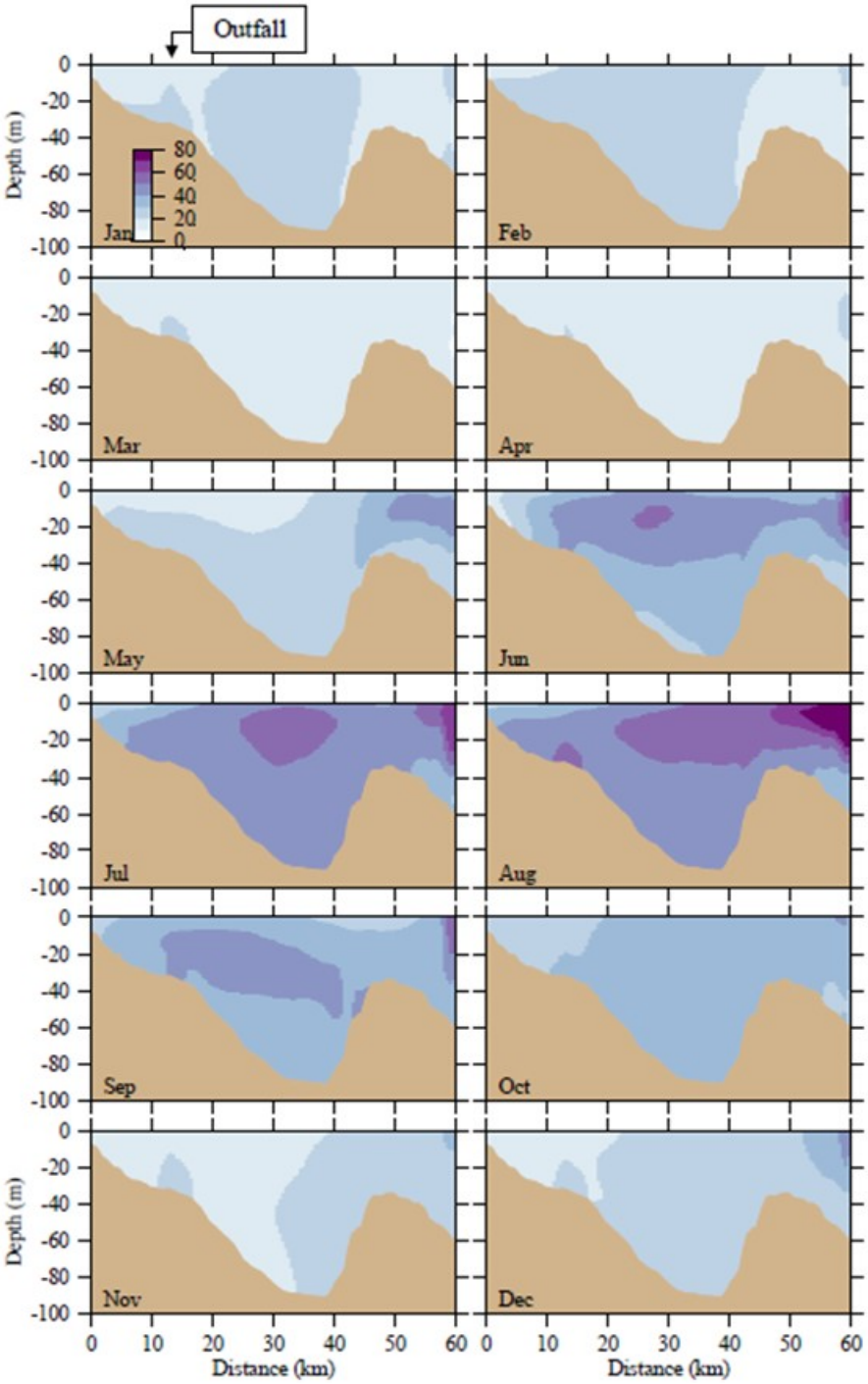

Figure 3-46 Particulate organic carbon (µM). Former BEM results for 2016 along east-west transect (Figure 3.1). Horizontal axis is distance eastward from coast; outfall is on seafloor at approximately 13 km (Zhao et al. 2017, Figure 5-8c).

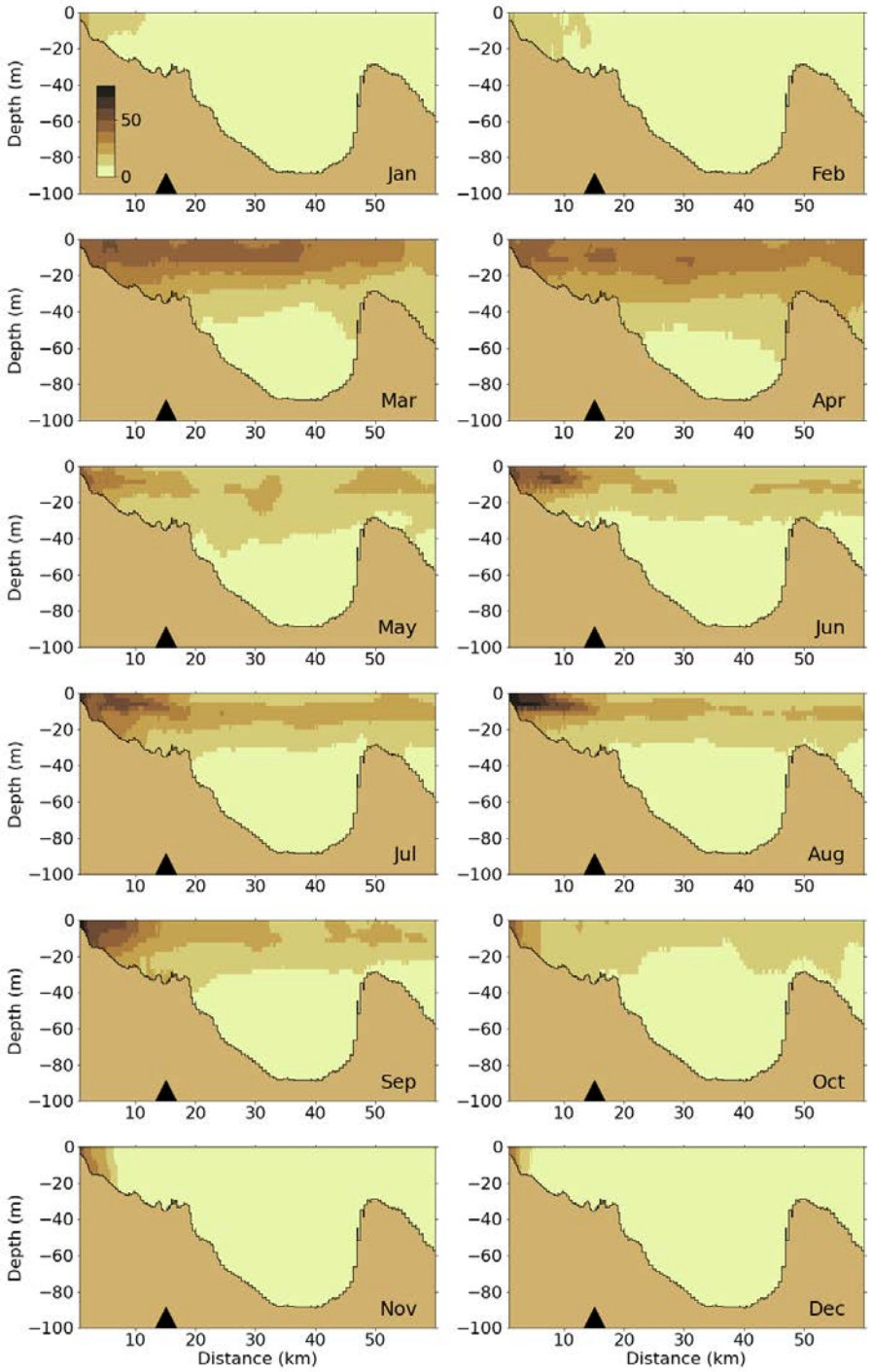

Figure 3-47 Particulate organic carbon (µM). Updated BEM results for 2016 along east-west transect (Figure 3.1). Horizontal axis is distance eastward from coast; black triangle indicates the location of the outfall on seafloor.

3.2.7 Dissolved Oxygen

Comparison of model-observation plots of dissolved oxygen (DO) concentrations for the former and updated BEM at Northern (Figure 3-48 and Figure 3-49) and Southern stations (Figure 3-50 and Figure 3-51) show that the updated BEM better reproduces differences between surface and bottom layers. The former BEM estimates very little variation of DO with depth. Bottom concentrations are well represented in both models. Surface concentrations are slightly underestimated in the former BEM, especially at Northern stations. The updated BEM generally represents surface DO very well. Bottom DO concentrations simulated with the updated BEM match observations from January to the end of the summer, but do not capture the sharp drop in fall at stations F22, N04, N07 and F29.

The vertical cross-sections of DO concentrations along the east-west transect for the former and updated BEMs show similar temporal and spatial patterns (Figure 3-52 and Figure 3-53), with the highest concentrations occurring near the surface between February and May. In the updated BEM, the highest concentrations occur slightly under the surface between March and July, which corresponds to the depths at which chlorophyll is the highest.

Comparisons of measured and modeled DO levels in the study area show differences between the Cape Cod Bay stations (F01 and F02) and the rest of the study area (e.g. measure DO appears to be consistently lower than modeled DO in late summer and early fall). This is not well reproduced, either by the former BEM or by the updated BEM (Figure 3-50 and Figure 3-51).

In addition to the time-series comparisons at the MWRA routine monitoring stations, DO results from the former and updated BEM were also compared to high-frequency measurements at the A01 mooring site (Figure 3-54 and Figure 3-55). As stated by Zhao et al. (2017), "…*in order to minimize the influence of intermittent sensor noise due to bubble sweep-down, daily medians of the raw hourly near-surface measurements are used. The daily medians are averaged over 3-day intervals to match the temporal resolution of the model output.*" For the updated BEM, the higher resolution model output has also been averaged over 3-day intervals for the sake of comparison. In the plots for the updated BEM, observation data are plotted using shaded areas that represent uncertainties around the measurements (linked to calibration issues). As advised by MWRA, an uncertainty of +/- 0.5 mg/L was used for DO concentrations, and an equivalent of 5 % for DO percent saturation. While the former BEM underestimates DO concentration and percent saturation at the 2 m-depth, the updated BEM shows a very good fit with the measurements. Both BEMs underestimate seasonal variations at 51 m deep, providing lower oxygen levels than measured for the first half of 2016, and higher for the second half.

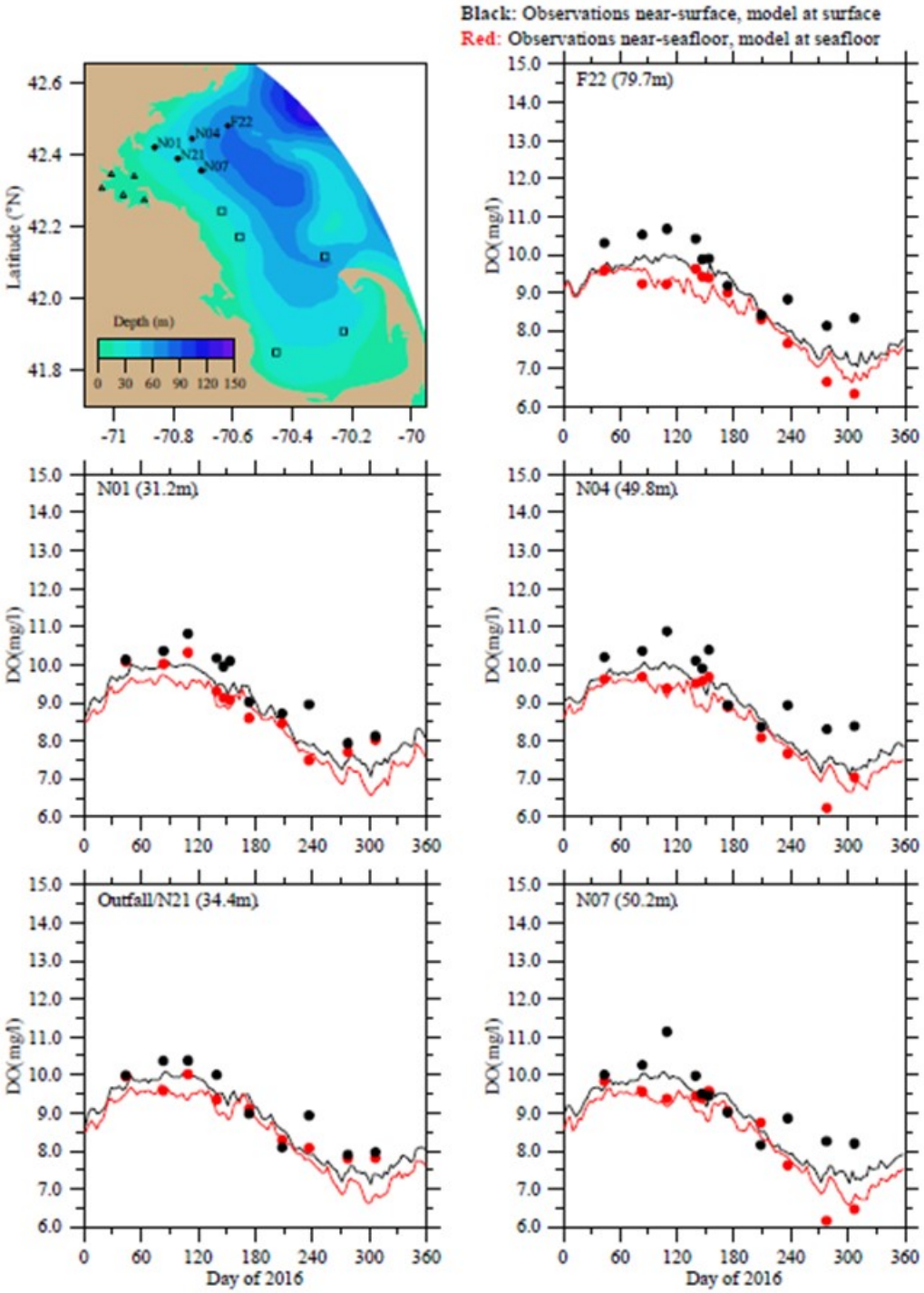

Figure 3-48 Oxygen concentrations at Northern stations. Model-observation comparisons for 2016 for former BEM (Zhao et al. 2017, Figure 5-9a).

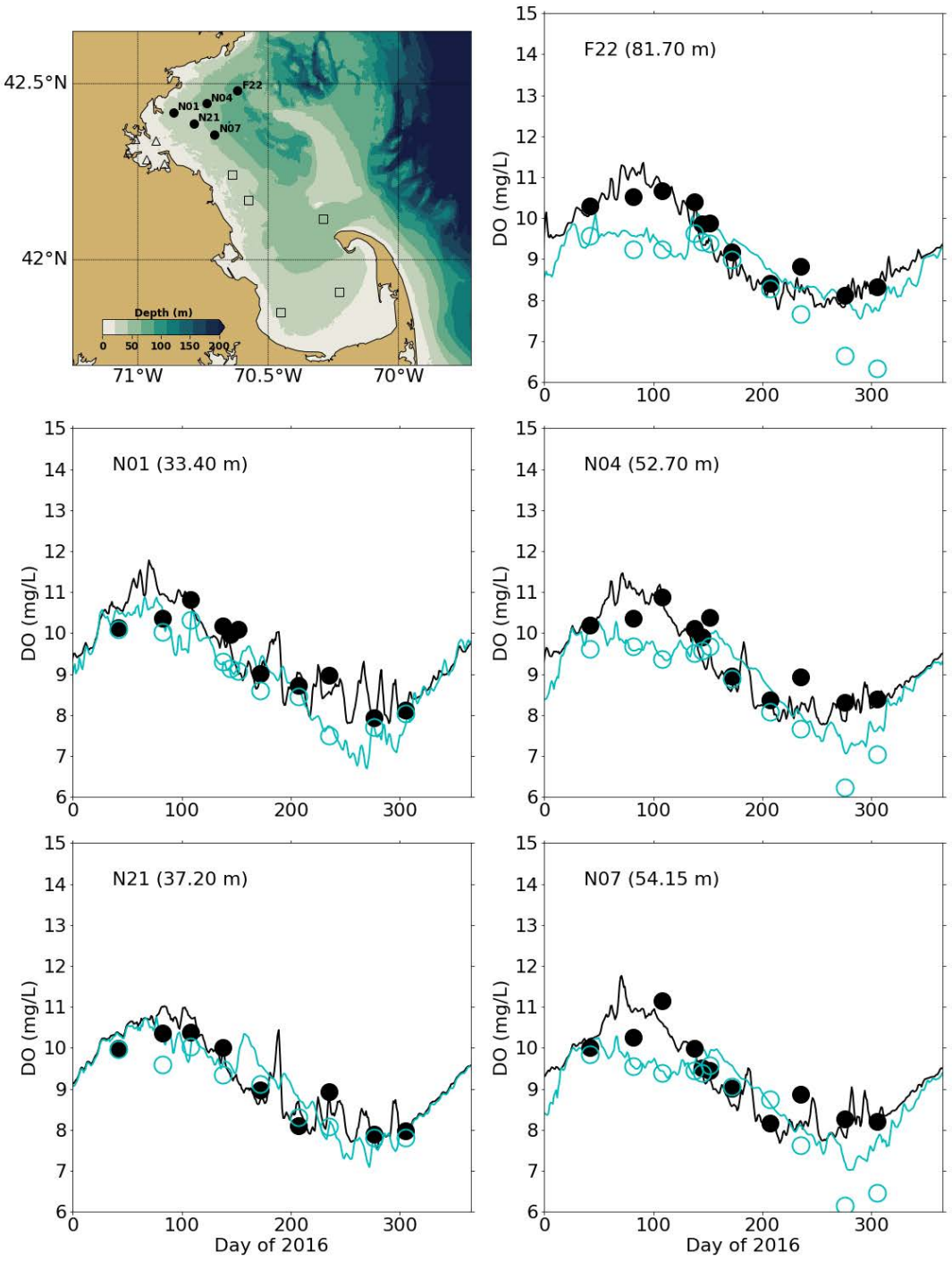

Figure 3-49 Oxygen concentrations at Northern stations. Model-observation comparisons for 2016 for updated BEM. Black: observations near surface, model at water surface. Blue: observations near seafloor, model at bottom.

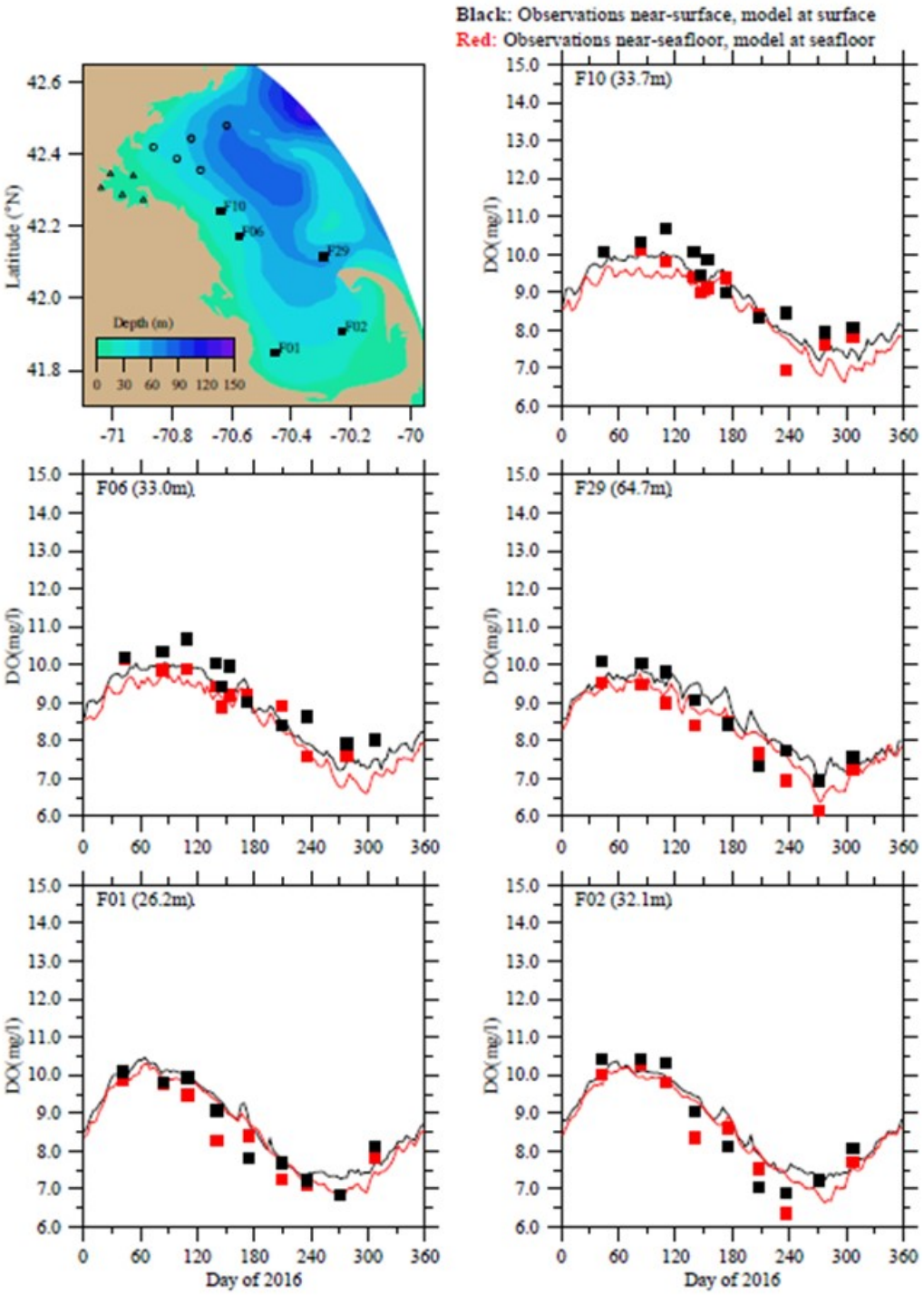

Figure 3-50 Oxygen concentrations at Southern stations. Model-observation comparisons for 2016 for former BEM (Zhao et al. 2017, Figure 5-9b).

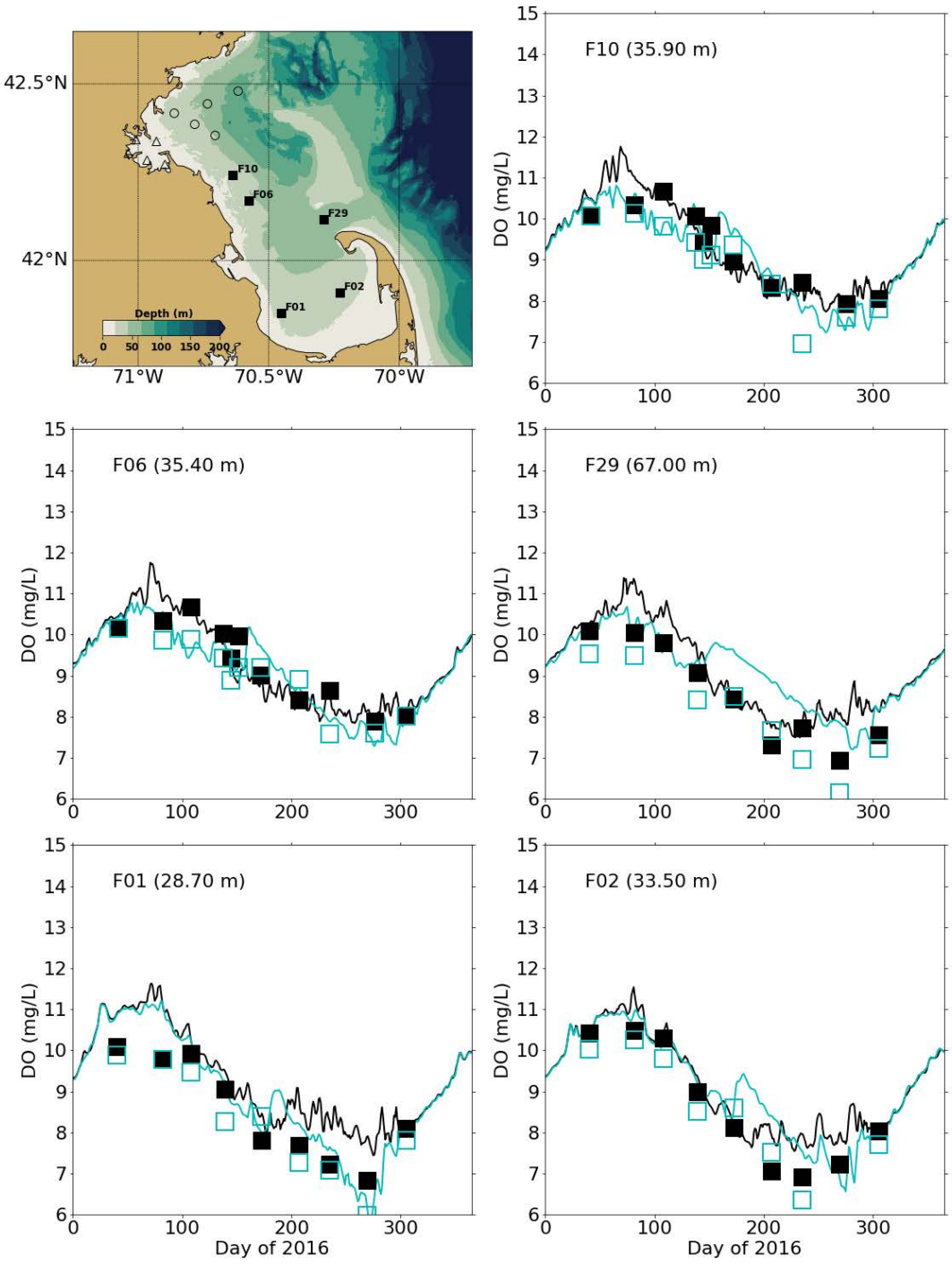

Figure 3-51 Oxygen concentrations at Southern stations. Model-observation comparisons for 2016 for updated BEM. Black: observations near surface, model at water surface. Blue: observations near seafloor, model at bottom.

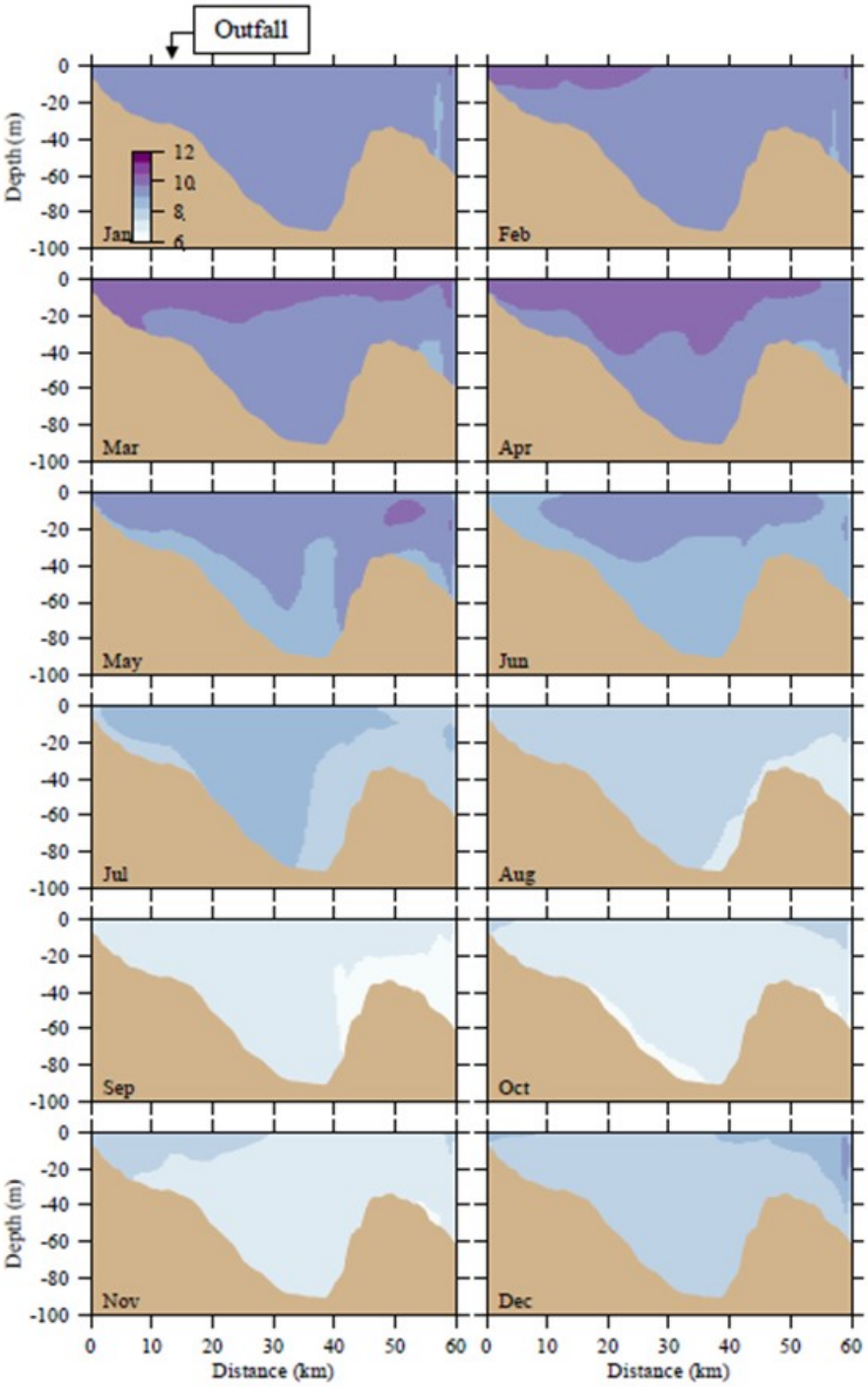

Figure 3-52 Oxygen concentration (mg L^{-1}). Former BEM results for 2016 along east-west transect (Figure 3.1). Horizontal axis is distance eastward from coast; outfall is on seafloor at approximately 13 km (Zhao et al. 2017, Figure 5-9c).

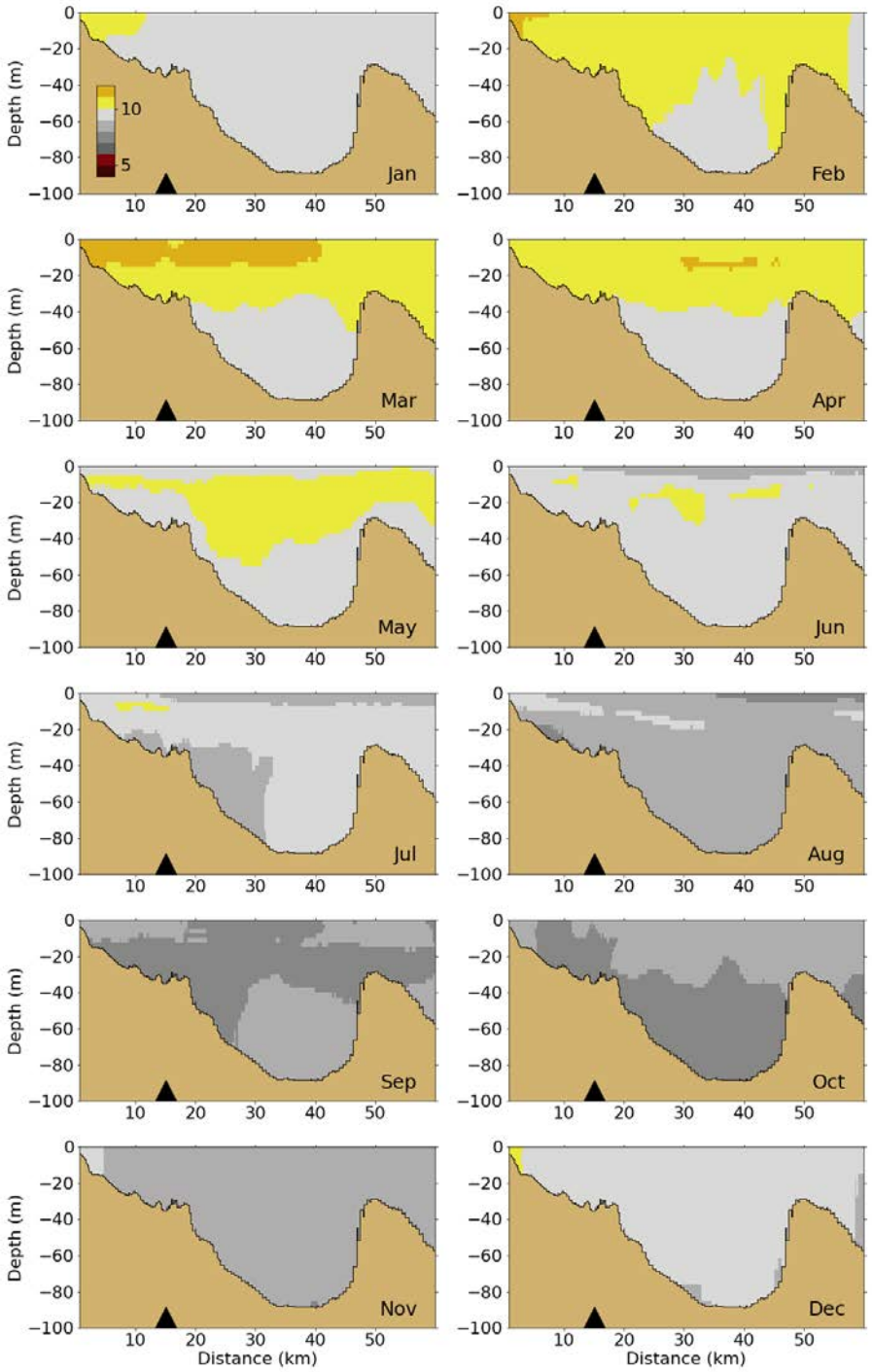

Figure 3-53 Oxygen concentration (mg L^{-1}). Updated BEM results for 2016 along east-west transect (Figure 3.1). Horizontal axis is distance eastward from coast; black triangle indicates the location of the outfall on seafloor.

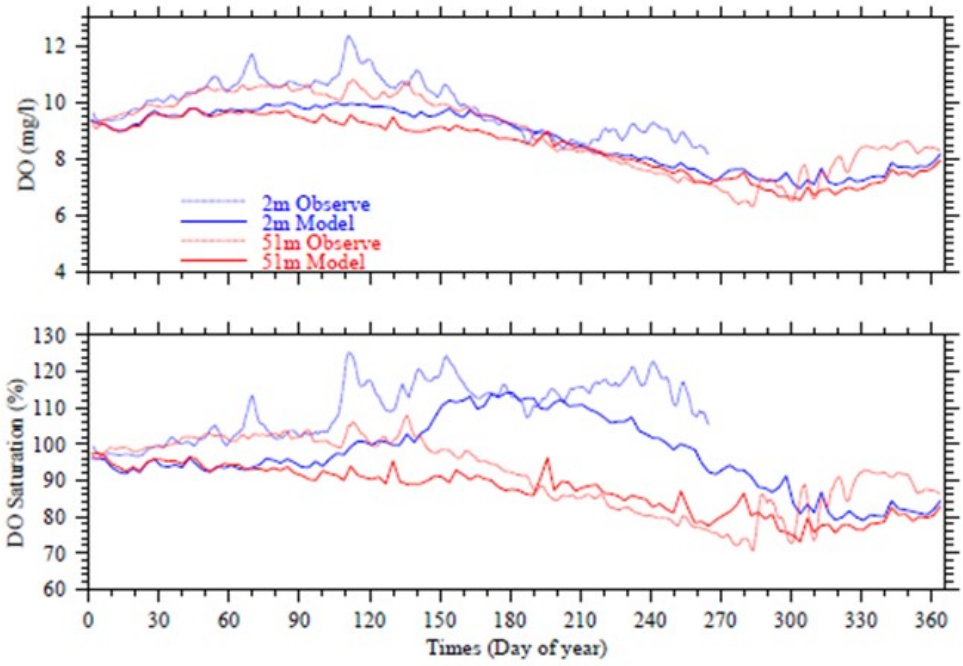

Figure 3-54 Oxygen time series at A01 mooring site, model-observation comparison for 2016 for former BEM. The 2-m depth observations after late September did not meet quality standards (Zhao et al. 2017, Figure 5-11).

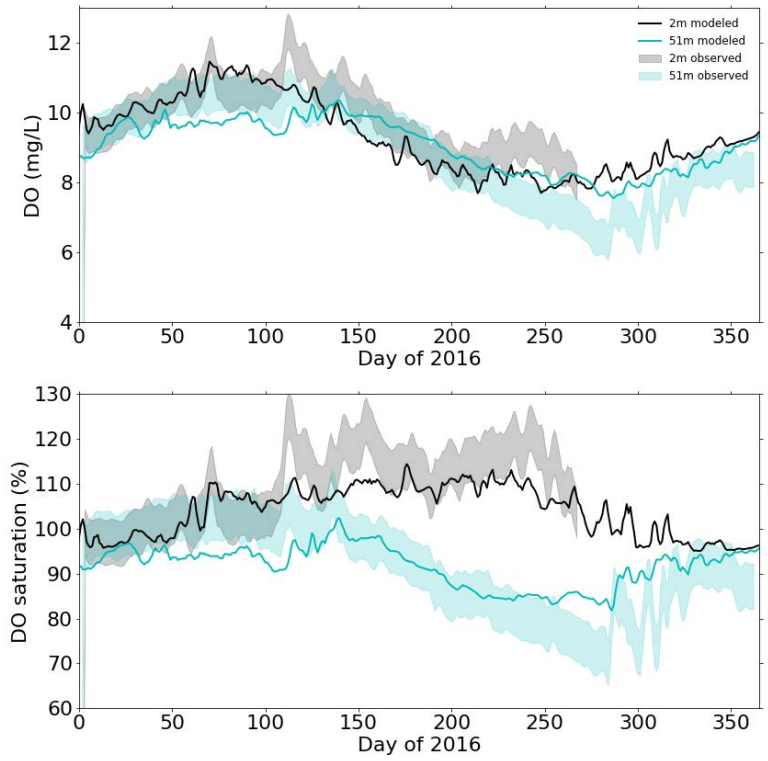

Figure 3-55 Oxygen time series at A01 mooring site, model-observation comparison for 2016 for updated BEM.

3.2.8 Sediment fluxes

Sediment ammonium (NH4) fluxes and sediment oxygen demand (SOD) are compared to box-whisker plots of measured benthic fluxes from 2000-2010 (see Tucker et al., 2010 and Zhao et al., 2017 for more details on the field methods). Although the monitoring program for sediment fluxes ended in 2010, the observations are still relevant for indicating historical magnitude of fluxes, as well as the geographic and seasonal patterns.

The NH4 sediment flux estimates from the former BEM are lower than historic measurements at harbor stations and match well with measurement ranges at the Massachusetts Bay stations (Figure 3-56). The updated BEM shows a different behavior: it estimates NH4 sediment fluxes in the range of the measurements (or slightly on the higher side) at harbor stations and overestimates them in Massachusetts Bay (Figure 3-57). Note that the y-axis range for fluxes at Massachusetts Bay stations (right side) is ~3 times smaller than that for the harbor stations (left side). These discrepancies are related to the simplified representation of sediment biogeochemical processes in the updated BEM (see Section 3.1.3.4).

Similarly, the SOD estimates from the former BEM are lower than historic measurements at harbor stations and match well with measurement ranges at the Massachusetts Bay stations (Figure 3-58). The updated BEM provides SOD fluxes well in the range of historic measurements at all stations, except at BH03 (harbor) and MB05 (Massachusetts Bay) where they are slightly lower than the observations (Figure 3-59).

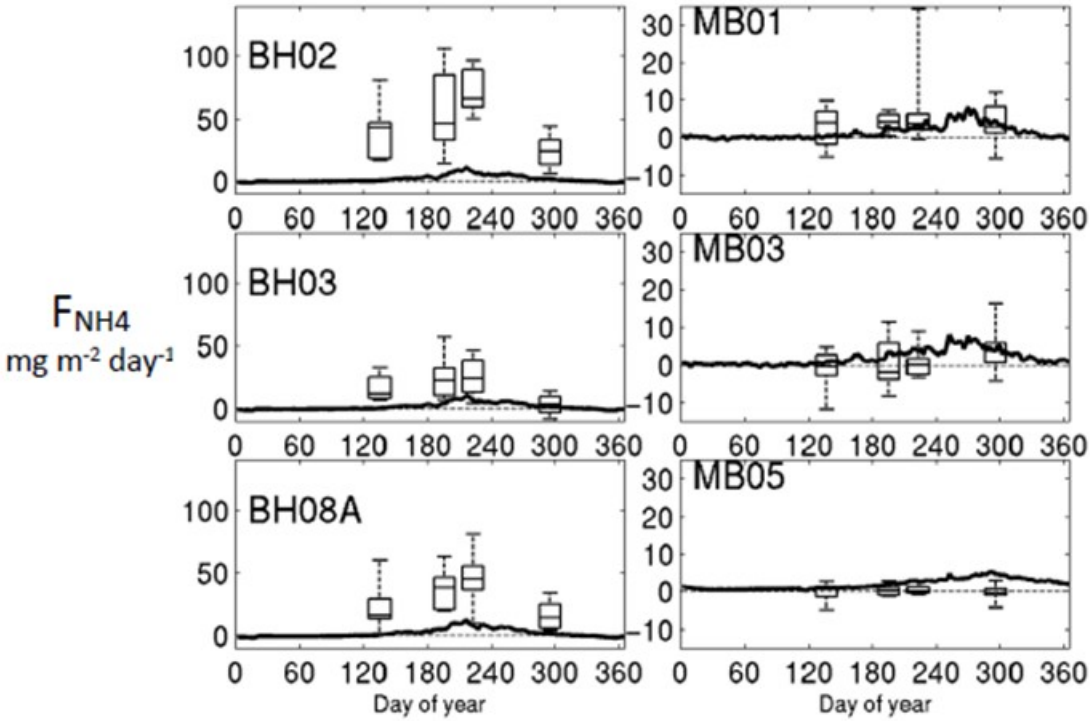

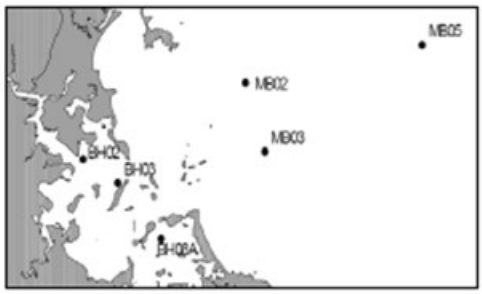

Figure 3-56 Sediment NH4+ flux. Former BEM 2016 results (line), and 2001-2010 observations (box-whiskers). Selected Boston Harbor stations (left column) and Massachusetts Bay stations (right column). (Zhao et al. 2017, Figure 5-12).

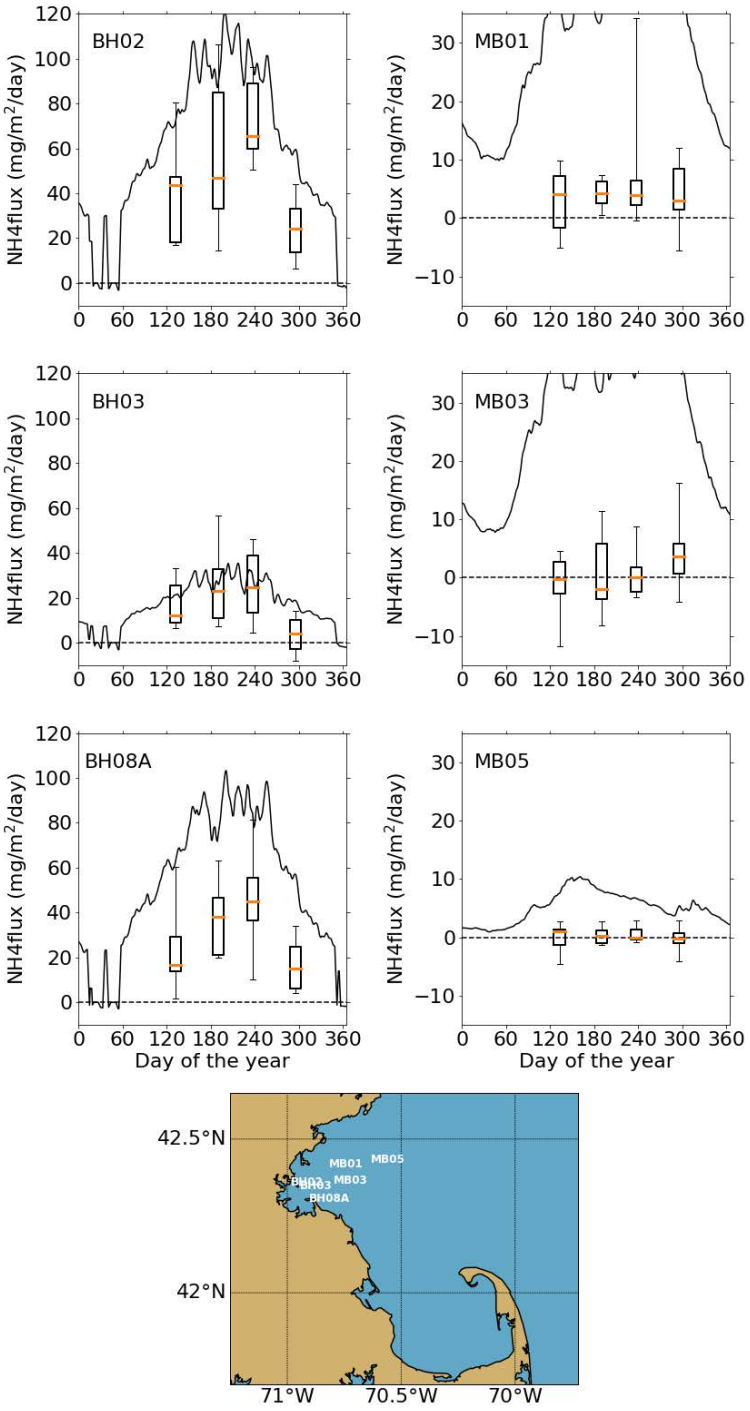

Figure 3-57 Sediment NH4+ flux. Updated BEM 2016 results (line), and 2001-2010 observations (box-whiskers).

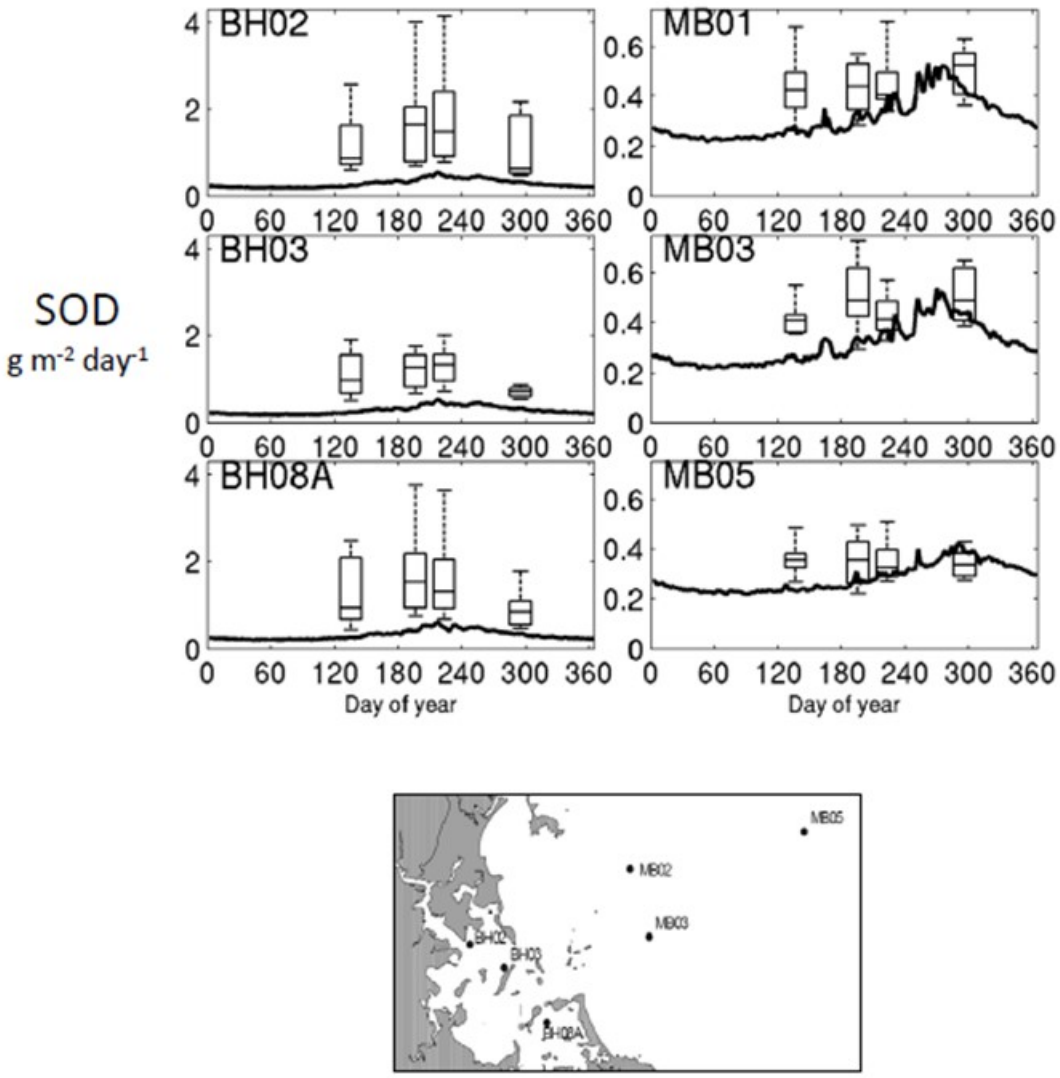

Figure 3-58 Sediment oxygen demand. Former BEM 2016 results (line), and 2001-2010 observations (box-whiskers). Selected Boston Harbor stations (left column) and Massachusetts Bay stations (right column). (Zhao et al. 2017, Figure 5-13).

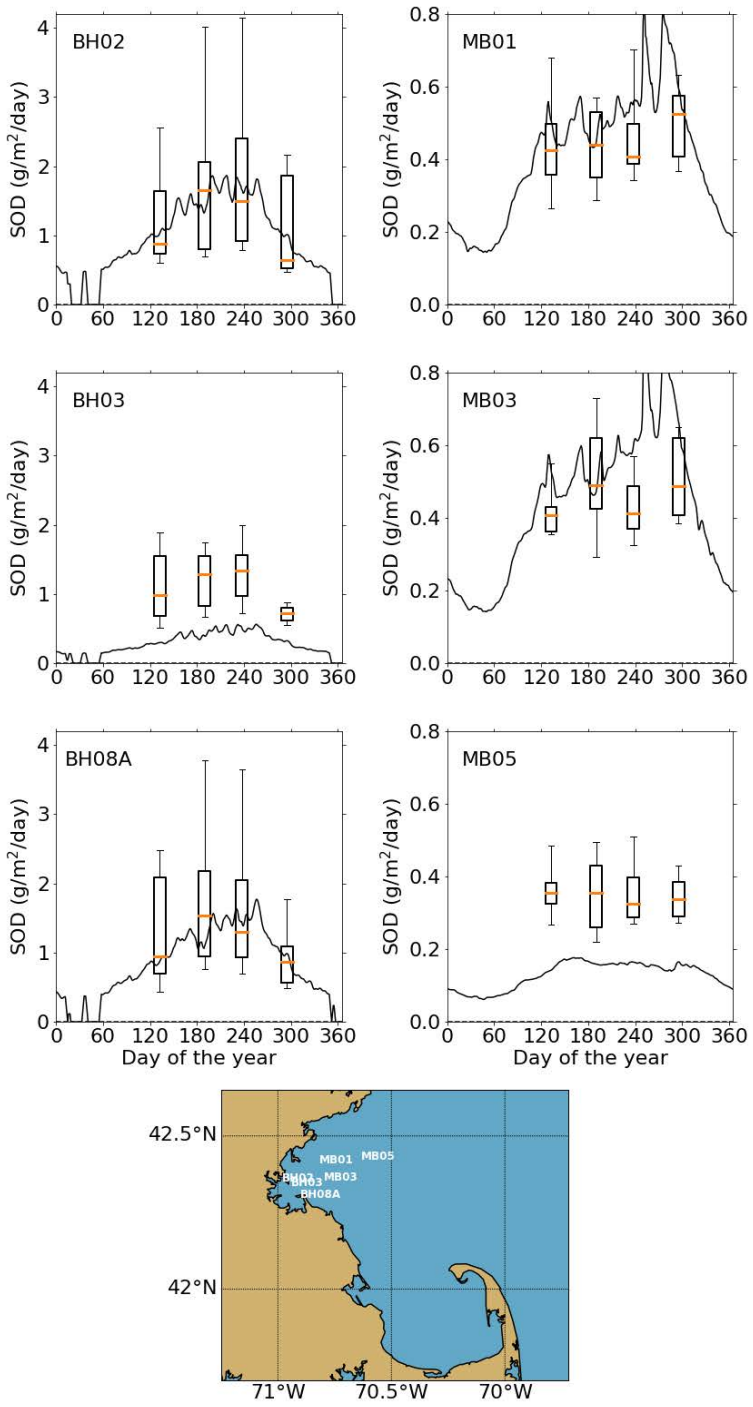

Figure 3-59 Sediment oxygen demand. Updated BEM 2016 results (line), and 2001-2010 observations (box-whiskers).

3.3 Discussion

3.3.1 Role of model boundary

The results from the updated BEM show some differences from the former BEM because of the different location of the model boundary. The monthly vertical cross-section plots clearly illustrate this. Toward the right-hand side of these plots, where the former BEM approaches its open boundary, sometimes clear horizontal gradients exist in the former BEM under the influence of the boundary condition (e.g. chlorophyll-*a*: Figure 3-26; POC: Figure 3-46). As the updated BEM does not have a boundary close to the study area, horizontal gradients are much smaller, which is more realistic (Figure 3-27 and Figure 3-47).

An initial concern was that the more distant open boundary of the updated BEM could have resulted in difficulties reproducing the observed water quality in and near the bays, for example at station F22. The comparison to the former BEM and field data presented here indicates that this is not the case.

3.3.2 Outfall plume

The mathematical equations used in the updated BEM to represent the hydrodynamics use the so-called hydrostatic assumption. This is a common approach for coastal waters and ocean modeling (also used by the former BEM). It implies that vertical momentum is not accounted for. This is almost never an issue, with the possible exception of outfall plumes close to their point of release.

The updated BEM releases the DITP discharge in the bottom water layer cells where the DITP discharges are situated. The initial rising of the plume due to its momentum is not accounted for. This causes the concentration in the line of bottom layer cells right on top of the outfall to be overestimated. This can be clearly observed from modeled near-bottom concentrations time series at station N21 (e.g. DIN in Figure 3-13).

After the momentum of the discharge is dissipated, the plume buoyancy becomes the driving force. The model equations do account for this. The plume can be observed to disperse in a horizontal direction and end up near the water surface in winter, while it is trapped in the lower part of the water column in summer (as seen in Figure 3-19 for DIN).

This is further illustrated in Figure 3-60, which shows the measured DIN levels at station N21 near the water surface, near the bottom (≈ 35m deep) and at an intermediate depth. While highest concentrations occur near the surface in winter, high DIN concentrations are observed at ~10 m above the seabed (~25m deep) during the summer of 2016.

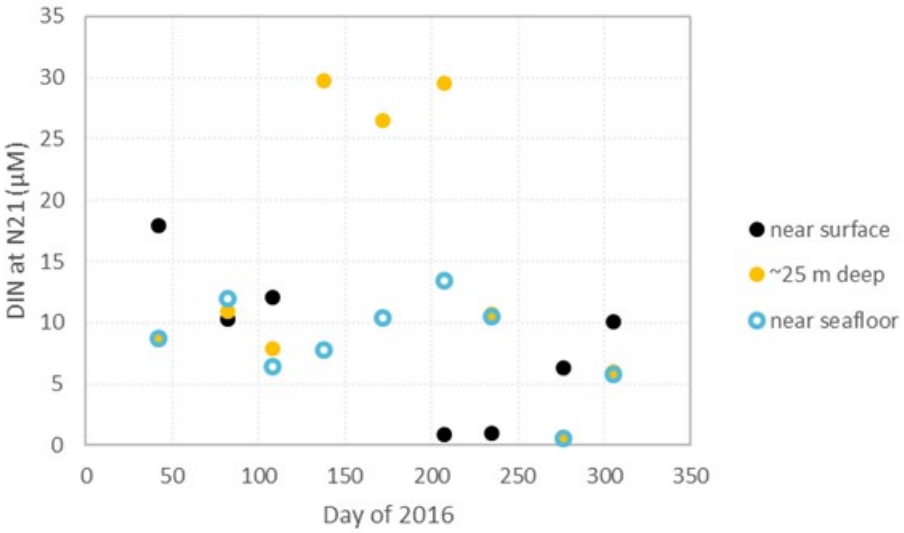

Figure 3-60 DIN measurements at MWRA station N21 (above outfall) at different water depths.

The vertical position of the discharge plume throughout the year could be simulated more accurately using a near-field model like CORMIX (Cornell Mixing Zone Expert System, e.g. Doneker and Jirka, 2007). The result could then be used in the updated BEM to distribute the discharge over the appropriate portion of the water column rather than in the bottom layer. However, as the discrepancy is expected to be local only, and as the simulated ultimate plume position in the updated BEM shows realistic behavior in summer and winter, such a procedure was not implemented.

The updated BEM overestimates concentrations for several water quality variables in the bottom layer of the water column over the DITP outfall (station N21). This is (partly) due to the above methodological issue associated with near-field modeling of the outfall discharge. Another part of the explanation is that station N21 is indicated to be located exactly on top of the outfall in the model. However, the actual location of sampling may well be somewhat removed from this location due to operational constraints on the positioning of the survey vessel. This means that the measured sample may in fact miss the plume. This is expected to be especially relevant close to the seafloor where the plume is still narrow.

3.3.3 Temporal variability of simulated concentrations

Many simulated variables show a much stronger temporal variability in the updated BEM than they did in the former BEM. This holds in particular for the near-surface concentrations of phytoplankton and associated variables (Chlorophyll-*a*, POC, PON). This behavior was confirmed to be consistent with mathematical formulations and model forcing. An important clarifying factor is the day-to-day wind variability. Also, the higher variability of modeled light extinction contributes to this. High frequency observations (e.g. at buoy A01) confirm that this behavior is realistic. In the plots of the updated BEM shown in this section, a 3-day running average transformation was applied for all time series comparisons.

3.3.4 Vertical gradients of simulated concentrations

Model results for many variables show much stronger vertical gradients in the updated BEM than they did in the former BEM. The comparison to field data showed that these gradients are mostly realistic, although they are sometimes a little overestimated. Vertical gradients are the combined result of horizontal transport, vertical mixing and biogeochemical processes like settling and primary production in parts of the water column. Section 2 argues that the updated BEM hydrodynamic model simulates realistic horizontal transport patterns and seasonally variable vertical mixing. In the current section it was demonstrated that the addition of biogeochemical processes provides realistic vertical gradients for most water quality variables.

3.3.5 Residence times and flushing of study area; relative importance of outfall

The updated BEM was used to carry out a tracer simulation to quantify the residence time in the study area and the dilution of the DITP outfall. The simulation was arranged and processed as follows:

- Years 2015 (spin-up) and 2016 (for results) were simulated.
- Two tracers were simulated: a conservative and a decaying tracer, the latter with a constant and homogeneous decay rate.
- The observed time series of the DITP discharge volume was used.
- The DITP discharge was assigned a constant and equal concentration of both tracers.
- The total mass of both tracers in sub-domain Mass Bay North (MBN, Figure 3-1) was recorded as a function of time, as well as the total water volume.
- From the above, the spatially averaged concentrations in MBN were calculated.
- The average “age” of the DITP release in MBN was calculated from the ratio of the masses of the two tracers and the known decay rate of the decaying tracer.
- The average “dilution” of the DITP release in MBN was calculated from the concentration released and the average simulated concentration of the conservative tracer.

The age of the DITP released water in MBN can be considered the residence time of the effluent in the Northern part of Massachusetts Bay. Averaged over 2016, the simulated age amounts to 17 days. The average simulated dilution rate over 2016 amounts to about 2,500. This means that on average one part of DITP effluent is diluted in 2,500 parts of water entering the area from other sources: mostly from GoM and a very small part from rainfall and from rivers. This dilution is for the entire MBN region and, as expected, is much higher than dilution rates applicable local to the outfall plume, as were the focus of earlier modeling and field studies specific to plume behavior (e.g. Hunt et al., 2010 and references cited therein).

These results illustrate that Massachusetts Bay is a “boundary dominated” system influenced strongly by exchanges of water with the GoM. The overall mass balance of nitrogen for 2016 derived from the complete updated BEM further illustrates this (see Appendix B). Of the total annual loads and inflows of tracers to MBN in the simulation, the DITP discharge accounts for 7%, the contribution from rivers is negligible and the inflows from GoM amount to 93%. This implies that on average, 7% of the nitrogen present in MBN stems from DITP. This is consistent with results of earlier studies (Hunt et al., 1999).

The boundary dominance of the system is highlighted here to emphasize the importance of not having a model boundary close to the study area. This is considered a very relevant aspect of the fitness-for-purpose of the updated BEM.

3.3.6 Processes controlling dissolved oxygen

Dissolved oxygen (DO) is an important water quality parameter and the simulation of realistic DO concentrations is therefore an important aspect of the fitness-for-purpose of the updated BEM. During the calibration process (see Appendix B), the reaeration rate had to be increased significantly as compared to the former BEM in order to reduce discrepancies between model results and observations (and between results from the updated and former BEM). The reaeration rate finally adopted in the study area is equivalent to the one used by Deltares in North Sea modeling studies. In addition, it was shown above that neither the former nor the updated BEM can reproduce the measured concentrations of DO at the Cape Cod Bay stations (F01 and F02) throughout the whole year very accurately (Figure 3-50 and Figure 3-51).

Because of the relevance of the issue, a comparison of oxygen fluxes linked to the different processes at play in the former and updated BEM was carried out. Xue et al. (2014) show results produced with the former BEM of monthly variations in the different oxygen production and consumption process fluxes at one station of the Cape Cod Bay (F02) in 2008 (Figure 3-61). The same fluxes were extracted from the updated BEM mass balances in the MBS-CCB area for comparison (Figure 3-62, see Figure 3-1 for location of the mass balance area).

Seasonal patterns of the oxygen fluxes in the two models appear very similar. However, the ratios between production (net primary production) and consumption (oxidation + SOD) process fluxes differ. Oxidation and SOD fluxes are comparable in both models, while estimated net primary production is higher in the updated BEM. To compensate for this, the reaeration process thus needs to be stronger in the updated BEM. This process causes a negative flux during summer: DO escapes to the atmosphere because of oversaturation near the surface as a result of primary production. This difference between the two models may be due to different formulas used for oxygen production in the two models. The formula reported by Xue et al. (2014), which is also mentioned in the RCA Manual (Hydroqual, 2004), results in a noticeably lower oxygen production than the formulation used in the updated BEM. The formulation of the updated BEM has been double checked and was confirmed to be consistent with the underlying biochemical reaction formulas.

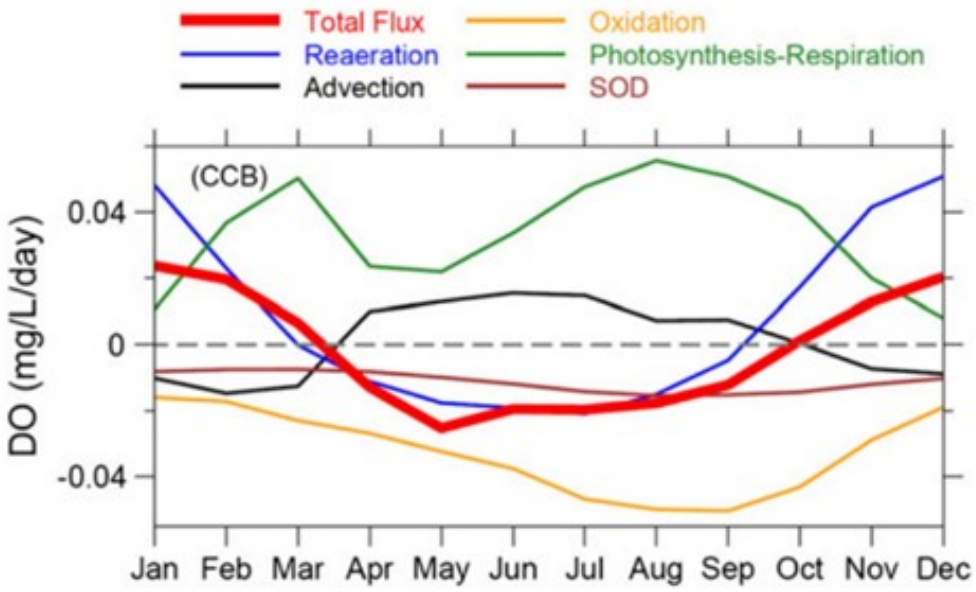

Figure 3-61 Model-computed vertically averaged monthly-mean values of DO fluxes in Cape Cod Bay for 2008 with the former BEM (Xue et al. 2014, figure 16). Fluxes are calculated for model grid cell at station F02.

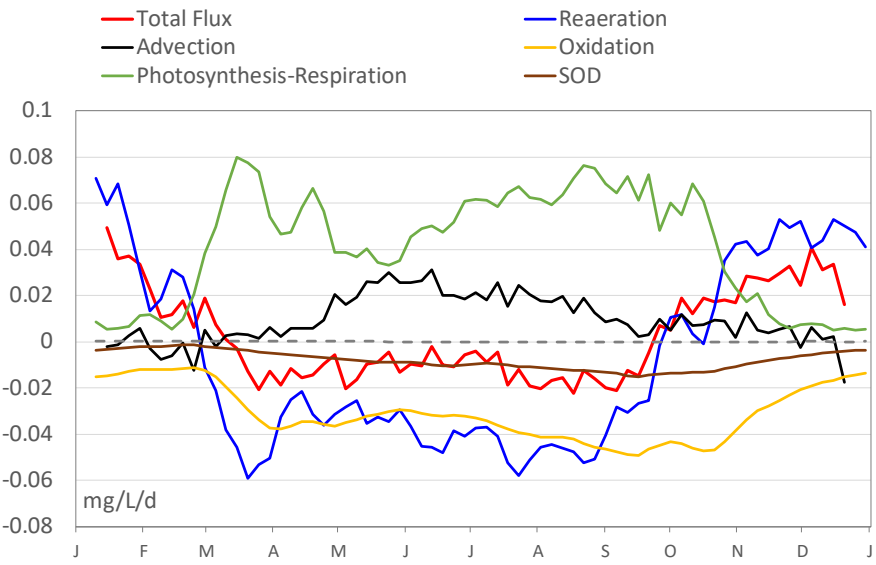

Figure 3-62 Model-computed averaged DO fluxes in the MBS-CCB mass balance area (Figure 3-1) for 2016 with the updated BEM. Results are calculated at a 5-day timestep, which limits the ability to filter out the tidal signal and explains the "shakiness" of the curves.

3.3.7 Relevance of sediments in mass balances

The relevance of the bottom sediments and related processes is evaluated based on annual mass balances from the simulation of 2016 for the MBN sub-domain (Figure 3-1). These reveal that the sediment contributes 17% to the total recycling flux of organic nitrogen, 18% to the total recycling flux of organic phosphorus and 23% to the total oxygen demand for the recycling of organic carbon. These shares are low enough as a proportion of annual mass balances that the differences in the model-observation comparisons discussed in Section 3.1.3.4 will not unduly impact fitness for purpose of the updated BEM.

3.4 Conclusions on update/former model comparisons for water quality

Based on the comparison between the former and the updated BEM the following conclusions can be made:

- A suitable water quality model configuration has been set-up and validated for the updated BEM that is comparable to the former BEM. Some model attributes are more elaborate and others somewhat simpler than the former BEM. All simplifications adopted were demonstrated not to compromise the fitness-for-purpose.
- The agreement between the updated BEM and field data is equally good or better than for the former BEM.
- The updated BEM shows noticeably stronger temporal variability and noticeably stronger vertical gradients than the former BEM. Comparison to field data reveals that both characteristics imply that the updated BEM provides a more realistic representation of the water quality in Massachusetts Bay.
- The updated BEM uses a much larger computational domain than the former BEM. This avoids the need to specify boundary concentrations at a location close to the area of interest that need to be derived from local observation values. This makes the updated BEM more suitable for evaluating the influence of the DITP outfall on the water quality of Massachusetts Bay and Cape Cod Bay as well as for conducting scenario simulations such as changes to effluent loads.

4 Conclusion

The updated BEM has been developed (as documented in Appendix A) and successfully calibrated with field observations for the period 2012-2016 (as documented in Appendix B). The performance of the updated model, as evaluated by comparisons to observations, has been demonstrated to be comparable to or better than that of the former model. In addition, the key differences between the updated and former models have been explained. This helps deliver full confidence in the performance of the updated BEM, support proper interpretation of annual assessments made with the updated BEM, and provide continuity with the assessments made using the former BEM. It is concluded that the updated model is valid and suitable for use by the MWRA in its permit-required annual simulations of the years from 2017 onward.

5 References

Alessi, Carol A., Beardsley, Robert C., Limeburner, Richard, Rosenfeld, Leslie K., Lentz, Steven J., Send, Uwe, Winant, Clinton D., Allen, John S., Halliwell, George R., Brown, Wendell S., Irish, James D.,1995. "CODE-2: moored array and large-scale data report", Woods Hole Oceanographic Institution Technical Report 85-35, DOI:10.1575/1912/1641.

Blauw, A.N., Los, H.F.J., Bokhorst, M., Erftemeijer, P.L.A., 2009. GEM: a Generic Ecological Model for estuaries and coastal waters. Hydrobiologia 618: 175-198.

Doneker, R.L. and G.H. Jirka, "CORMIX User Manual: A Hydrodynamic Mixing Zone Model and Decision Support System for Pollutant Discharges into Surface Waters", EPA-823-K-07-001, Dec. 2007.

Hunt, C.D., Kropp, R.K., Fitzpatrick, J.J., Yodzis, P, Ulanowicz R.E., 1999. A review of issues related to the development of a food web model for important prey of endangered species in Massachusetts and Cape Cod Bays. Boston: Massachusetts Water Resources Authority. Report 1999-14. 62 p.

Hunt, C.D., Mansfield, A.D., Mickelson, M.J., Albro, C.S., Geyer, W.R., Roberts, P.J.W., 2010. Plume tracking and dilution of effluent from the Boston sewage outfall, Marine Environmental Research, 70(2), 150-161, https://doi.org/10.1016/j.marenvres.2010.04.005.

Hydroqual, 2004. User's Guide for RCA (Release 3.0), June 2004.

Keay, K. E., W. S. Leo, and P. S. Libby, 2012. Comparisons of Model-Predicted and Measured Productivity in Massachusetts Bay. Boston: Massachusetts Water Resources Authority. Report 2012-03. 11 p. plus Appendix. http://www.mwra.state.ma.us/harbor/enquad/pdf/2012-03.pdf.

Los, F.J., Villars, M.T., Van der Tol, M.W.M., 2008. A 3-dimensional primary production model (BLOOM/GEM) and its applications to the (southern) North Sea (coupled physical-chemical-ecological model). Journal of Marine Systems, 74 (1-2): 259-294. https://doi.org/10.1016/j.jmarsys.2008.01.002

Los, F.J., 2009. Eco-hydrodynamic modeling of primary production in coastal waters and lakes using BLOOM. Ph.D. Thesis, Wageningen University, 2009.

Smits, J.G.C. and J.K.L. van Beek, 2013. ECO: A Generic Eutrophication Model Including Comprehensive Sediment-Water Interaction. PLoS ONE 8(7), 2013: e68104.

Tucker, J., S. Kelsey, and A. E. Giblin, 2010. 2009 benthic nutrient flux annual report. Boston: Massachusetts Water Resources Authority. Report 2010-10. 27 p. http://www.mwra.state.ma.us/harbor/enquad/pdf/2010-10.pdf.

Xue, P., Chen C., Qi J., Beardsley R.C., Tian R., Zhao L., Lin H. 2014. Mechanism studies of seasonal variability of dissolved oxygen in Mass Bay: A multi-scale FVCOM/UG-RCA application. Journal of Marine Systems, 131, 102–119.

Zhao L., Chen C., Beardsley R.C., Codiga D.L., Leo W.S. 2016. Simulations of Hydrodynamics and Water Quality in the Massachusetts Bay System during 2014 using the Bays Eutrophication Model. Boston: Massachusetts Water Resources Authority. Report 2016-03. 103p.

Zhao L., Beardsley R.C., Chen C., Codiga D.L., Wang L. 2017. Simulations of 2016 Hydrodynamics and Water Quality in the Massachusetts Bay System using the Bays Eutrophication Model. Boston: Massachusetts Water Resources Authority. Report 2017-13. 111p.

Appendix A: Model attributes and methods

Appendix A is in a separate file, available online at:
www.mwra.com/media/file/demonstration-updated-bays-eutrophication-model-2021-02A

Appendix B: Multi-year calibration

Appendix B is in a separate file, available online at:
https://www.mwra.com/media/file/demonstration-updated-bays-eutrophication-model-2021-02B

Massachusetts Water Resources Authority
100 First Avenue • Boston, MA 02129
www.mwra.com
617-242-6000